Summer School
"Turbulence and fluctuations in the microphysics and dynamics of clouds"
Porquerolles, France
September 1-10, 2010

Integration of simulations and experiments to study inertial particles in turbulence: <u>one-particle statistics</u>

Lance R. Collins
Cornell University

Acknowledgments

Collaborators:

- Zellman Warhaft
- Hui Meng
- Raymond Shaw
- Don Koch
- Eberhard Bodenschatz
- Haitao Xu
- Greg Voth

Students:

- Shivshankar Sundaram
- Walter Reade
- Arun Keswani
- Aruj Ahluwalia
- Juan Salazar

Students of Collaborators

- Armann Gylfason
- Sathya Ayyalasomalajula
- Nicholas Ouellette

International Collaboration for Turbulence Research

Topics

Talk 1: Discuss how simulations and experiments have helped us understand the motion of a <u>single</u> inertial particle in turbulence.

- Homogeneous isotropic turbulence
- Mean shear (boundary layer)
- Entrainment

Talk 2: Discuss the motion of <u>particle pairs</u> in turbulence with the goal of analyzing the interparticle collision rate.

Comprehensive Strategy

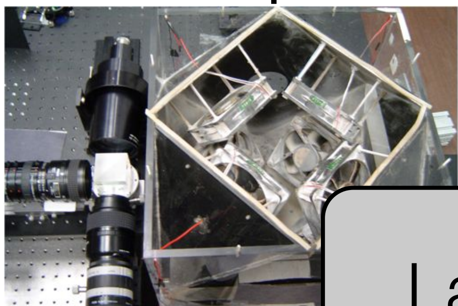

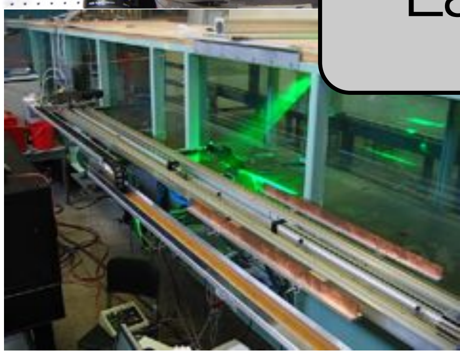

Laboratory

DNS

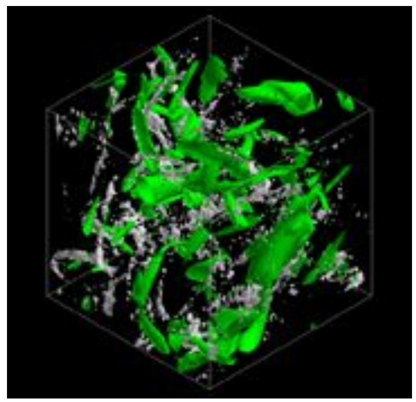

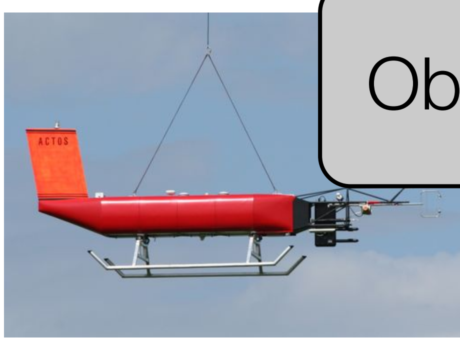

Observations

Modeling

- RANS
- LES

Atmospheric Research 97 (2010) 426–437

Contents lists available at ScienceDirect

Atmospheric Research

journal homepage: www.elsevier.com/locate/atmos

Towards understanding the role of turbulence on droplets in clouds: In situ and laboratory measurements

H. Siebert [a,e,*], S. Gerashchenko [b,e], A. Gylfason [c,e], K. Lehmann [a,e], L.R. Collins [b,e], R.A. Shaw [a,d,e], Z. Warhaft [b,e,f]

[a] Leibniz-Institute for Tropospheric Research, Leipzig, Germany
[b] Sibley School of Mechanical & Aerospace Engineering, Cornell University, Ithaca, NY 14853-7501, USA
[c] School of Science & Engineering, Reykjavik University, Reykjavik, Iceland
[d] Department of Physics, Michigan Technological University, Houghton, MI 49931-1295, USA
[e] International Collaboration for Turbulence Research
[f] Cornell Center for a Sustainable Future, Ithaca, NY, USA

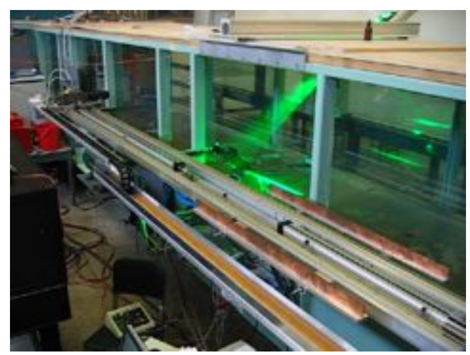

Is turbulence in the lab and cloud the same?

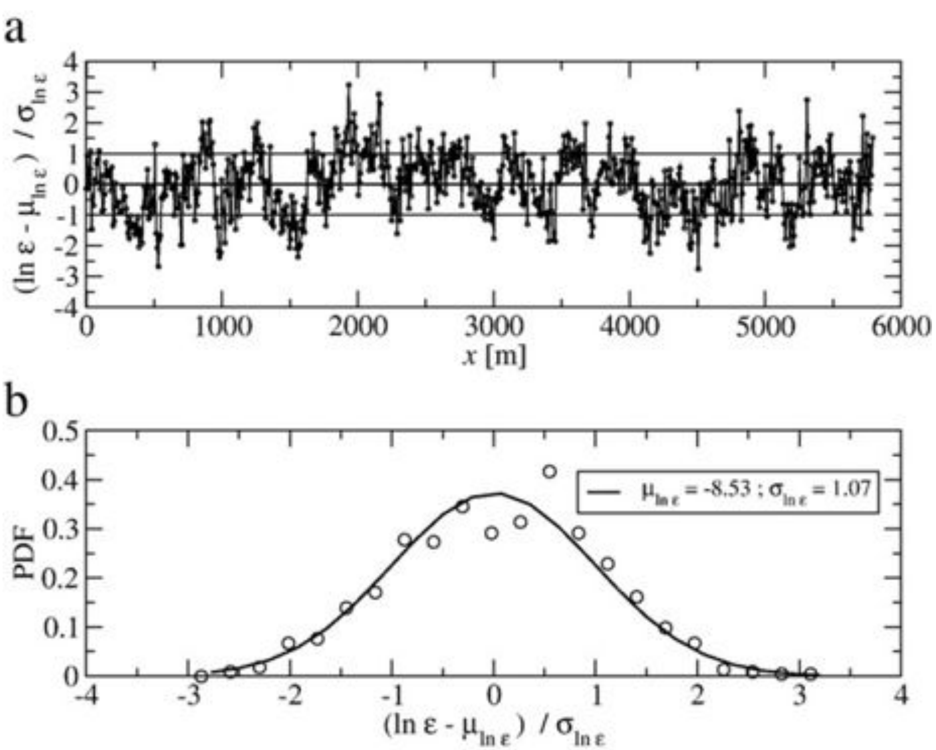

Fig. 6. Time series of normalized local energy dissipation derived from a 6 km long record in a stratocumulus field (upper panel) with PDF (lower panel).

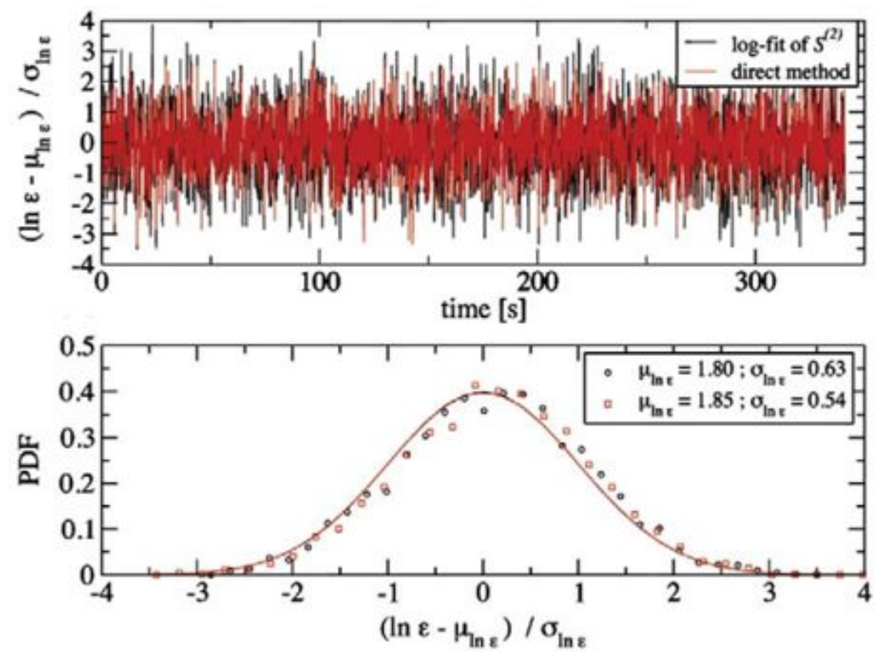

Fig. 7. Upper panel: Time series of normalized local energy dissipation rate $(\ln\varepsilon - \mu_{\ln}\varepsilon)/\sigma_{\ln}\varepsilon$ derived from wind-tunnel data with two different methods (red line: direct method $\varepsilon = 15\nu\left(\partial_t u(t)/\bar{U}\right)^2$, where $\bar{U}$ is the mean wind speed; black line: ε estimated from the 2nd-order structure function after applying non-overlapping block averages over ten samples to fit the resolution of the cloud data). The lower panel shows the corresponding PDFs.

Is turbulence in the lab and cloud the same?

$$\sigma^2_{\ln \epsilon} \sim \left(\frac{L}{\eta}\right)^{\mu}$$

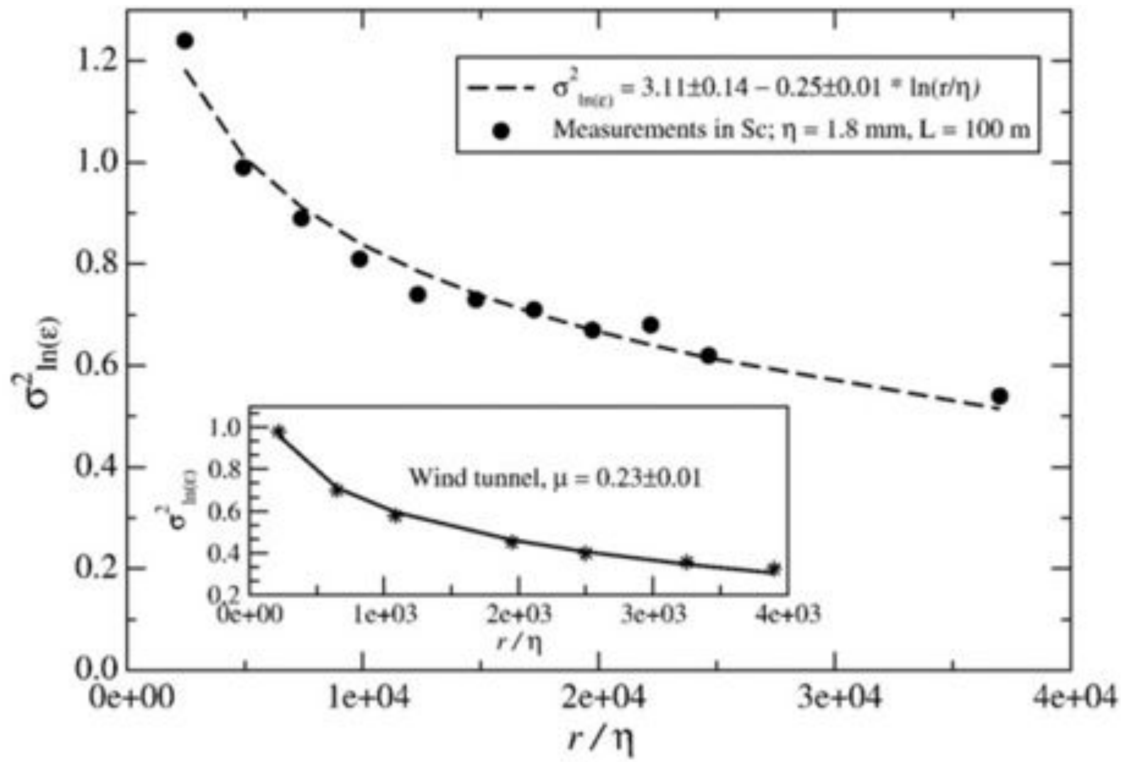

Fig. 8. Variance $\sigma^2_{\ln(\varepsilon_r)}$ as a function of the integration length r normalized with the Kolmogorov length $\eta \approx 1.8$ mm. An integral length scale $L \approx 100$ m limits $r/\eta < L/\eta \approx 5 \cdot 10^4$. A logarithmic fit (dashed line) yields an intermittency exponent $\mu = 0.25$ with a standard error of 0.01. The insert shows the same statistical quantity taken from the laboratory data.
Modified from Siebert et al. (2010).

Is turbulence in the lab and cloud the same?

$$\sigma^2_{\ln \epsilon} \sim \left(\frac{L}{\eta}\right)^{\mu}$$

Yes!

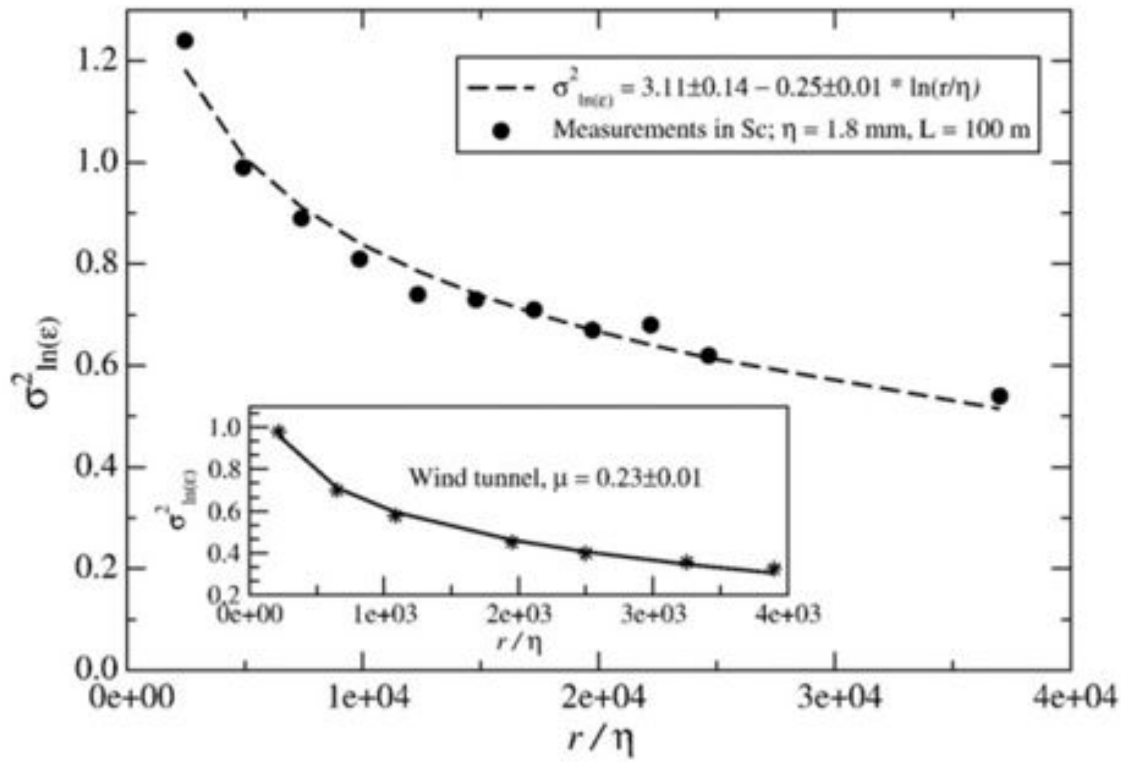

Fig. 8. Variance $\sigma^2_{\ln(\varepsilon_r)}$ as a function of the integration length r normalized with the Kolmogorov length $\eta \approx 1.8$ mm. An integral length scale $L \approx 100$ m limits $r/\eta < L/\eta \approx 5 \cdot 10^4$. A logarithmic fit (dashed line) yields an intermittency exponent $\mu = 0.25$ with a standard error of 0.01. The insert shows the same statistical quantity taken from the laboratory data.
Modified from Siebert et al. (2010).

Motion of an inertial particle (low inertia)

$$\frac{dX_i}{dt} = v_i \qquad \frac{dv_i}{dt} = \frac{u_i\left(X_i\right) - v_i}{\tau_p} + g_i + \cdots$$

$$\boxed{\begin{aligned} v_i &= u_i\left(X_i\right) + \tau_p g_i - \tau_p a_i\left(X_i\right) + \cdots \\ a_{p,i} &= a_i\left(X_i\right) + \cdots \end{aligned}}$$

$$a_i\left(X_i\right) \equiv \left[\frac{\partial u_i}{\partial t} + u_j \frac{\partial u_i}{\partial x_j}\right]_{X_i}$$

Maxey (1987)

Motion of an inertial particle (low inertia)

$$\frac{dX_i}{dt} = v_i \qquad \frac{dv_i}{dt} = \frac{u_i\left(X_i\right) - v_i}{\tau_p} + g_i + \cdots$$

$$v_i = u_i\left(X_i\right) + \tau_p g_i - \cancel{\tau_p a_i}\left(X_i\right) + \cdots$$

$$a_{p,i} = a_i\left(X_i\right) + \cdots$$

$$a_i\left(X_i\right) \equiv \left[\frac{\partial u_i}{\partial t} + u_j \frac{\partial u_i}{\partial x_j}\right]_{X_i} \qquad \epsilon = 0.001 - 0.01$$

$$Fr = \frac{g}{\langle a^2 \rangle^{1/2}} = \frac{\nu^{1/4} g}{a_0 \epsilon^{3/4}} \approx 5 - 20$$

Maxey (1987)

Wind tunnel measurements of near isotropic turbulence

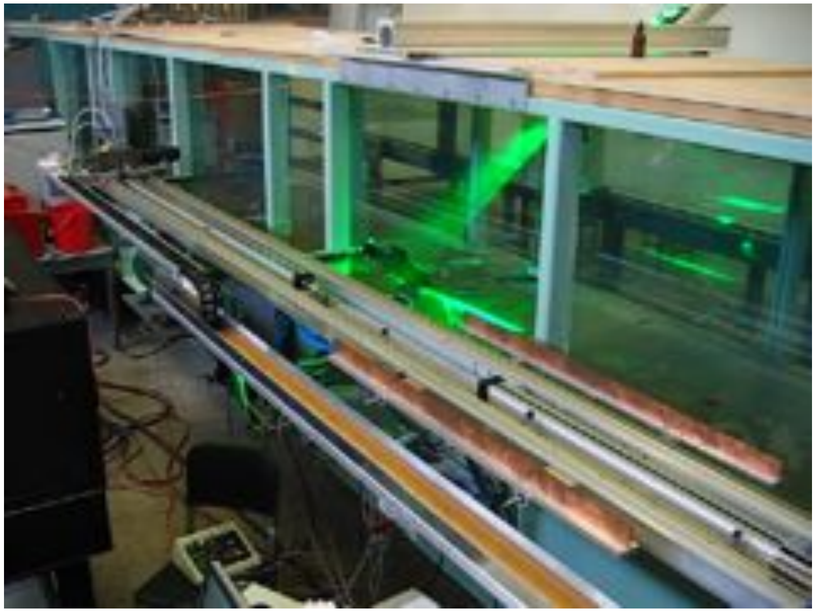

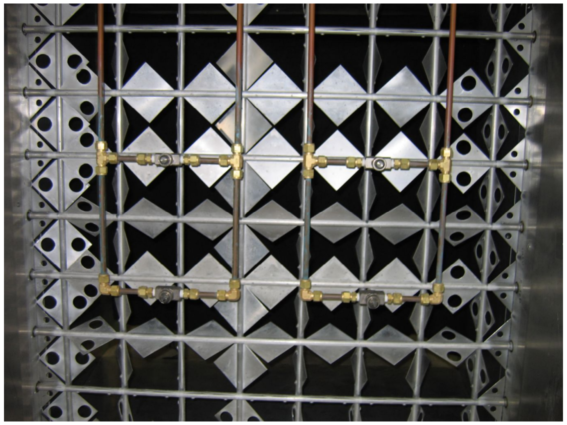

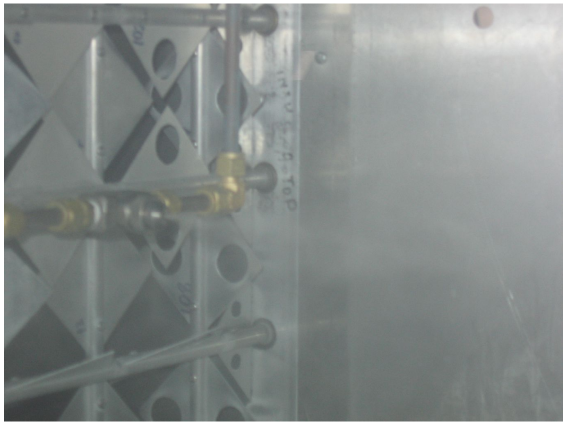

Ayyalasomayajula et al. 2006

Particle Trajectories

Ayyalasomayajula et al. 2006

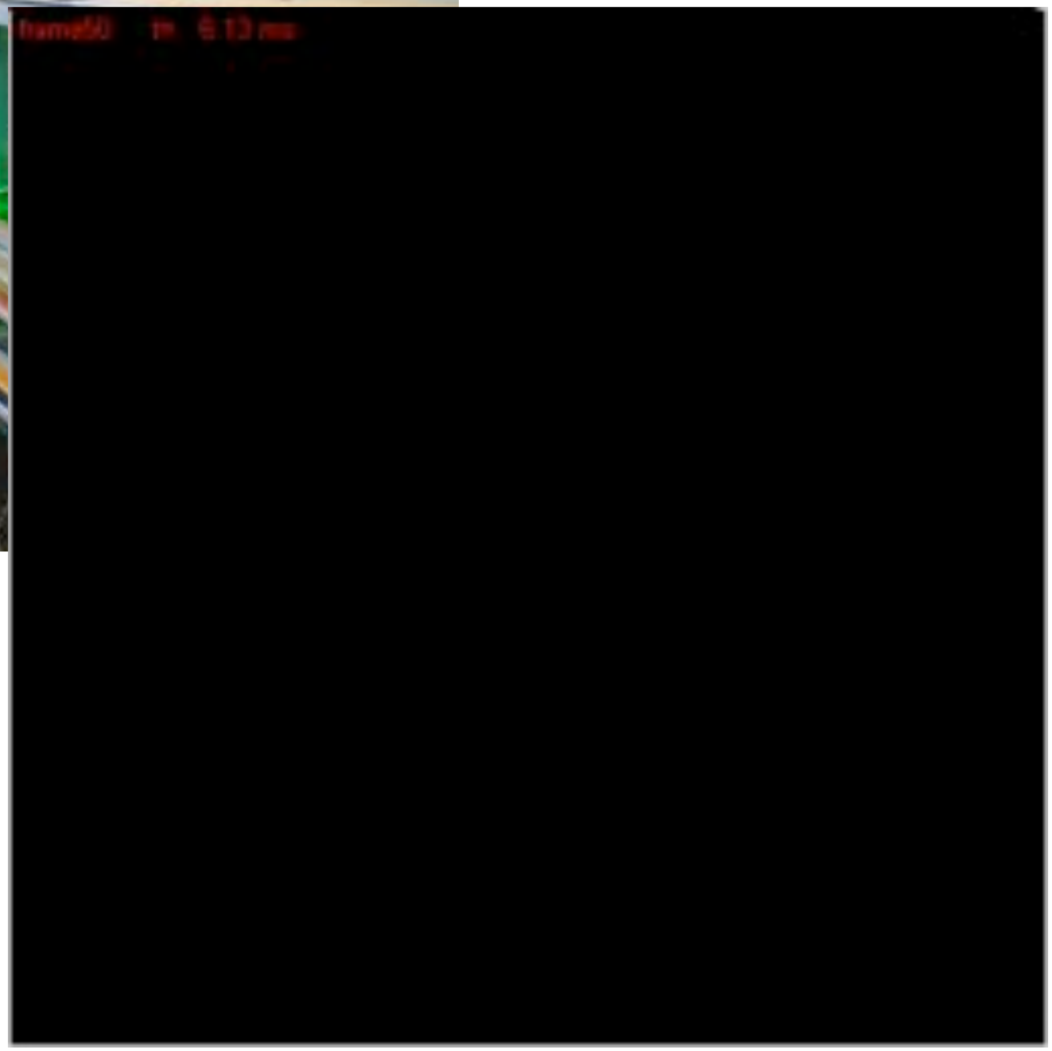

Probability Density Function (PDF) of Acceleration

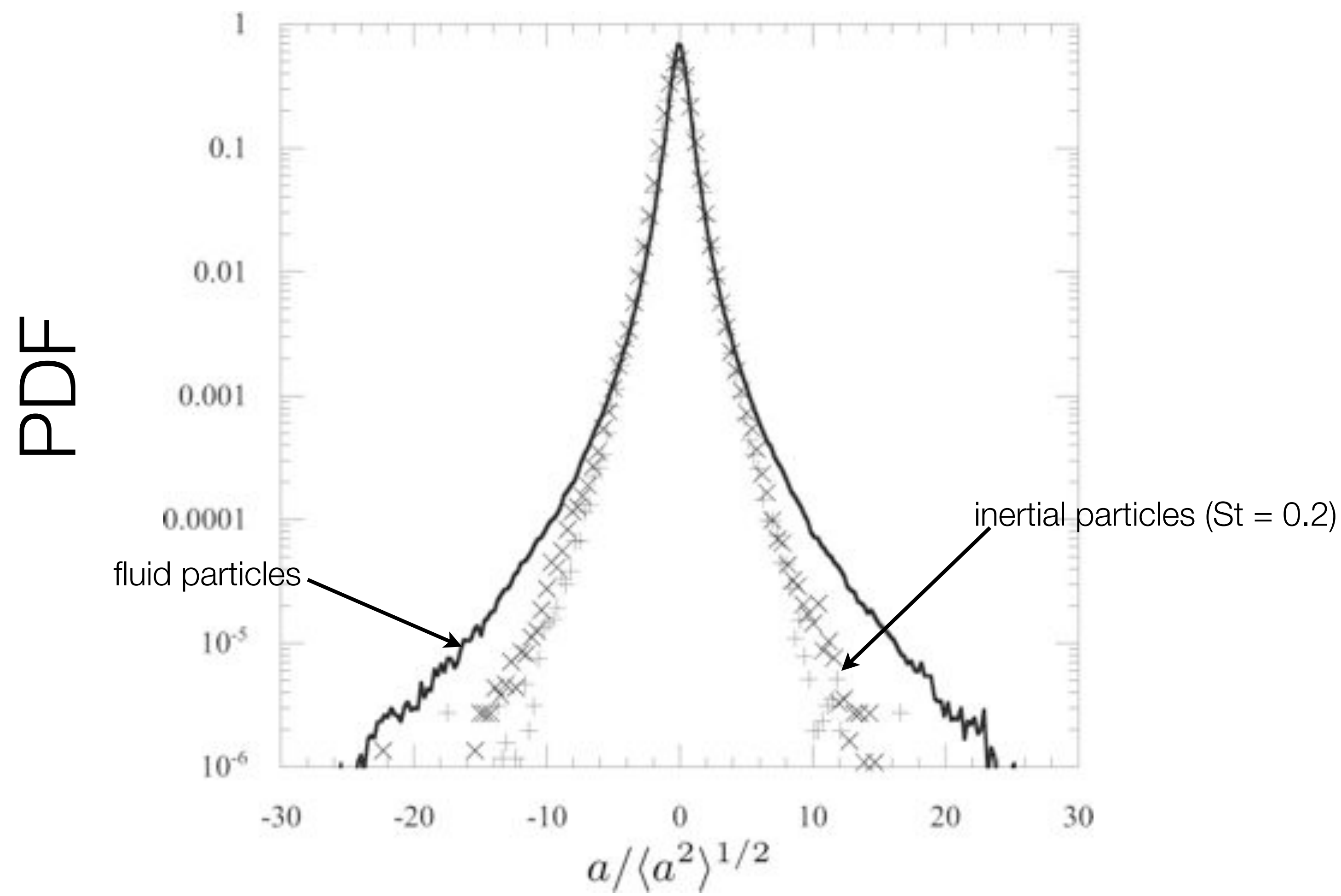

Ayyalasomayajula et al. 2006

DNS - Fluid

$$\frac{\partial u_i}{\partial t} + \epsilon_{ijk}\omega_j u_k = -\frac{\partial p^\star}{\partial x_i} + \nu \frac{\partial^2 u_i}{\partial x_j \partial x_j} + F_i$$

$$\frac{\partial u_j}{\partial x_j} = 0$$

$$\omega_i = \epsilon_{ijk}\frac{\partial u_k}{\partial x_j}$$

$$p^\star = \frac{p}{\rho} + \frac{1}{2}u_i u_i$$

- De-aliased pseudospectral code
- Number of grid points 512^3
- Deterministic forcing to maintain statistically stationary turbulence
- Temporal resolution $\frac{\sqrt{3}\Delta t_f |u_i u_i|_{\max}}{\Delta x} \leq \frac{1}{2}$
- Spatial resolution $\kappa_{\max}\eta > 2$

DNS - Particles

$$0 \leq St \equiv \tau_p/\tau_\eta \leq 2$$

- $\mathrm{Re}_p = \dfrac{|u_i - v_i|d}{\nu} \ll 1$
- $\beta = \rho_p/\rho_f \gg 1$
- $d/\eta \ll 1$
- $\Phi_V \sim O(10^{-7})$
- $\Phi_M \sim O(10^{-4})$

$$\frac{dXi}{dt} = v_i(\mathbf{x} = \mathbf{X})$$

$$\frac{dv_i}{dt} = \frac{u_i(\mathbf{x} = \mathbf{X}) - v_i}{\tau_p}$$

Inertial Particles

$$\frac{dXi}{dt} = u_i(\mathbf{x})$$

$$\frac{du_i(\mathbf{x})}{dt} = -\frac{1}{\rho_f}\nabla p(\mathbf{x}) + \nu\nabla^2 u_i(\mathbf{x})$$

Fluid Particles

Heavy particle dynamics

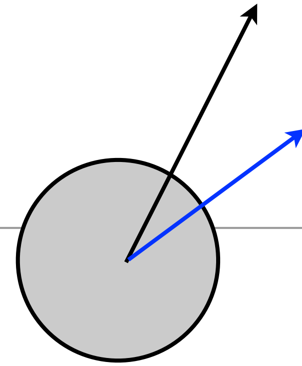

Maxey & Riley, PoF 26, 883 (1983)

$$\frac{d\mathbf{X}}{dt} = \mathbf{v}$$

$$\frac{d\mathbf{v}}{dt} = \frac{\mathbf{u}(\mathbf{x},t) - \mathbf{v}}{\tau_p} + \left(1 - \frac{1}{\beta}\right)\mathbf{g}$$

$$+ \sqrt{\frac{9}{2\beta\tau_p}} \int_0^t \frac{d/d\tau\,[\mathbf{u} - \mathbf{v}]}{\sqrt{t-\tau}} d\tau \quad \text{Basset}$$

$$+ \frac{1}{\beta}\frac{d\mathbf{u}}{dt} \quad \text{pressure}$$

$$+ \frac{1}{2\beta}\left[\frac{d\mathbf{u}}{dt} - \frac{d\mathbf{v}}{dt}\right] \quad \text{added mass}$$

$$\beta \equiv \frac{\rho_p}{\rho} \qquad \tau_p \equiv \frac{\beta d^2}{18\nu}$$

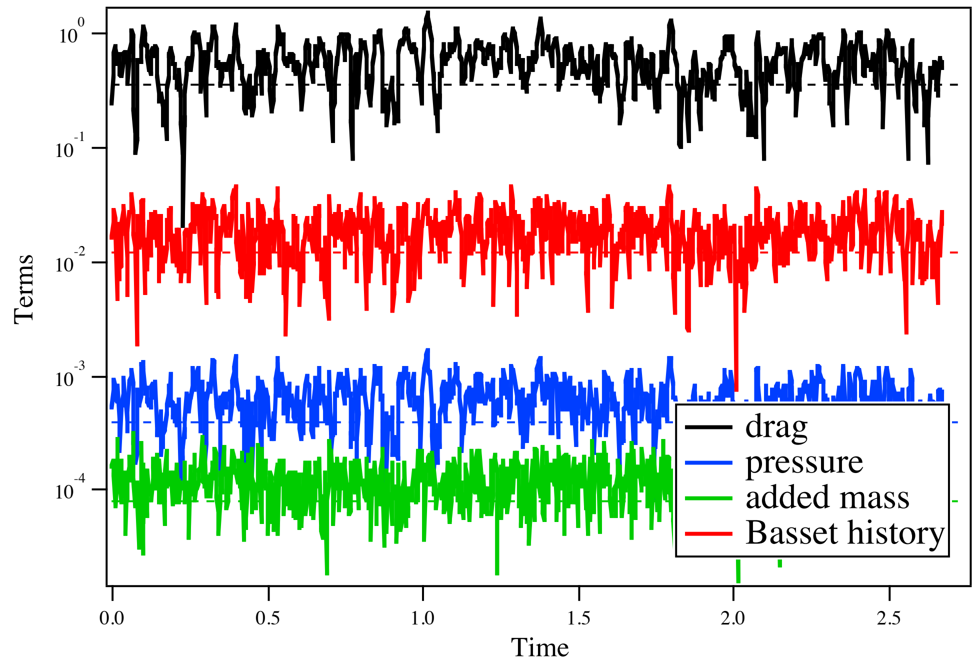

Elghobashi & Truesdell, JFM 242:655 (1992)
Hill, PoF 17:037103 (2005)

DNS acceleration statistics

- Overall agreement with the experiments is good
- Use the DNS to separate the effects due to “sampling” and “filtering” by simulating unphysical particles

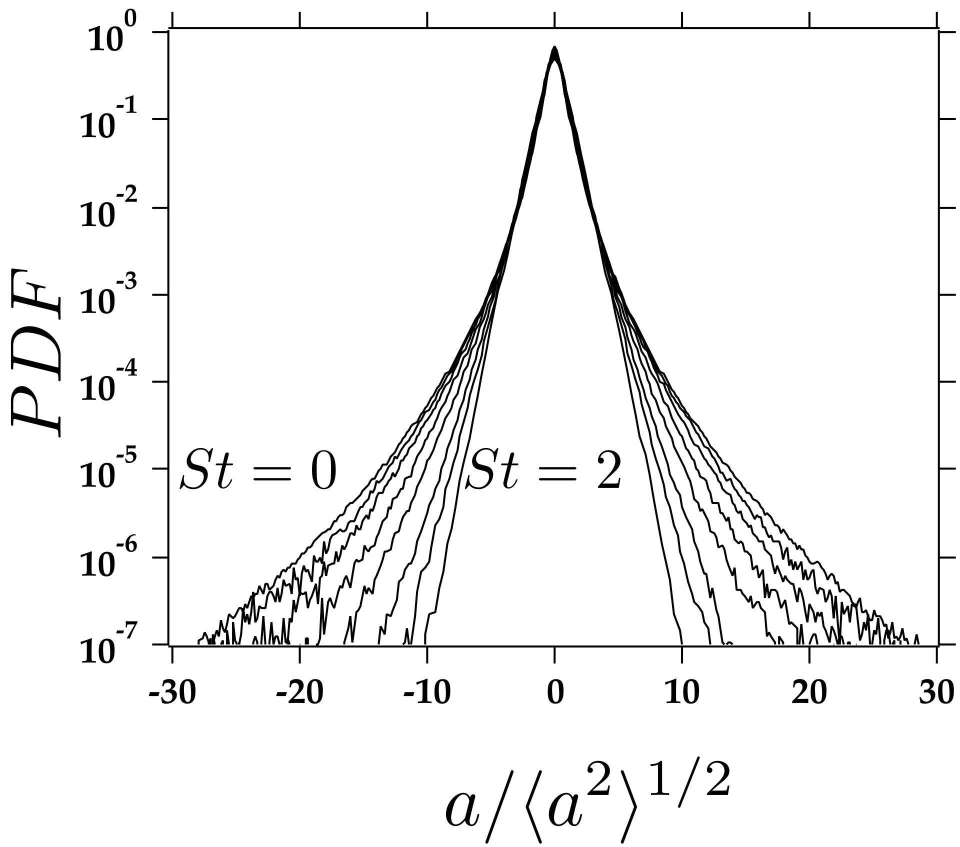

Eulerian view of clustering

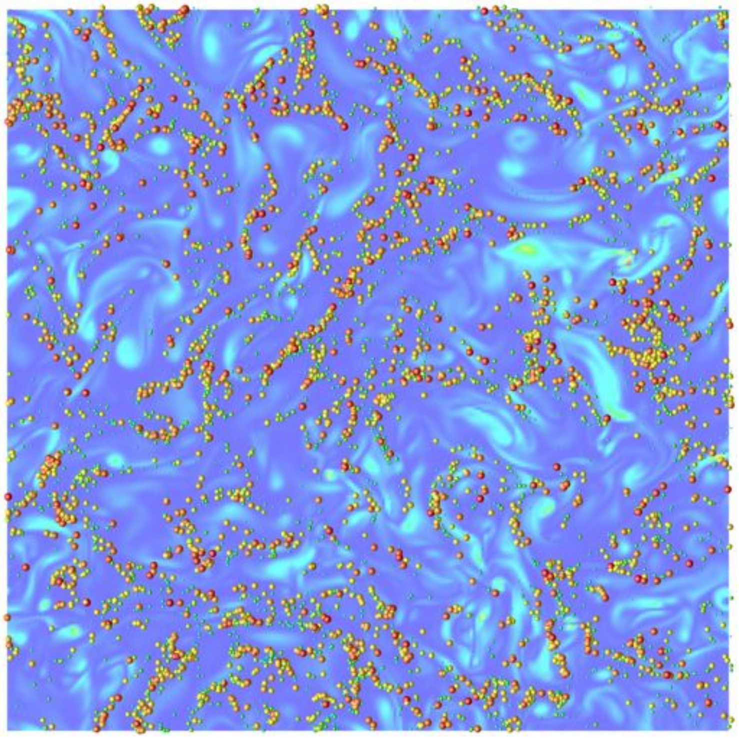

DNS

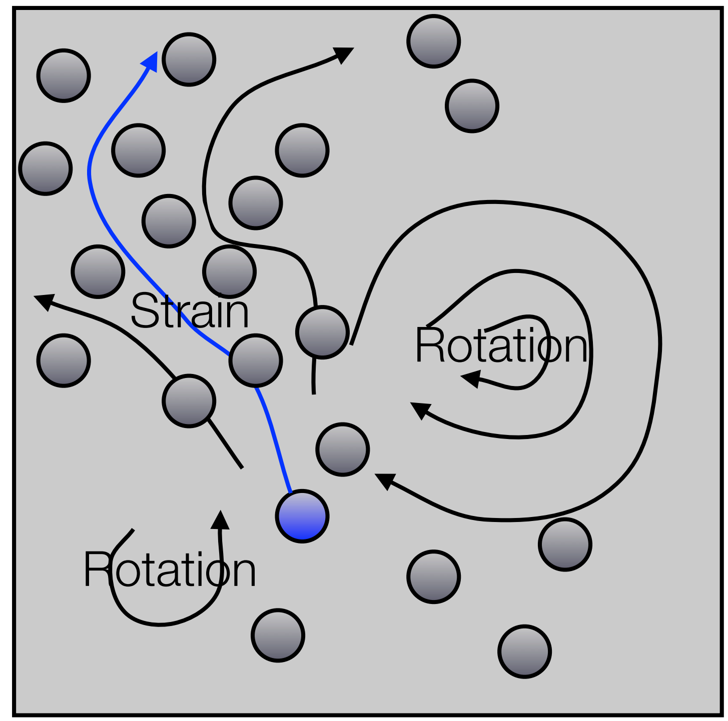

Schematic

Maxey 1987; Squires & Eaton 1991; Wang & Maxey 1993
Sundaram & Collins 1997; Reade & Collins 2000
Falkovich et al. 2002; Zaichik & Alipchenkov 2003; Chun et al. 2005

The concept of biased filtering Ayyalasomayajula et al. (2008)

- In their study, a vortex model showed that even at low St some discrepancy remained in the tails of the acceleration PDF.
- If the timescale of an acceleration event is a function of its magnitude, then there will be a biased filtering of the velocity field, i.e., a particle will sample small- and large-magnitude events differently.
- Filtering is a function of $\mathcal{A}$ inasmuch as ω is a function of $\mathcal{A}$.
- Results from the vortex model support a functional form $\omega = f(\mathcal{A})$

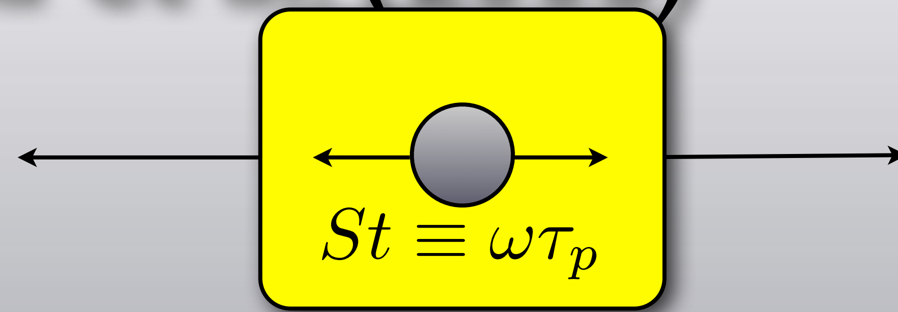

$$u = \sqrt{2}\mathcal{A}\sin\omega t$$

$$\frac{dv}{dt} = \frac{u - v}{\tau_p}$$

$$St_\omega = \omega\tau_p$$

$$\frac{\langle a_p^2\rangle}{\langle a_f^2\rangle} = \frac{1}{1 + St_\omega^2}$$

Generalized particles

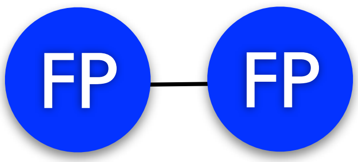

$$\frac{d\mathbf{x}}{dt} = \mathbf{u}$$

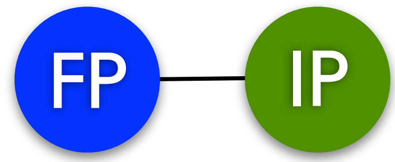

$$\frac{d\mathbf{x}}{dt} = \mathbf{v} \qquad \mathbf{u}(\mathbf{x})$$

“sampling” no “filtering”

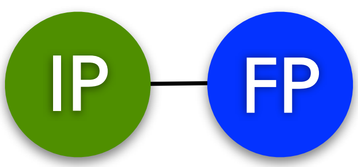

$$\frac{d\mathbf{x}}{dt} = \mathbf{u} \qquad \frac{d\mathbf{v}}{dt} = \frac{(\mathbf{u} - \mathbf{v})}{\tau_p}$$

“filtering” no “sampling”

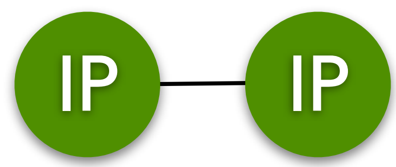

$$\frac{d\mathbf{x}}{dt} = \mathbf{v} \qquad \frac{d\mathbf{v}}{dt} = \frac{(\mathbf{u} - \mathbf{v})}{\tau_p}$$

Revisiting the role of biased sampling and filtering in the acceleration PDF

- Particle inertia has a significant effect on acceleration variance, even at St as low as 0.1.
- For St≤0.2 the effect of particle inertia on the acceleration variance is captured by biased sampling.
- For St>2 it is filtering that captures the effect of inertia.
- Contributions to acceleration variance come predominantly from the central portion of the PDF.

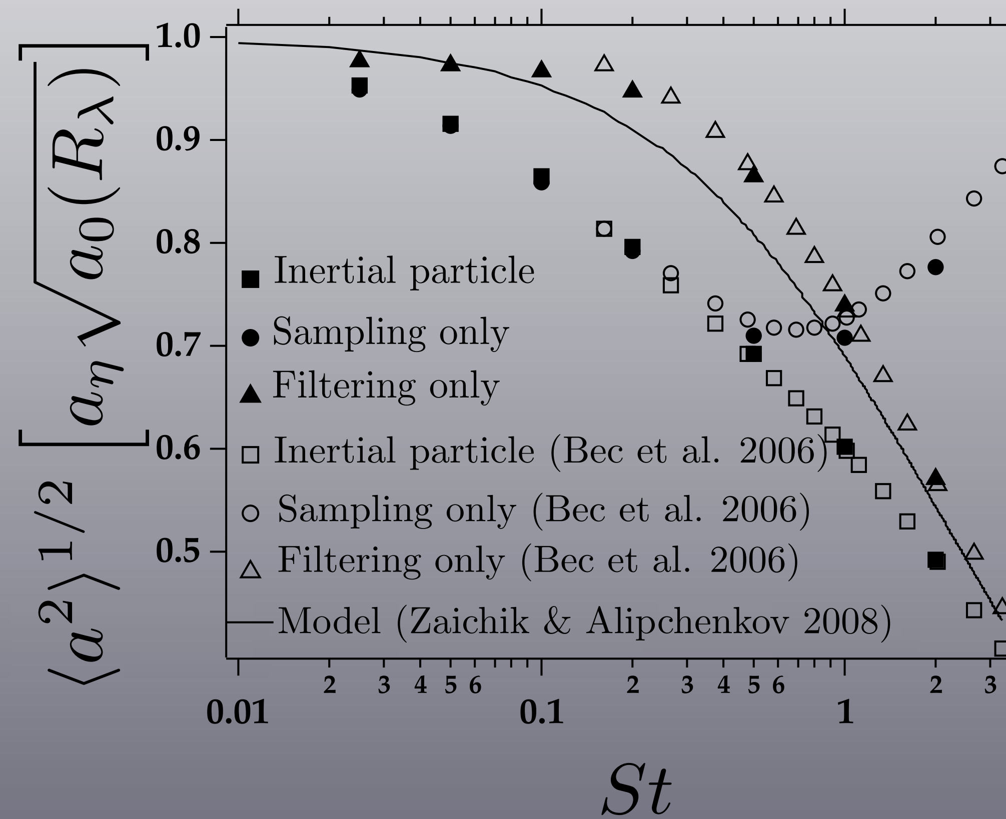

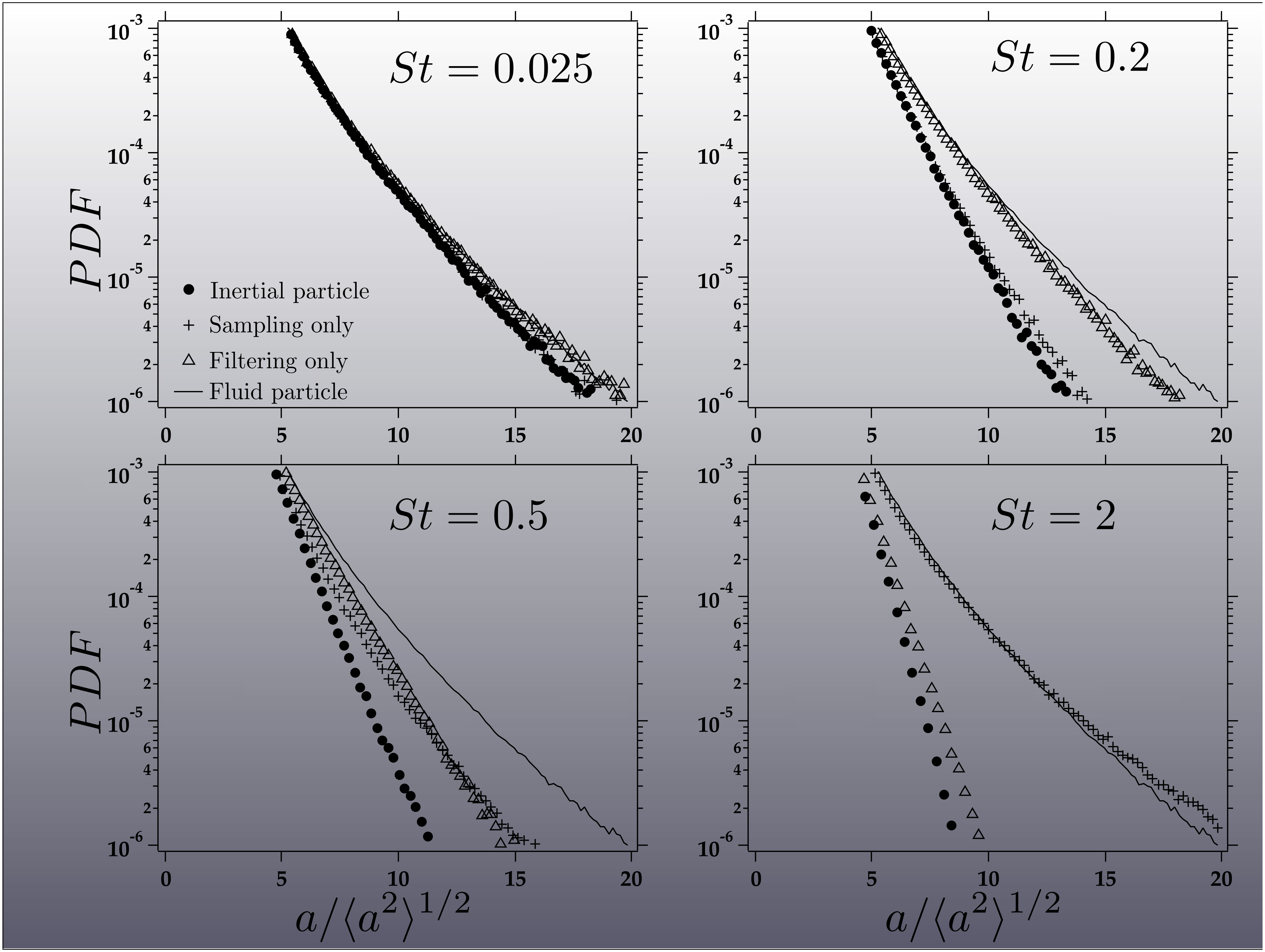

$St = 0.025$
$St = 0.2$
$St = 0.5$
$St = 2$
PDF
$a/\langle a^2 \rangle^{1/2}$
Inertial particle
Sampling only
Filtering only
Fluid particle
10^{-3}
10^{-4}
10^{-5}
10^{-6}
0
5
10
15
20

Acceleration timescale as a function of acceleration magnitude

- We test the conjecture of Ayyalasomayajula et al. (2008) by computing the single-component acceleration autocorrelation function of fluid particles sampled along inertial particle trajectories conditioned on the magnitude of the acceleration event.
- The correlation times, defined as the first zero-crossing, are a decreasing function of acceleration magnitude.
- We conclude that biased filtering does occur and is important in determining the shape of the normalized acceleration PDF.

$$\rho_{a|N} = \left.\frac{\langle a(t)a(t+\Delta t)\rangle}{\langle a^2\rangle}\right|_{a^2\geq N\langle a^2\rangle}$$

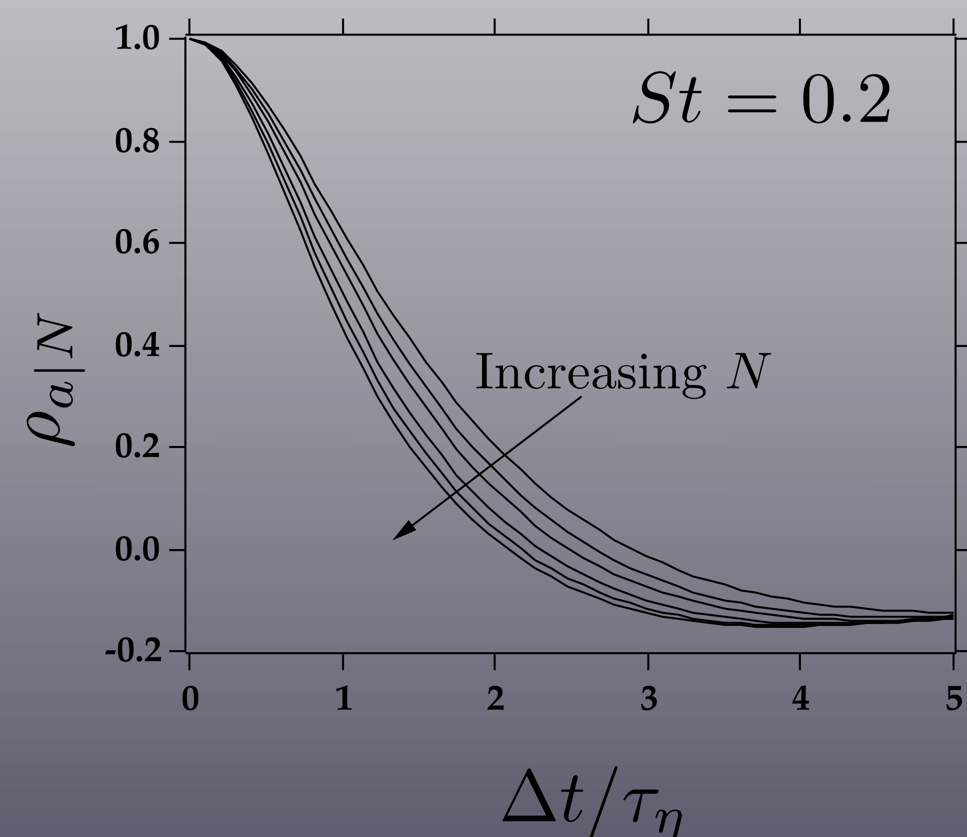

Cloud parameters

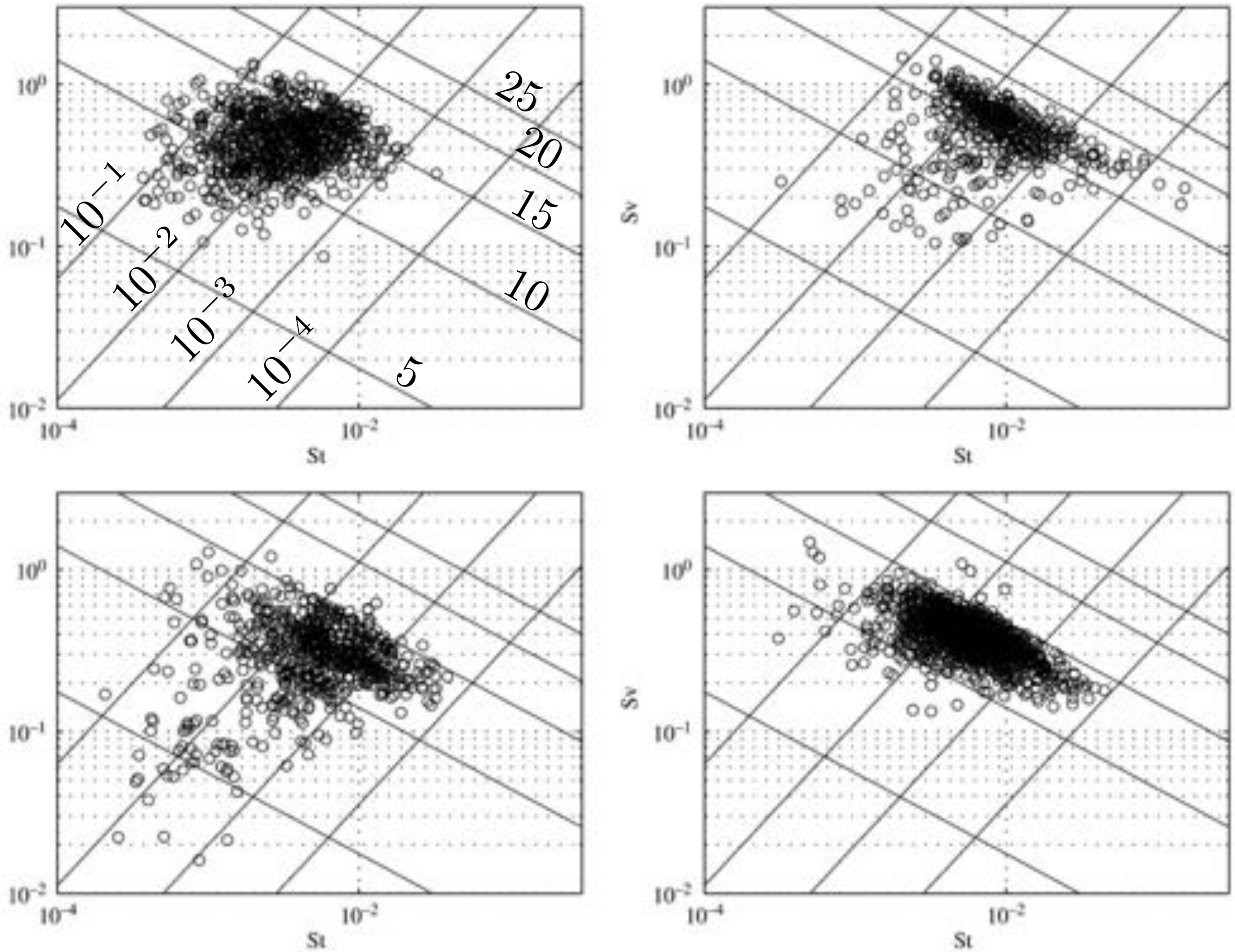

Fig. 9. The distribution of cloud microphysical and turbulence properties in a dimensionless Stokes–settling parameter space. The upper left plot is for a stratocumulus cloud and the remaining three are for small cumulus clouds. Each point represents data in a 1-second (approximately 15 m) average. Diagonal lines with positive slope are contours of constant turbulent energy dissipation rate, ε, at values of 10^{-4}, 10^{-3}, 10^{-2}, and 10^{-1} (lower right to upper left corners). Diagonal lines with negative slope are contours of constant droplet diameter at values of 5, 10, 15, 20 and 25 μm (lower left to upper right corners).

Froude number distribution

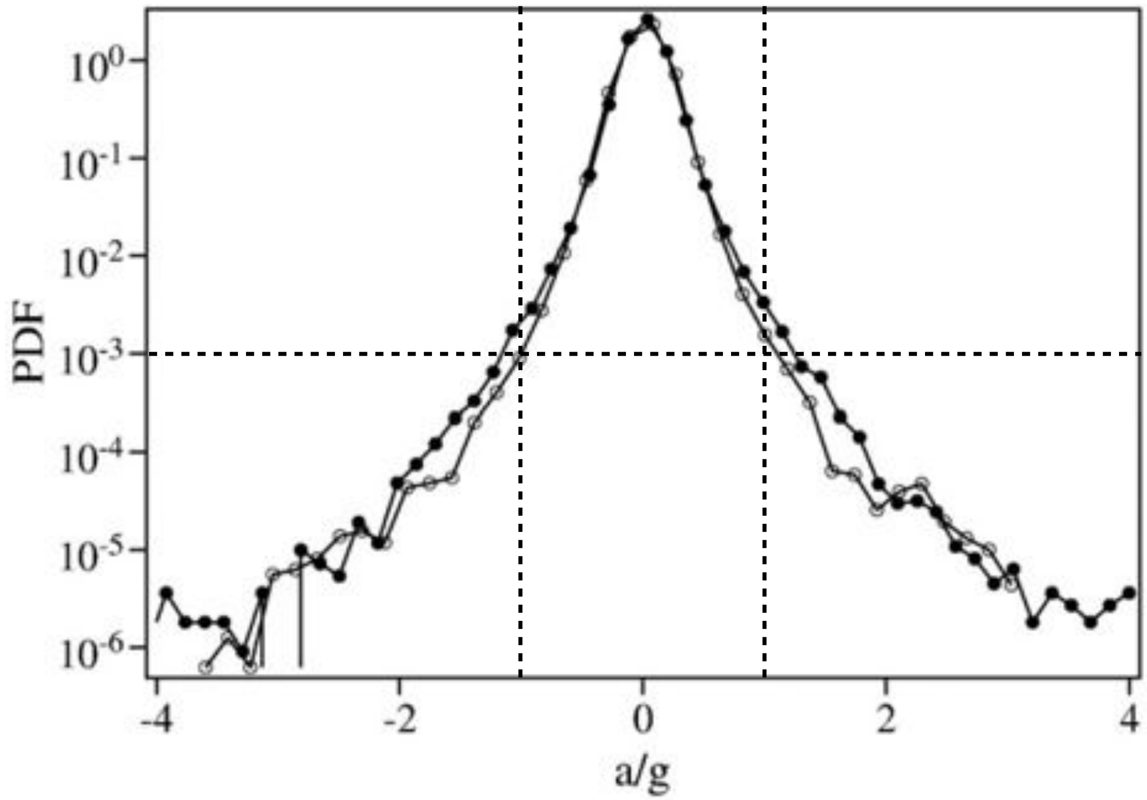

Fig. 12. Probability density function of the Lagrangian acceleration of droplets in a turbulent wind-tunnel flow. The accelerations have been normalized by the gravitational acceleration and scaled to reflect atmospheric conditions (see text). The two PDFs are for flows with Taylor microscale Reynolds numbers $R_\lambda = 100$ (open circle) and 240 (filled circle) and Stokes number $St = 0.072$. Notice that the tails clearly show droplets undergoing accelerations greater than those due to gravity.
Modified from Gerashchenko et al. (2008).

Summary for isotropic turbulence

- Turbulence inside a cumulus cloud is similar to turbulence in a laboratory
- Particle accelerations measured in a wind tunnel are less intermittent than the equivalent fluid particle at the same conditions
- Same result found in DNS
- Using DNS we can separate sampling and filtering effects; sampling is dominant for low-order moments (consistent with Bec et al. 2006); filtering effects found in the tails of the PDF; result traced to "biased filtering"
- Combination of results allows us to estimate the distribution of Froude numbers in a weakly turbulent cumulus cloud; 1 part in 1000 has turbulent accelerations of the same order as gravity

Boundary layer experiment

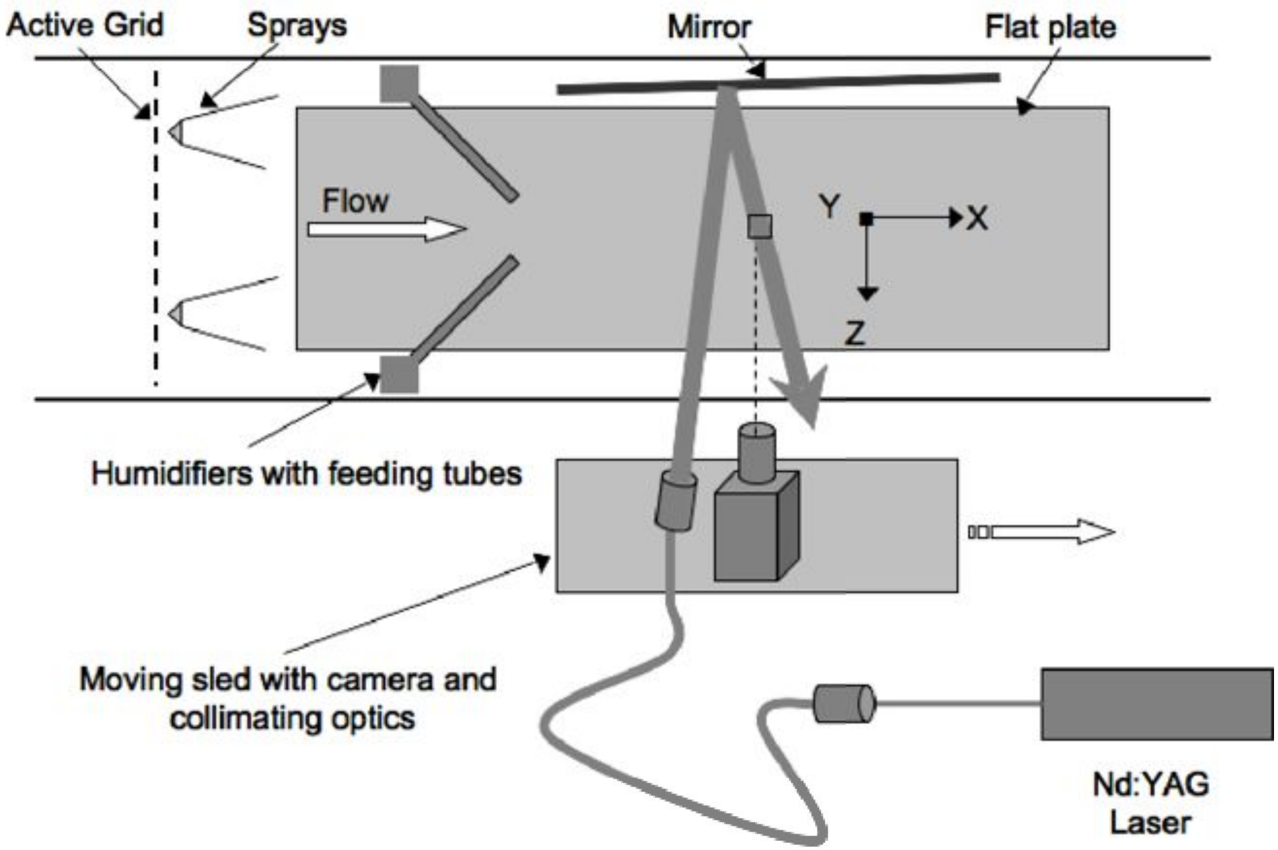

Gerashchenko et al., *J. Fluid Mech*. **617**:255-281, 2008

Plate and optical setup

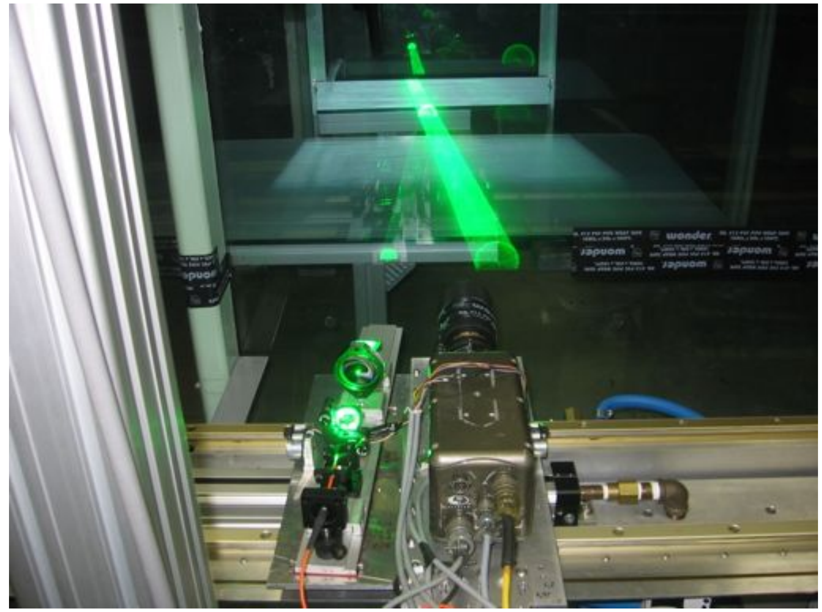

Horizontal plate

3.3 m X 0.67 m plexiglass plate
Sunbeam ultrasonic humidifier
Spraying systems company

Optical setup

Phantom v7.1 camera (8 kHz)
TSI phase Doppler particle analyzer
Hot wire velocimeter (2 components)

Gerashchenko et al., *J. Fluid Mech*. **617**:255-281, 2008

Parameters

Case	U_∞ (m/s)	$\langle u^2 \rangle^{1/2}/U_\infty$	u^* (m/s)	R_λ	$\langle d^2 \rangle^{1/2}$ (μm)	$St_{\eta\infty}$
Low	2.37	4.7%	0.117	100	16	0.035
Med	2.39	11.6%	0.124	240	16	0.07
High	2.39	11.6%	0.124	240	41	0.47

Gerashchenko et al., *J. Fluid Mech*. **617**:255-281, 2008

Experimental results

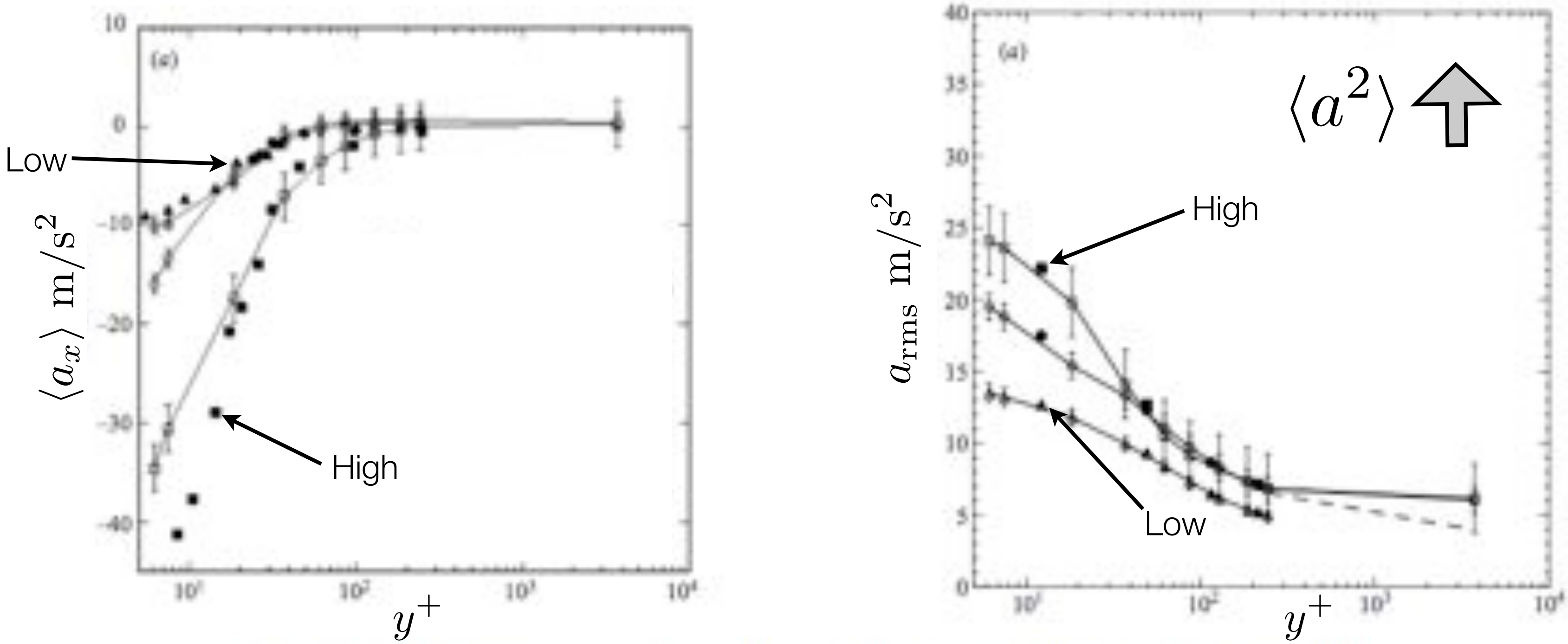

FIGURE 14. Acceleration r.m.s. *vs* y^+ for (a) x and (b) y components: squares, $St_0 = 0.47$, $Re_{\lambda 0} = 240$; circles, $St_0 = 0.07$, $Re_{\lambda 0} = 240$; triangles, $St_0 = 0.035$, $Re_{\lambda 0} = 100$. Filled symbols correspond to a strip width two times larger than for the open symbols.

Gerashchenko et al., *J. Fluid Mech*. **617**:255-281, 2008

J. Fluid Mech. (2010), *vol.* 658, *pp.* 229–246.
doi:10.1017/S0022112010001655

On the role of gravity and shear on inertial particle accelerations in near-wall turbulence

V. LAVEZZO[1], A. SOLDATI[1] S. GERASHCHENKO[2], Z. WARHAFT[2] AND L. R. COLLINS[2]†

[1]Dipartimento di Energetica e Macchine, Università degli Studi di Udine, 33100 Udine, Italy

[2]Sibley School for Mechanical and Aerospace Engineering, Cornell University, Ithaca, NY 14853, USA

(Received 25 September 2009; revised 1 April 2010; accepted 1 April 2010; first published online 15 June 2010)

Recent experiments in a turbulent boundary layer by Gerashchenko *et al.* (*J. Fluid Mech.*, vol. 617, 2008, pp. 255–281) showed that the variance of inertial particle accelerations in the near-wall region increased with increasing particle inertia, contrary to the trend found in homogeneous and isotropic turbulence. This behaviour was attributed to the non-trivial interaction of the inertial particles with both the mean shear and gravity. To investigate this issue, we perform direct numerical simulations of channel flow with suspended inertial particles that are tracked in the Lagrangian frame of reference. Three simulations have been carried out considering (i) fluid particles, (ii) inertial particles with gravity and (iii) inertial particles without gravity. For each set of simulations, three particle response times were examined, corresponding to particle Stokes numbers (in wall units) of 0.9, 1.8 and 11.8. Mean and r.m.s. profiles of particle acceleration computed in the simulation are in qualitative (and in several cases quantitative) agreement with the experimental results, supporting the assumptions made in the simulations. Furthermore, by comparing results from simulations with and without gravity, we are able to isolate and quantify the significant effect of gravitational settling on the phenomenon.

Key words: boundary layers, particle/fluid flows, simulation

Direct numerical simulations

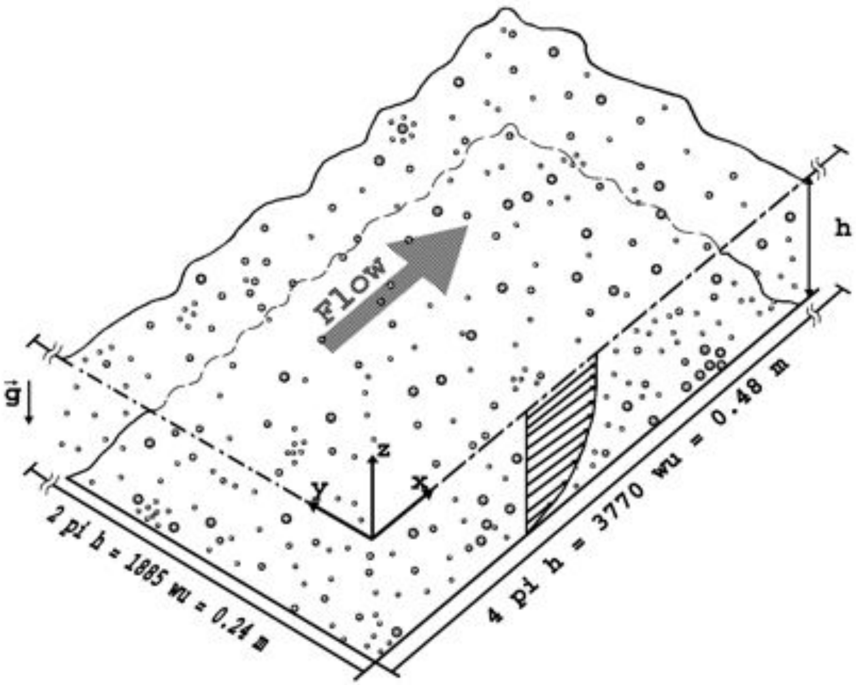

Lavezzo et al., *J. Fluid Mech.* (2010)

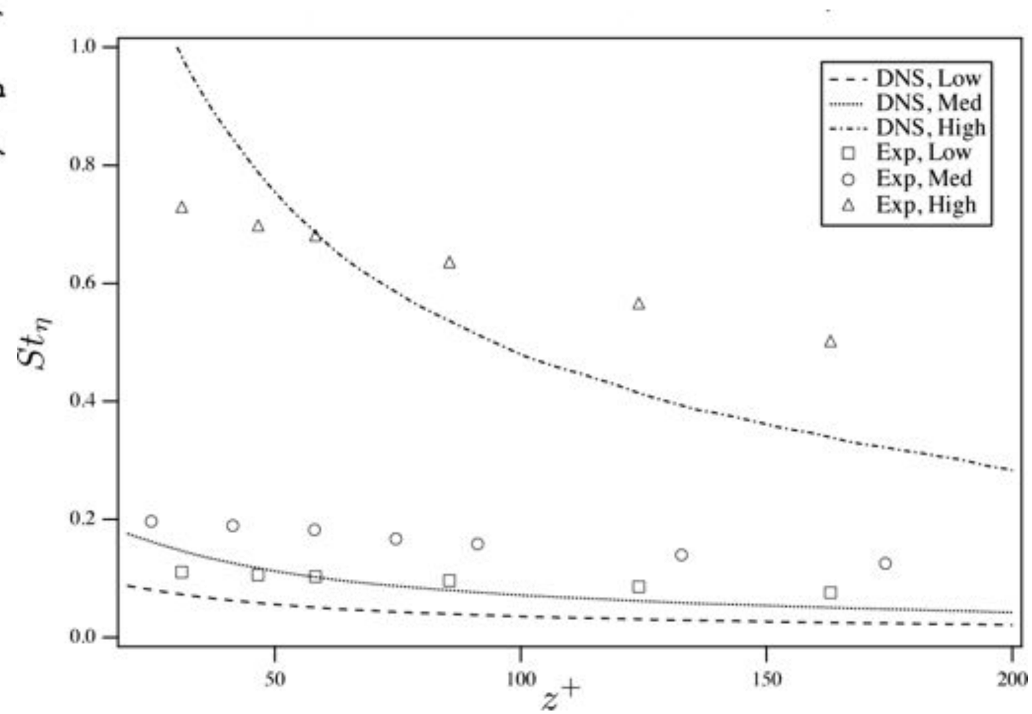

$$\frac{d\mathbf{x}}{dt} = \mathbf{v}$$

$$\frac{d\mathbf{v}}{dt} = \frac{[\mathbf{u}(\mathbf{x}) - \mathbf{v}]}{\tau_p} \left(1 + 0.15 Re_p^{0.687}\right) - \left(1 - \frac{1}{\beta}\right)\mathbf{g} \qquad \tau_p \equiv \frac{\beta d^2}{18\nu} \qquad \beta \equiv \frac{\rho_p}{\rho}$$

Mean flow

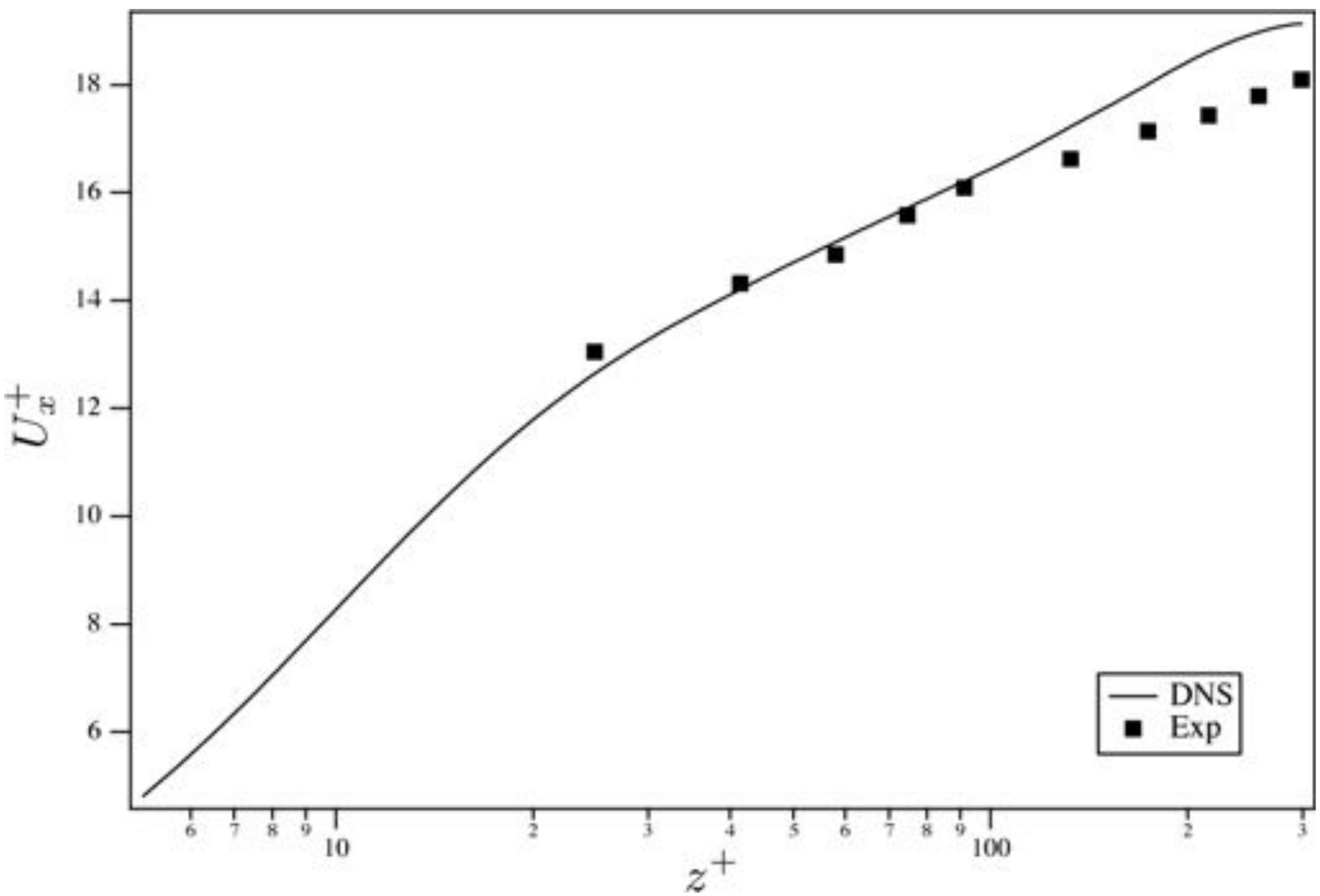

Lavezzo et al., *J. Fluid Mech.* (2010)

Mean acceleration comparison

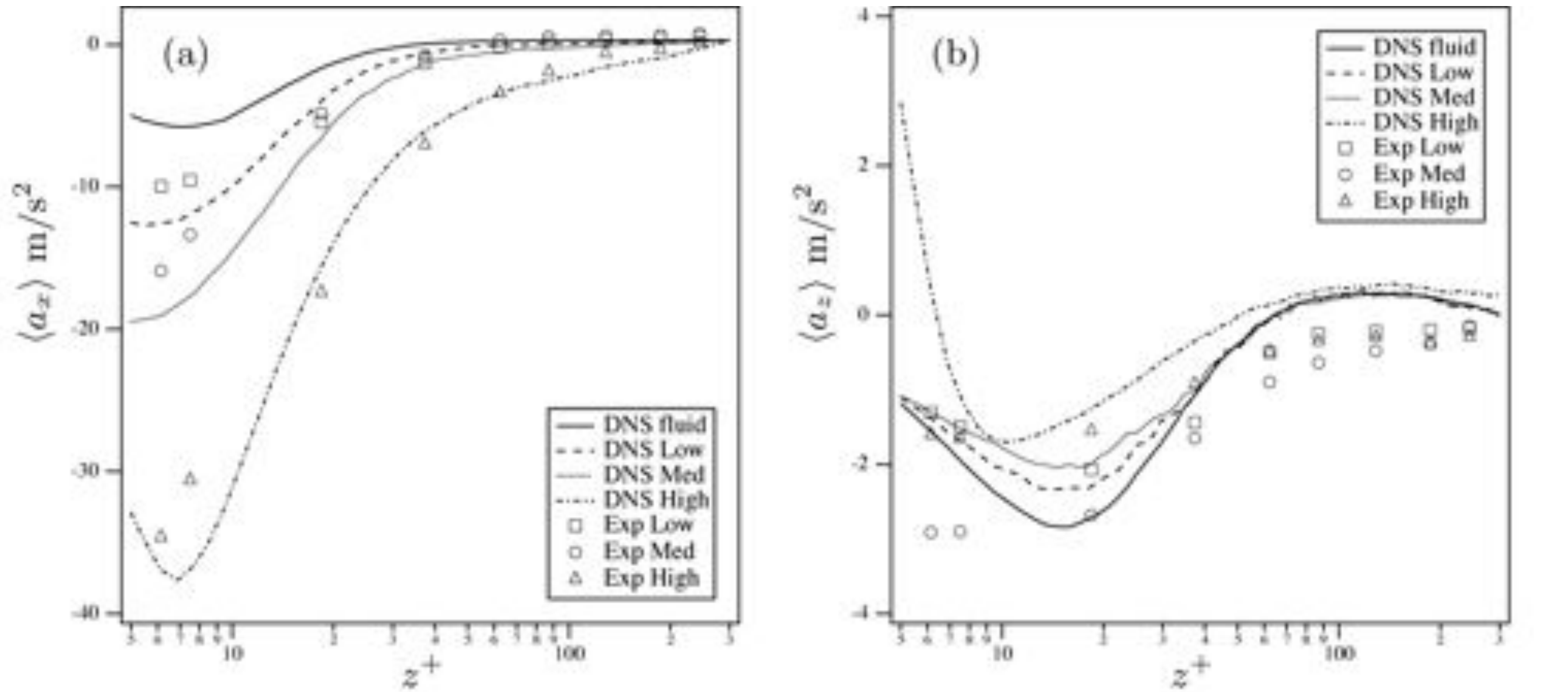

FIGURE 5. Mean particle acceleration in the (a) streamwise and (b) wall-normal directions as a function of z^+. Lines and symbols represent the simulation and experiments at low, medium and high Stokes numbers, as indicated (see table 1 for details).

Acceleration variance comparison

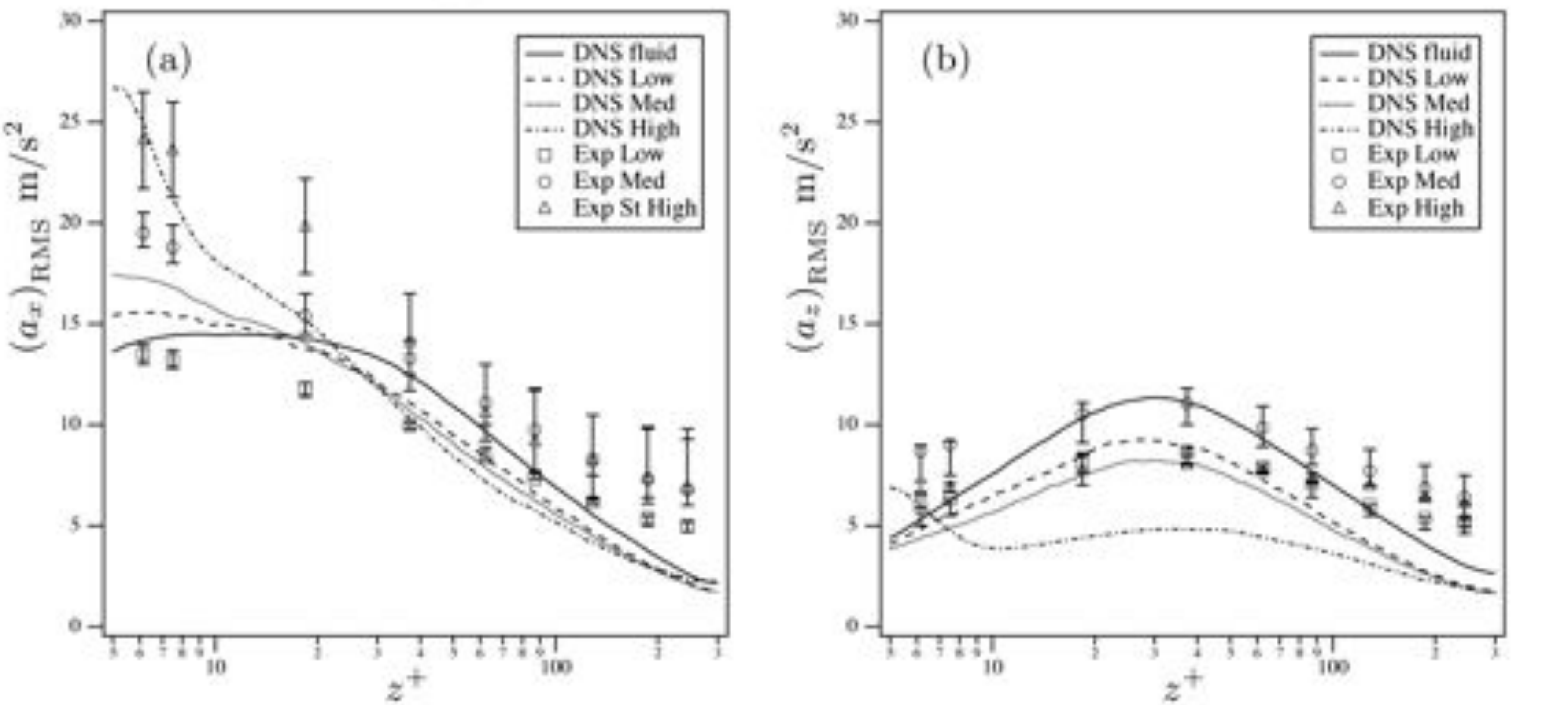

FIGURE 6. RMS of particle acceleration fluctuations in the (a) streamwise and (b) wall-normal directions as a function of z^+. Lines represent the DNS results and the symbols are from the experiments at low, medium and high Stokes numbers, as indicated.

Acceleration probability density functions (experiment vs DNS)

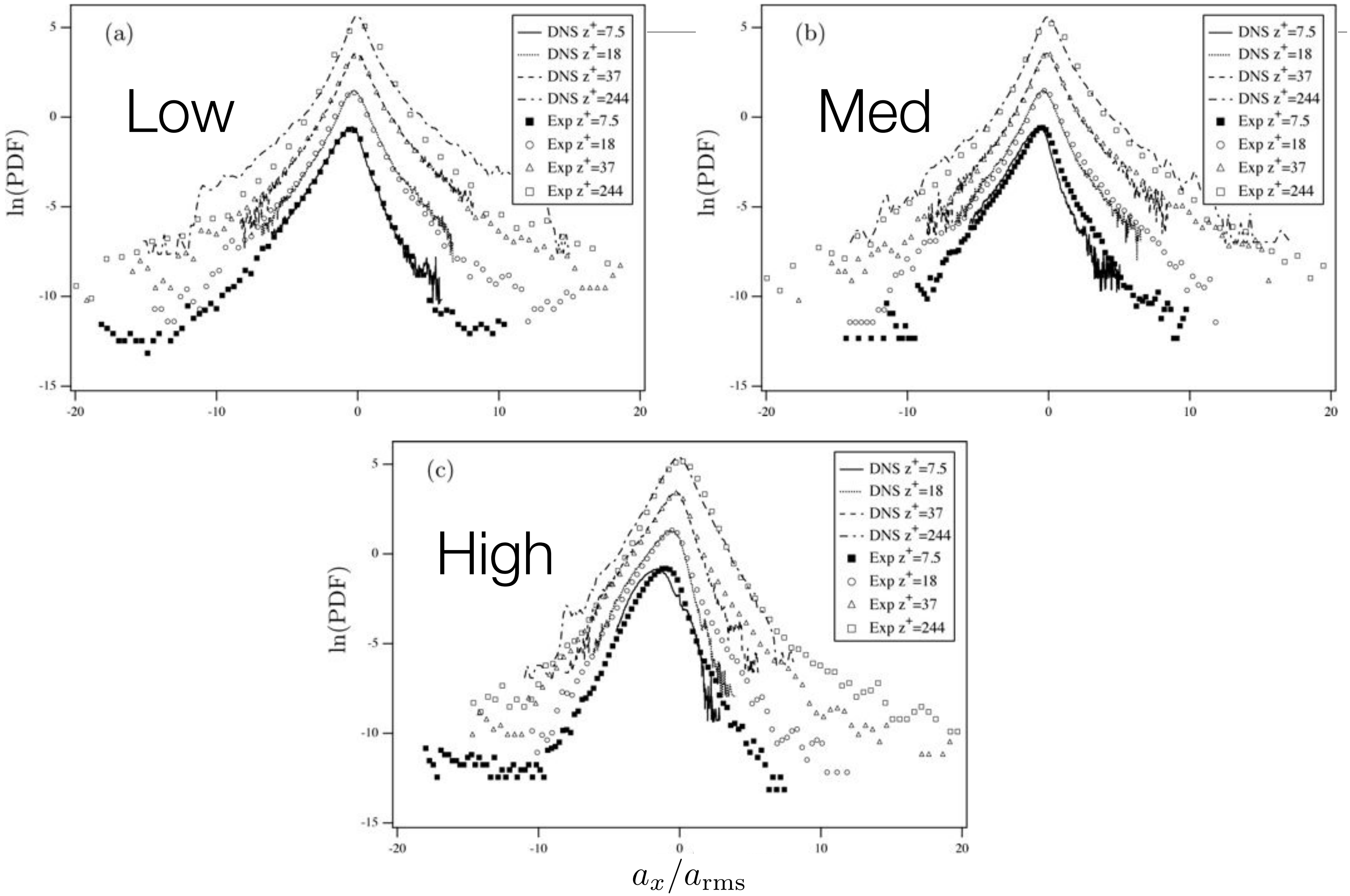

What is the role of gravitational settling and the mean shear?

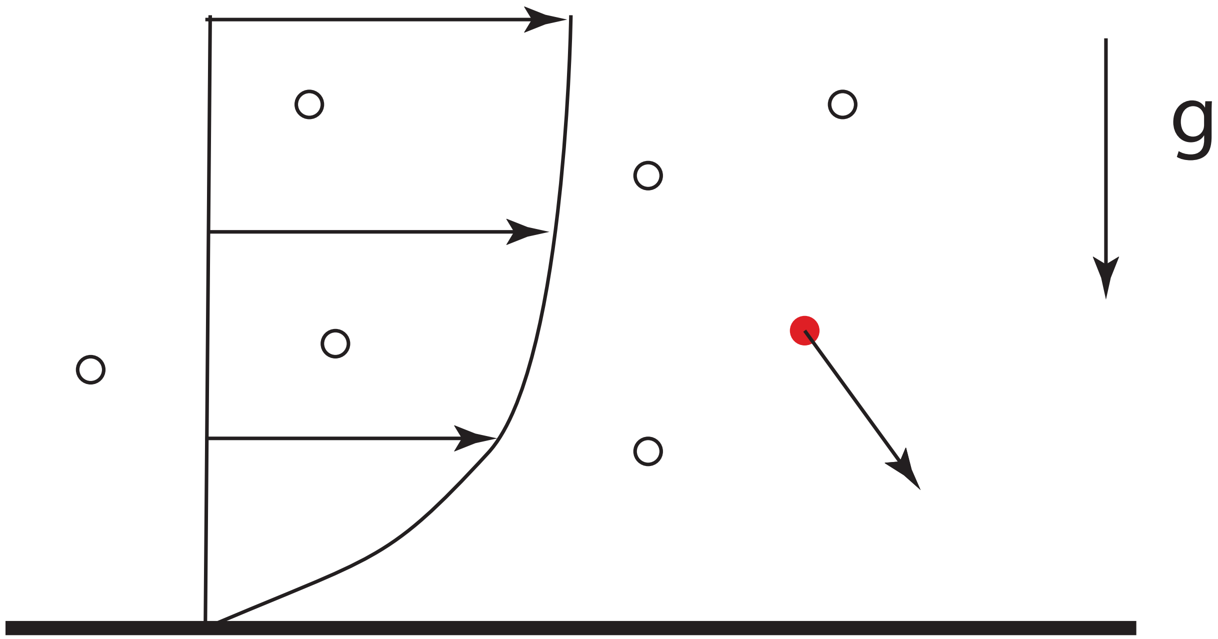

What is the role of gravitational settling and the mean shear?

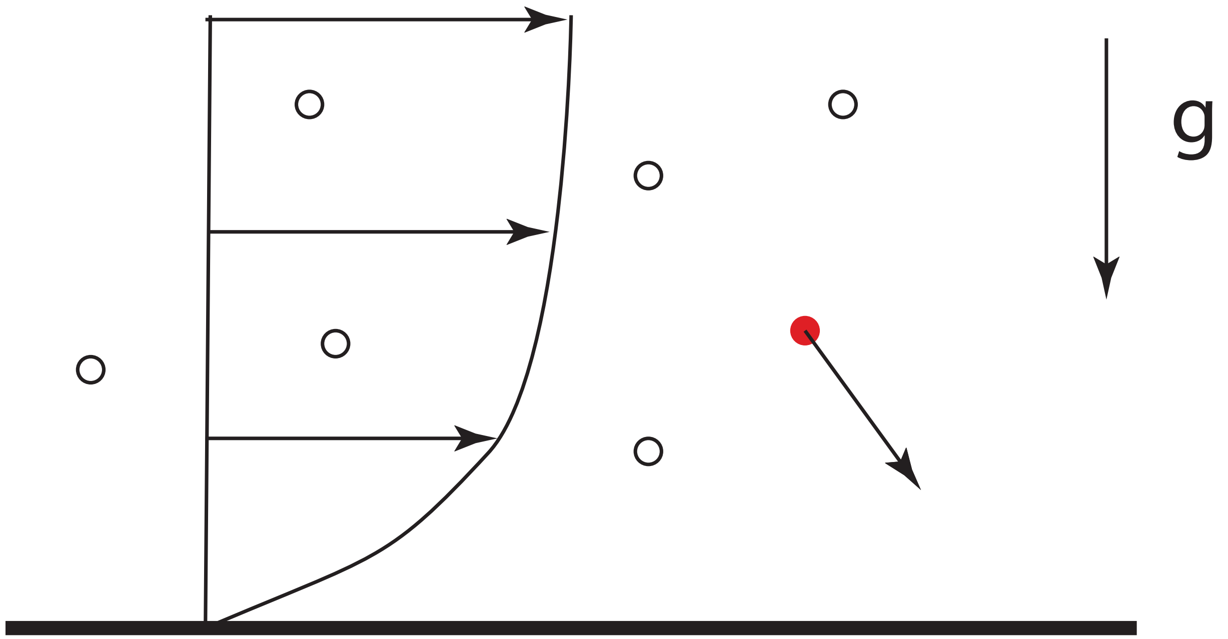

We can explore this by neglecting gravity in the particle motion

$$\frac{d\mathbf{v}}{dt} = \frac{[\mathbf{u}(\mathbf{x}) - \mathbf{v}]}{\tau_p}\left(1 + 0.15 Re_p^{0.687}\right) - \cancel{\left(1 - \frac{1}{\beta}\right)}\mathbf{g}$$

Acceleration mean and variance (no gravity)

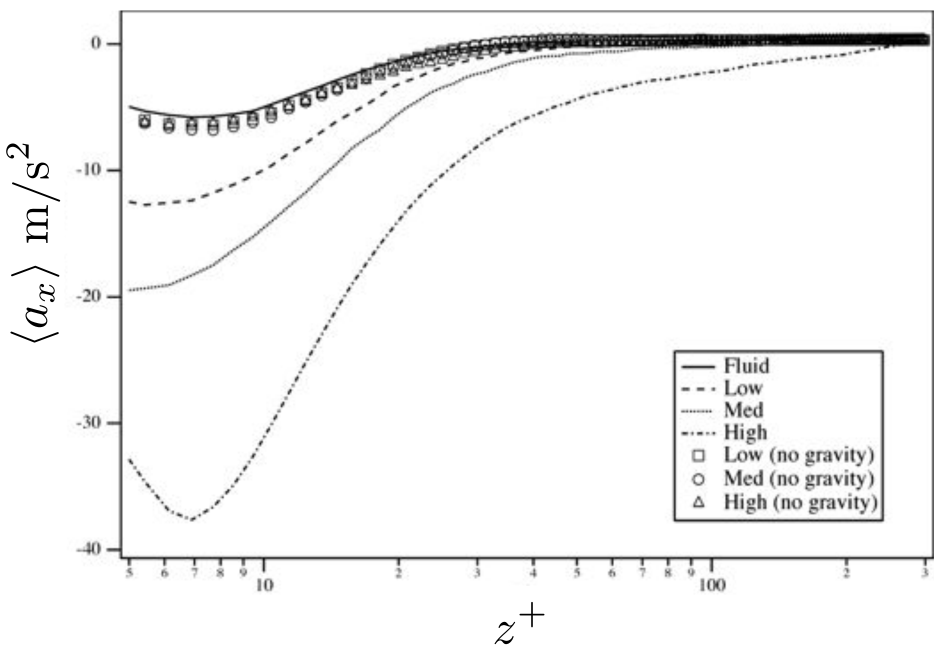

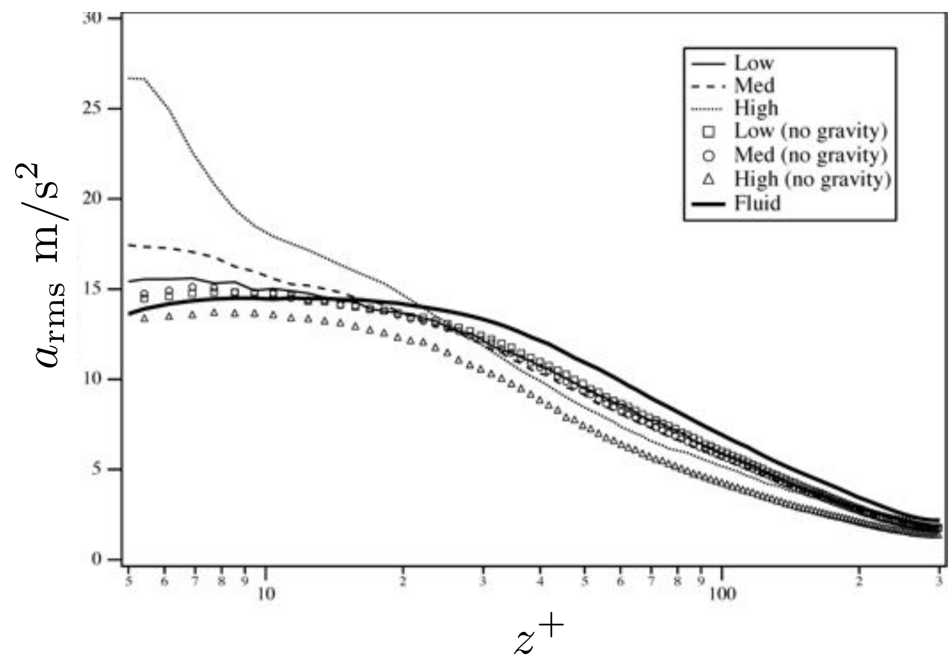

Lavezzo et al., *J. Fluid Mech.*, in review

Mean acceleration and Reynolds stress

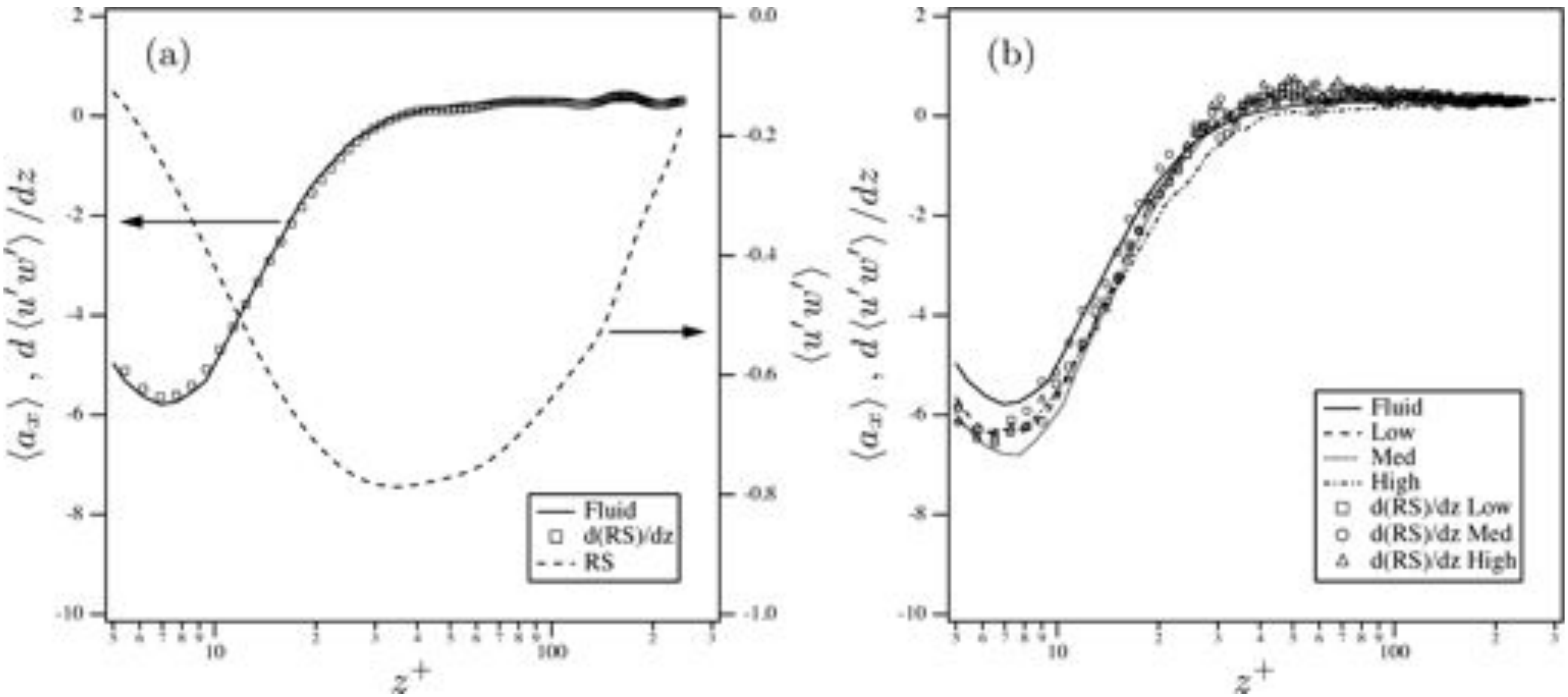

$$\langle a_x \rangle = \frac{d\langle u'w' \rangle}{dz} \qquad \langle a_{xp} \rangle = \frac{d\langle u'_p w'_p \rangle}{dz}$$

Lavezzo et al., *J. Fluid Mech.* (2010)

Effect of gravity on acceleration PDFs

$z^+ = 7.5$

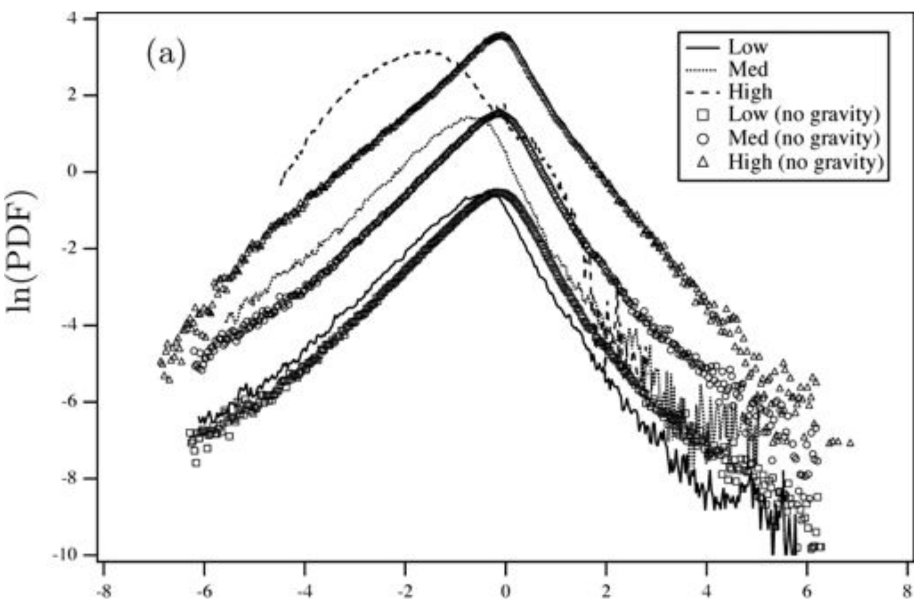

a_x / a_{rms}

$z^+ = 37$

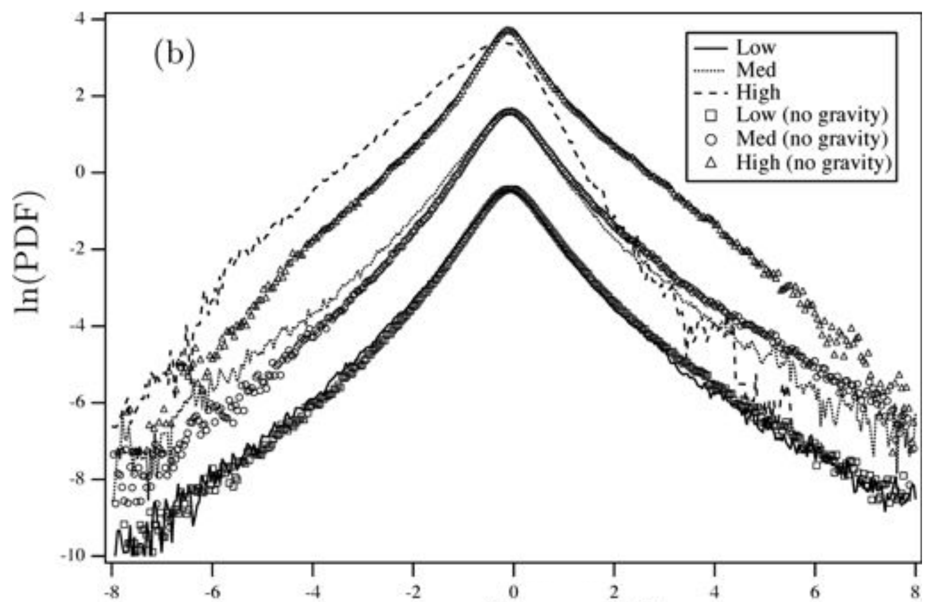

a_x / a_{rms}

Lavezzo et al., *J. Fluid Mech.* (2010)

Summary

- Direct numerical simulations of droplet acceleration statistics in channel flow are in good agreement with recent experiments in a boundary layer (mean, variance and PDFs).

- DNS allowed us to isolate the effect of gravity. We have demonstrated that the coupling of gravitational settling and the mean velocity gradient is responsible for

  - the dependence of the mean acceleration on Stokes number

  - reversal in the trend of the RMS with Stokes number (in the absence of gravity the trend in the RMS is consistent with isotropic turbulence)

- The study demonstrates some of the power of coordinated DNS and experimental studies of turbulence.

Entrainment experiment with and without gravity

Sergiy Gerashchenko, Garrett Good, Zellman Warhaft

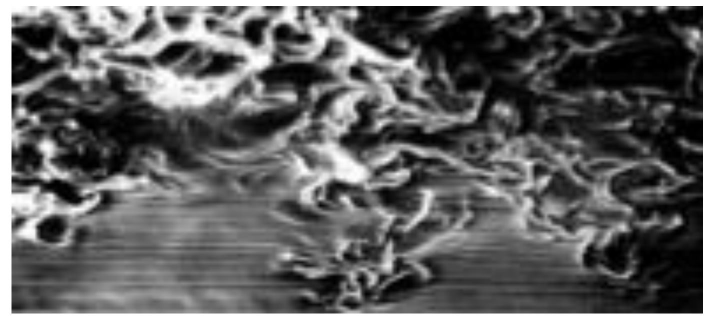

Veervali & Warhaft (1989)

Mixing of droplets across a turbulent non-turbulent interface (TNI)
Mixing of droplets across a turbulent turbulent interface (TTI)
Conditions such that evaporation and collision are negligible

Re_λ	$U(m/s)$	$u_{rms}(m/s)$	$v_{rms}(m/s)$	$TI(\%)$	$\epsilon(m^2/s^{-3})$	$\eta(mm)$
275(12)	2.15(0.05)	0.31(0.01)	0.24(0.01)	14.4(0.8)	0.138(0.006)	0.397(0.006)

$\tau_\eta(s)$	$\lambda(cm)$	$l(cm)$	St_η	St_l	Fr
0.0105(0.0003)	1.3(0.04)	24(2)	0.2(0.03)	0.0028(0.0001)	0.54(0.01)

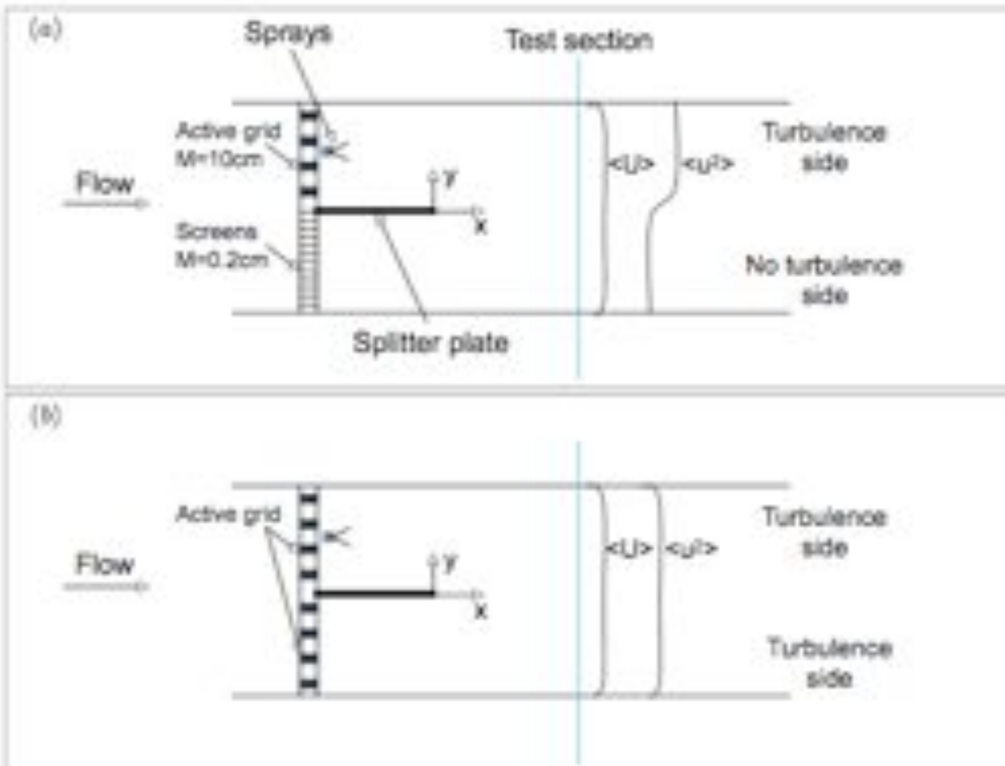

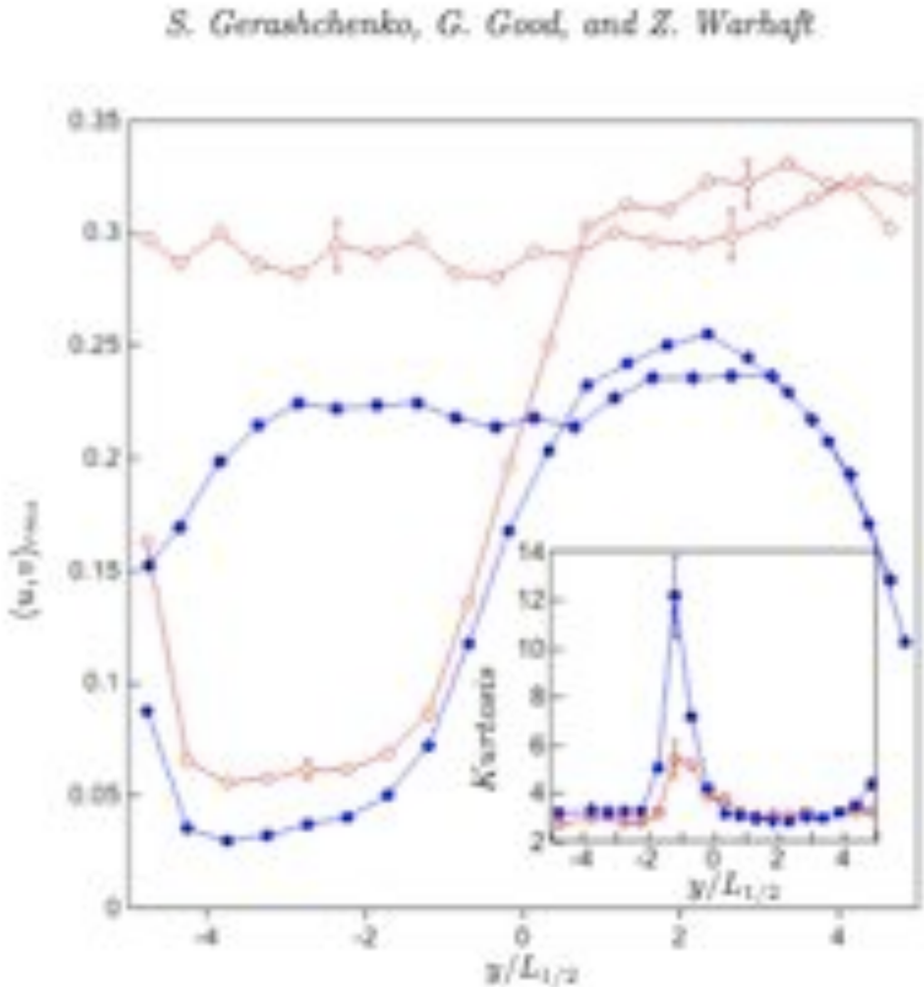

RMS velocity and 4th moment from HWA

Concentration profiles for TTI (squares) and TNI (circles); Red with g, Blue no g

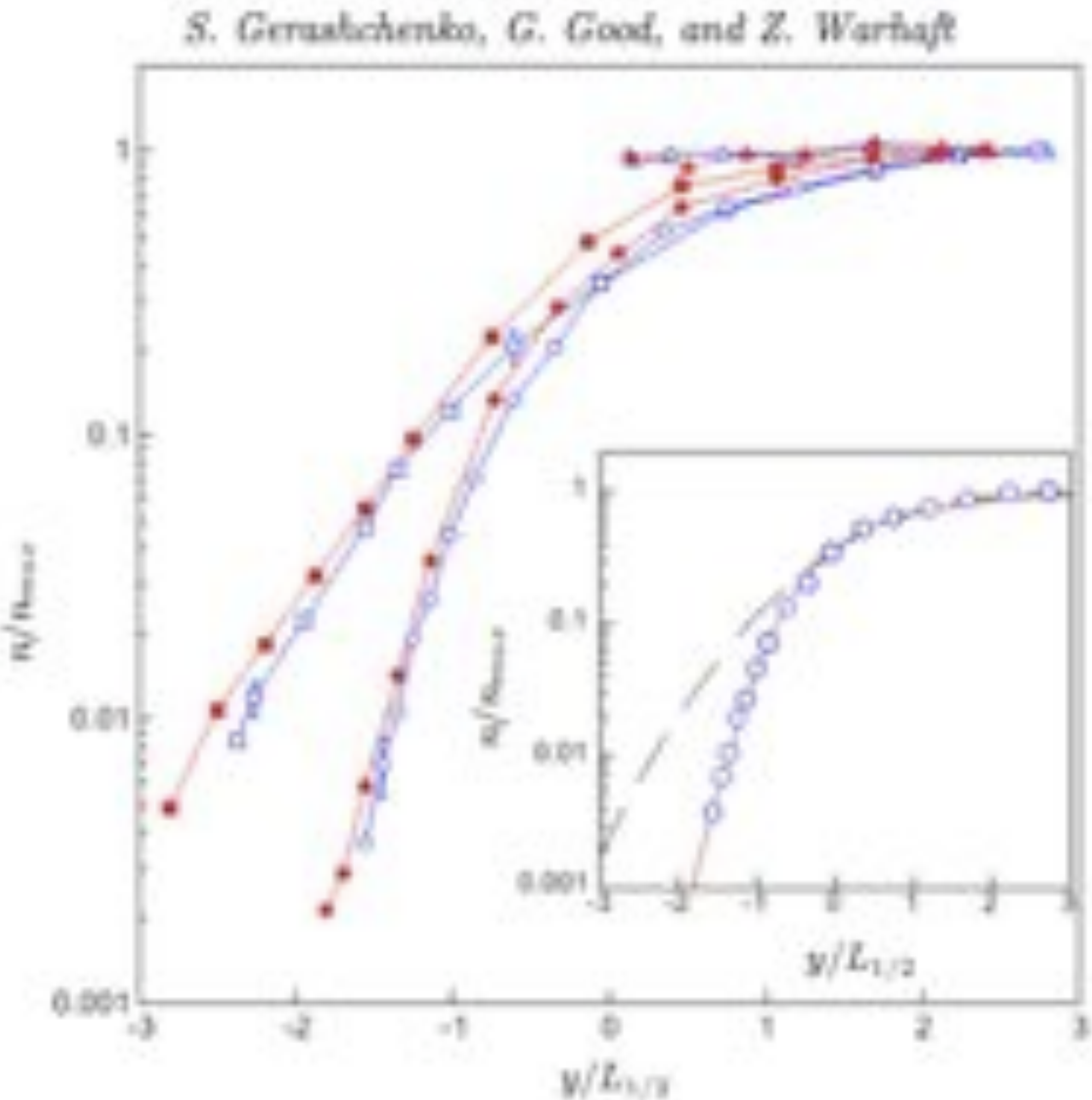

DNS Strategy (Peter Ireland and L R Collins)

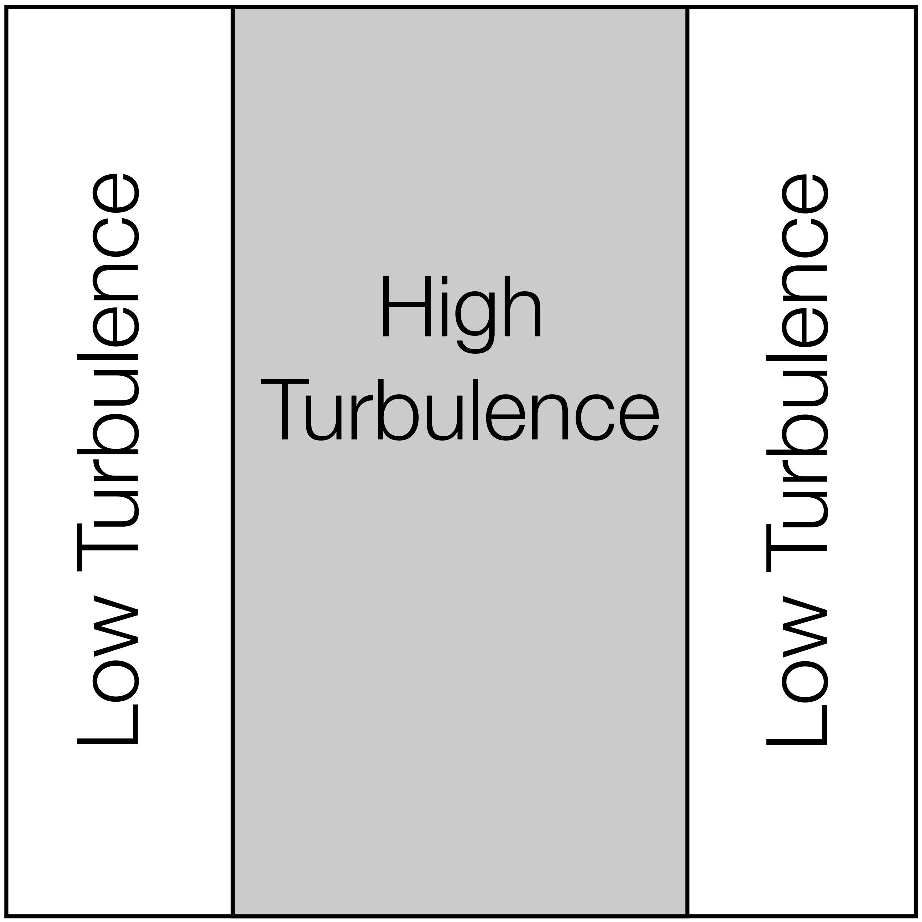

Particle Concentration Profiles

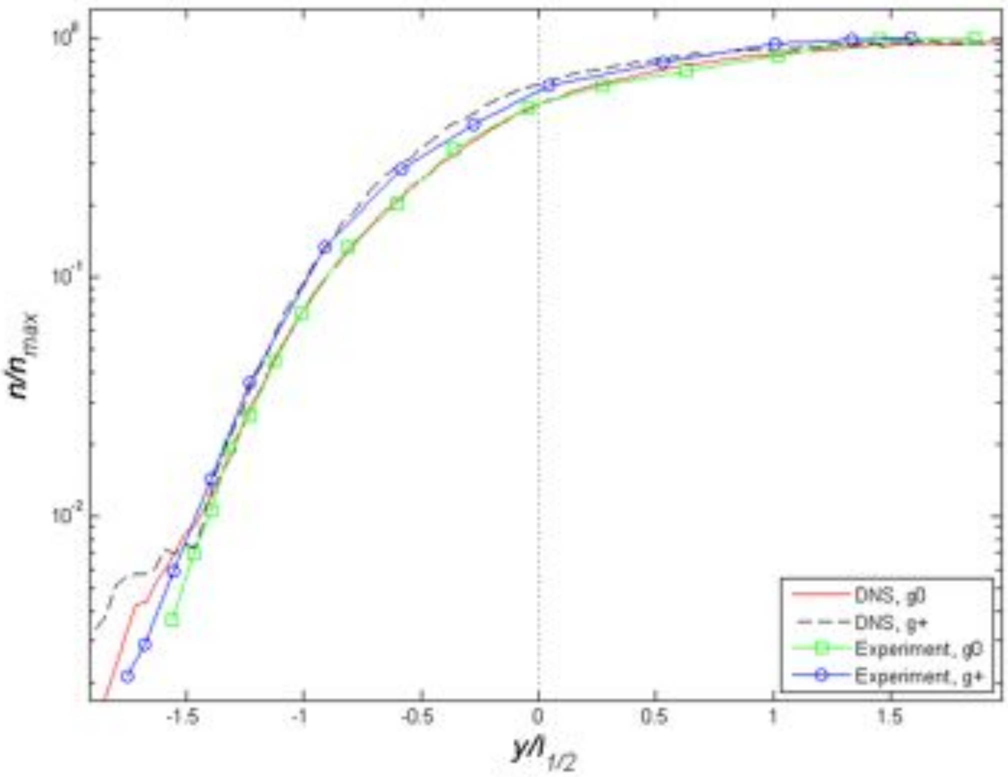

Summary of Preliminary Entrainment Experiments

- Particle mixing resembles that of a passive scalar (appropriate Stokes number is defined in terms of the large eddy turnover time)
- Gravitational settling does effect mixing rates
- DNS with a turbulent non-turbulent interface can mimic experiment
- Plan to perform Lagrangian tracking experiments of particles crossing the interface

Summer School

"Turbulence and fluctuations in the microphysics and dynamics of clouds"

Porquerolles, France

September 1-10, 2010

Integration of simulations, experiments *and theory* to study inertial particles in turbulence: <u>two-particle statistics</u>

Lance R. Collins
Cornell University

Topics

Talk 1: Discuss how simulations and experiments have helped us understand the motion of a single inertial particle in turbulence.

Talk 2: Discuss the motion of particle pairs in turbulence with the goal of analyzing the interparticle collision rate.

- Background on collision
- RDF and relative velocity PDF in isotropic turbulence (DNS then experiments)
- Clustering in the Lagrangian frame
- 2nd order structure function and “caustics”
- Effect of velocity filtering (towards LES)

Comprehensive Strategy

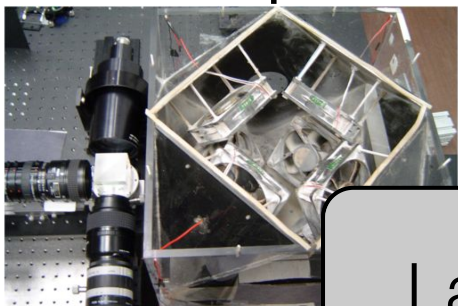

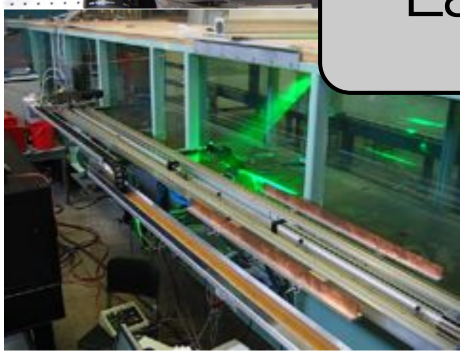

Laboratory

DNS

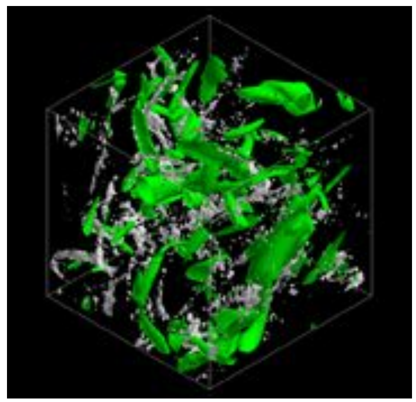

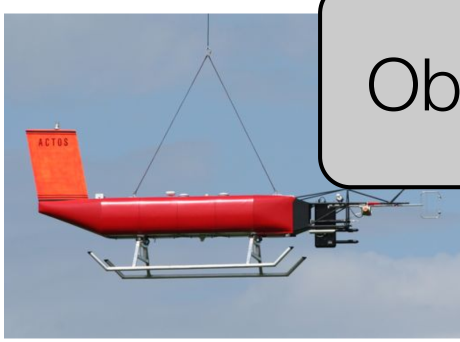

Observations

Modeling

- RANS
- LES

Generalized Collision Kernel

$$N_{ij}^{C} = 4\pi\sigma_{ij}^{2} n_i n_j g_{ij}\left(\sigma_{ij}\right) \int_{-\infty}^{0} -w_r P_{ij}\left(w_r|\sigma_{ij}\right) dw_r$$

$$n_i = \text{number of i} - \text{mers}$$

$$g_{ij}(r) = \text{radial distribution function}$$

$$P_{ij}(w_r|r) = \text{relative velocity PDF conditioned on } r$$

$$\sigma_{ij} = \left(\sigma_i + \sigma_j\right)/2 = \text{collision diameter}$$

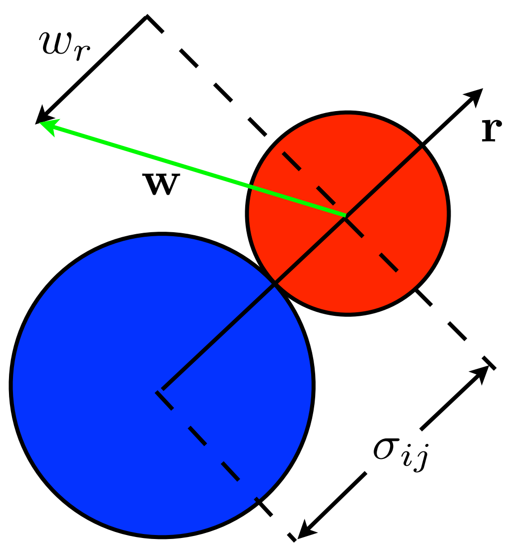

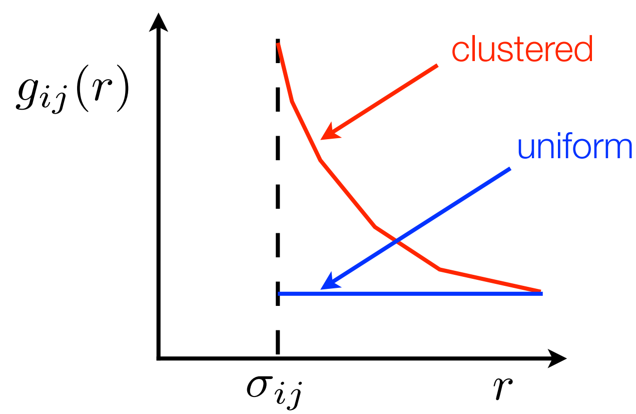

Sundaram & Collins, JFM 335, 75 (1997)
Wang et al. PoF 10:266 (1998)

Direct Numerical Simulation

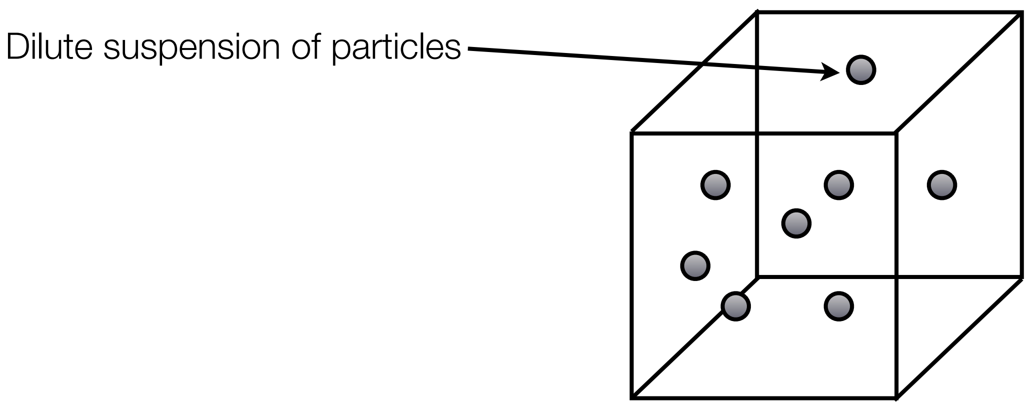

$$\frac{d\mathbf{x}}{dt} = \mathbf{v}$$

$$\frac{d\mathbf{v}}{dt} = \frac{[\mathbf{u}(\mathbf{x}) - \mathbf{v}]}{\tau_p} + \mathbf{g}$$

$$\tau_p \equiv \frac{\rho_p d^2}{18\mu}$$

$$\nabla \cdot \mathbf{u} = 0$$

$$\frac{\partial \mathbf{u}}{\partial t} + \mathbf{u} \cdot \nabla \mathbf{u} + \frac{\nabla p}{\rho} = \nu \nabla^2 \mathbf{u} + \mathbf{F}$$

Particle-particle Interactions

Elastic Rebound

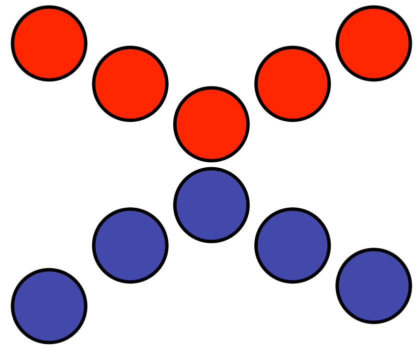

Coalescence

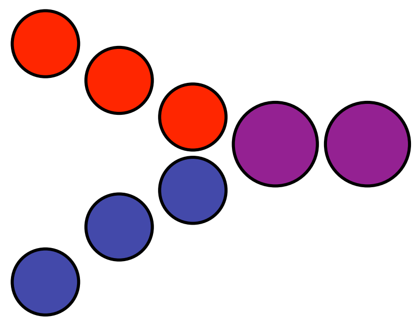

Ghost

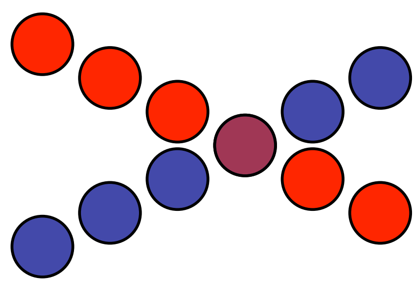

Parameters

U'	turbulence intensity	d	diameter
ϵ	dissipation rate	ρ_p	density
ν	kinematic viscosity	n	number density

$$R_\lambda \equiv {U'}^2 \sqrt{\frac{15}{\nu\epsilon}}$$

$St \equiv \dfrac{\tau_p}{\tau_\eta}$ Stokes number

d/η size parameter

Φ volume fraction

$S_v \equiv \dfrac{v_T}{u_\eta}$ settling parameter

Parameters

U'	turbulence intensity	d	diameter
ϵ	dissipation rate	ρ_p	density
ν	kinematic viscosity	n	number density

$$R_\lambda \equiv {U'}^2 \sqrt{\frac{15}{\nu\epsilon}}$$

$$St \equiv \frac{\tau_p}{\tau_\eta}$$ Stokes number

understood $\longrightarrow$ $\cancel{d/\eta}$ ~~size parameter~~

neglected $\longrightarrow$ $\cancel{\Phi}$ ~~volume fraction~~

$$St \propto \epsilon^{1/2}$$

$$S_v \propto \epsilon^{-1/4}$$

$$S_v \equiv \frac{v_T}{u_\eta}$$ settling parameter

Cloud parameters

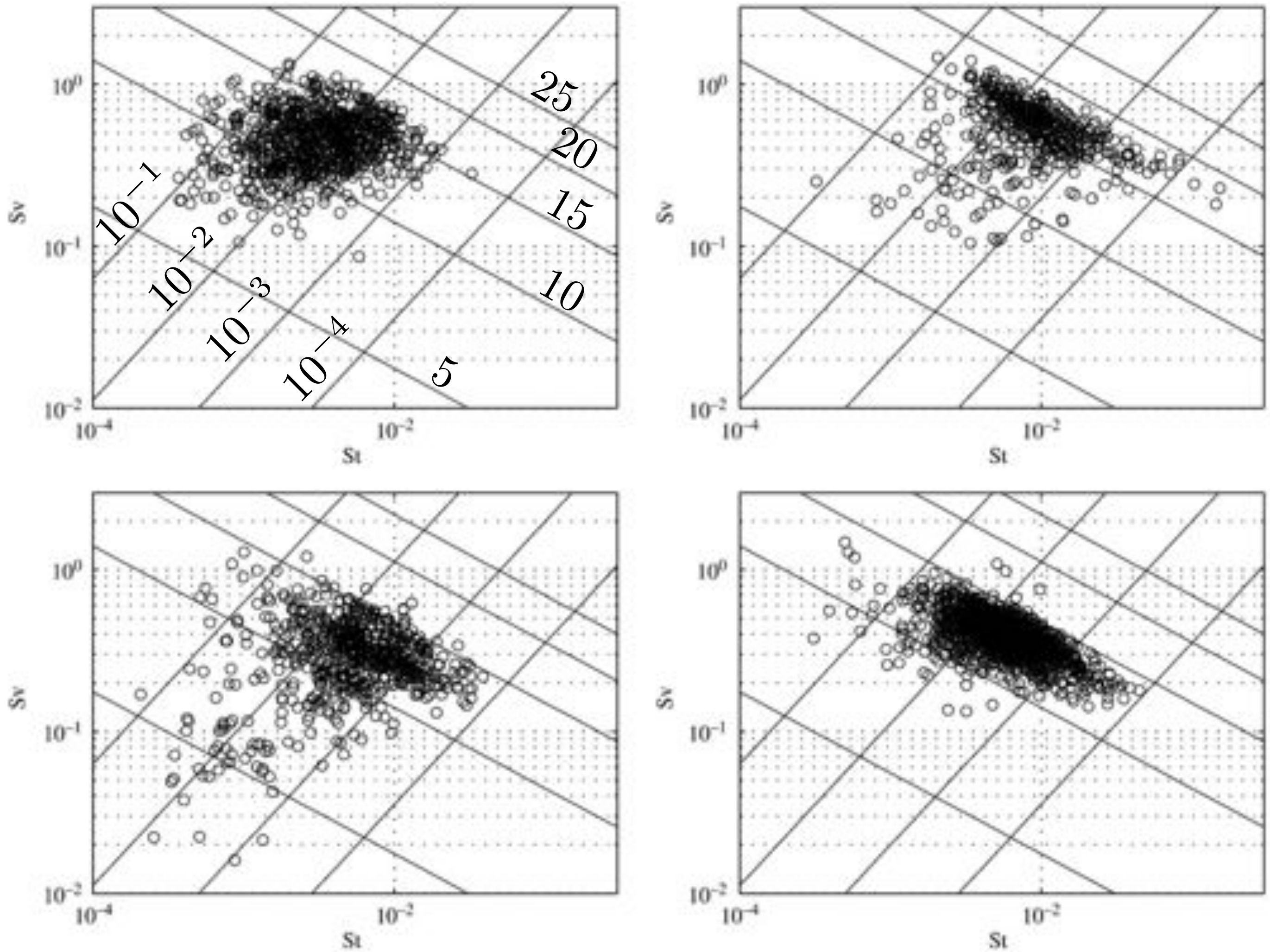

Fig. 9. The distribution of cloud microphysical and turbulence properties in a dimensionless Stokes–settling parameter space. The upper left plot is for a stratocumulus cloud and the remaining three are for small cumulus clouds. Each point represents data in a 1-second (approximately 15 m) average. Diagonal lines with positive slope are contours of constant turbulent energy dissipation rate, ε, at values of 10^{-4}, 10^{-3}, 10^{-2}, and 10^{-1} (lower right to upper left corners). Diagonal lines with negative slope are contours of constant droplet diameter at values of 5, 10, 15, 20 and 25 μm (lower left to upper right corners).

Limiting theories for turbulent collision

Saffman & Turner (1956)
zero Stokes number

$$N_c = \frac{1}{2} n^2 d^3 \left(\frac{8\pi\epsilon}{15\nu} \right)^{1/2}$$

Abrahamson (1975)
infinite Stokes number

$$N_c = \frac{1}{2} n^2 d^2 \left(\frac{16\pi\langle v^2 \rangle}{3} \right)^{1/2}$$

$$n = \text{number density}$$

$$\frac{1}{2}\langle v^2 \rangle = \text{particle energy}$$

Collision vs Stokes number

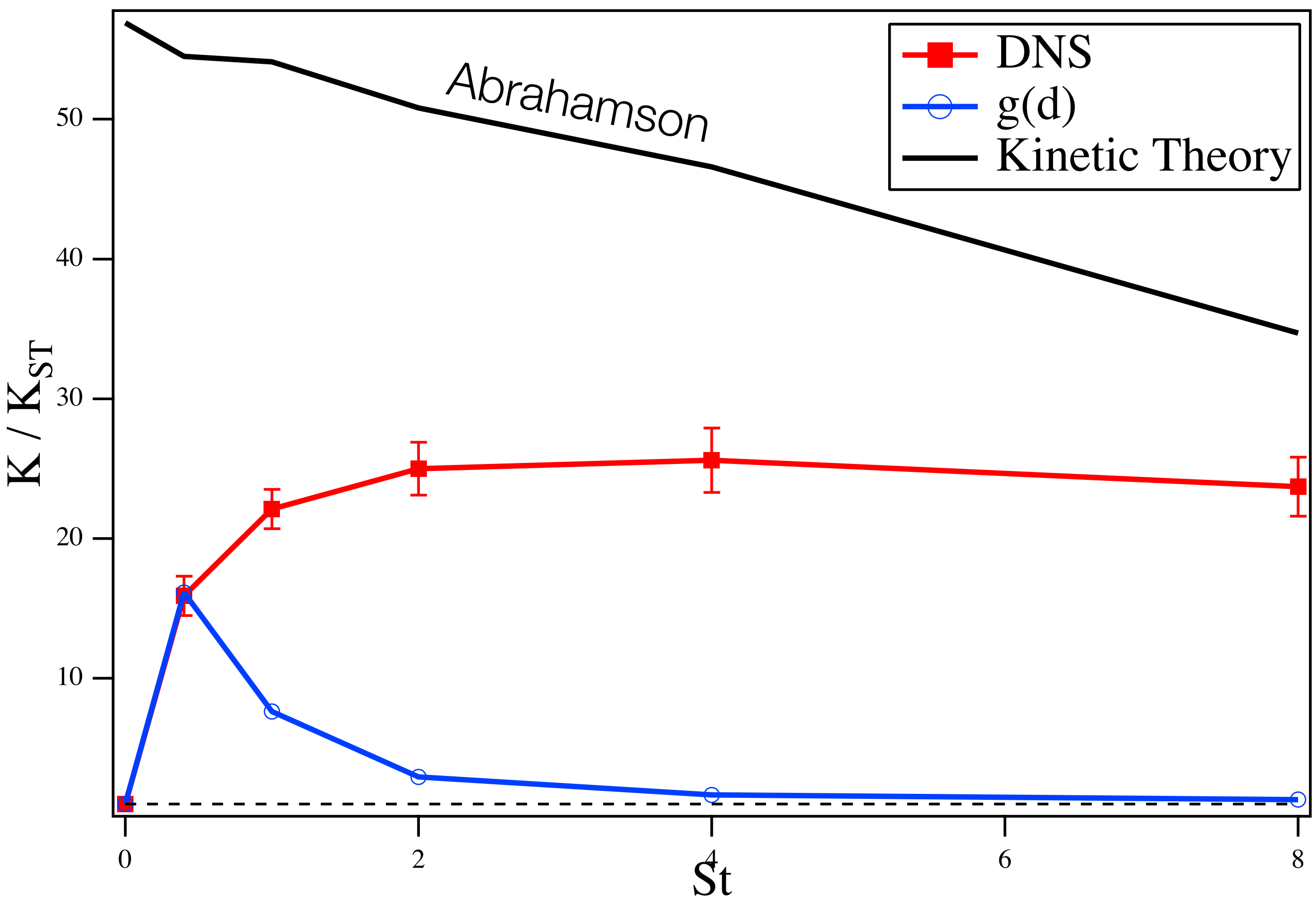

Sundaram & Collins (1997)

Evolution of the size distribution

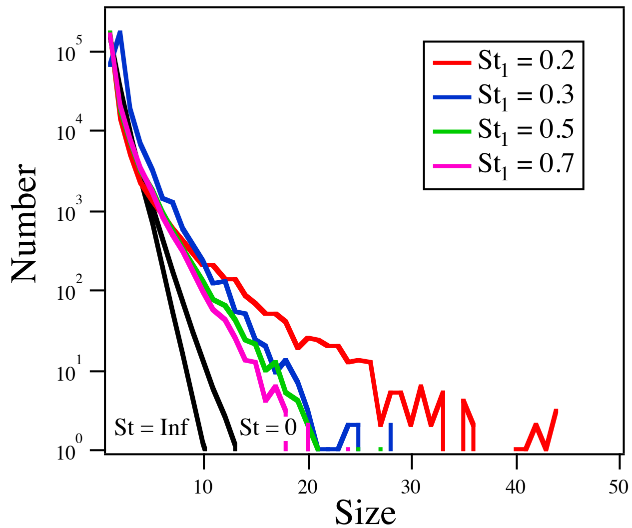

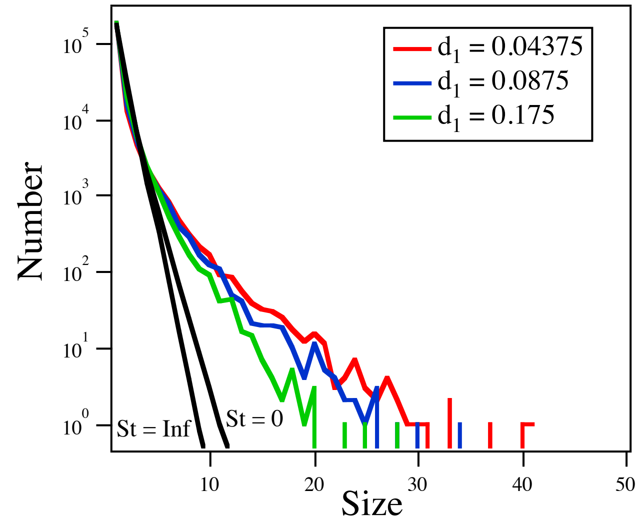

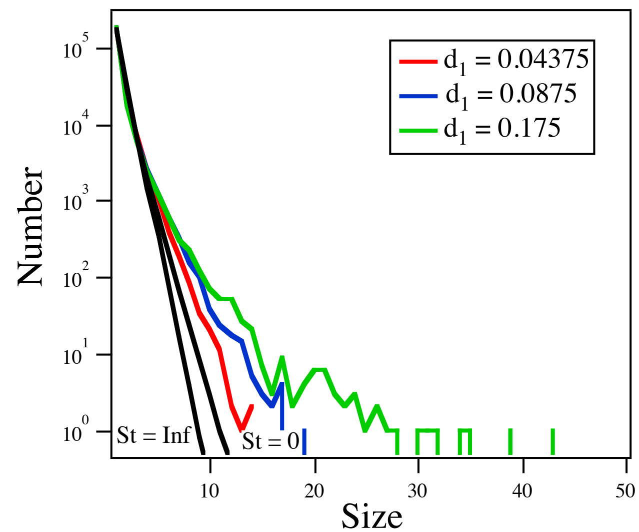

Reade & Collins (2000)

Radial Distribution Function (RDF)

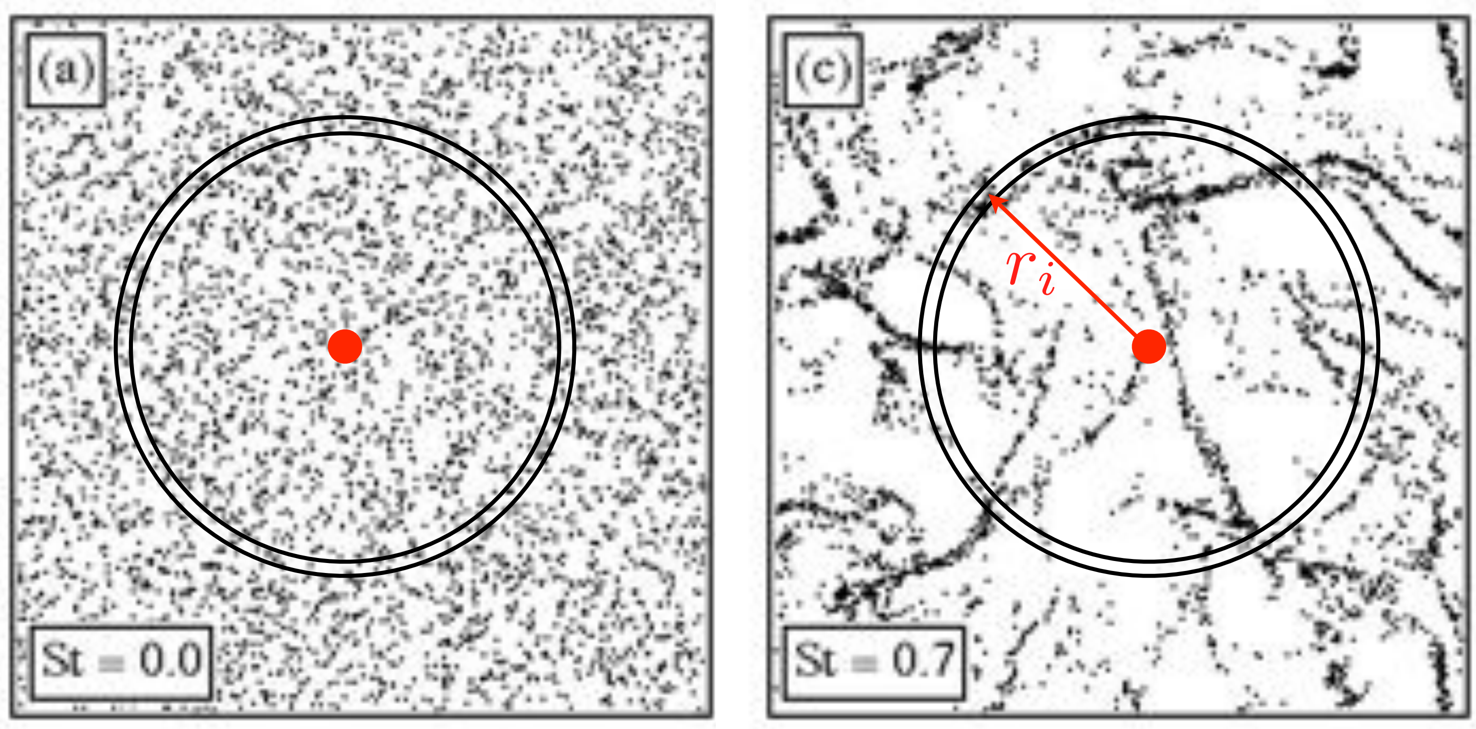

$$g\left(r_i\right) \equiv \frac{N_i/\Delta V_i}{N/V}$$

Sundaram & Collins 1997

Stokes Number Dependence

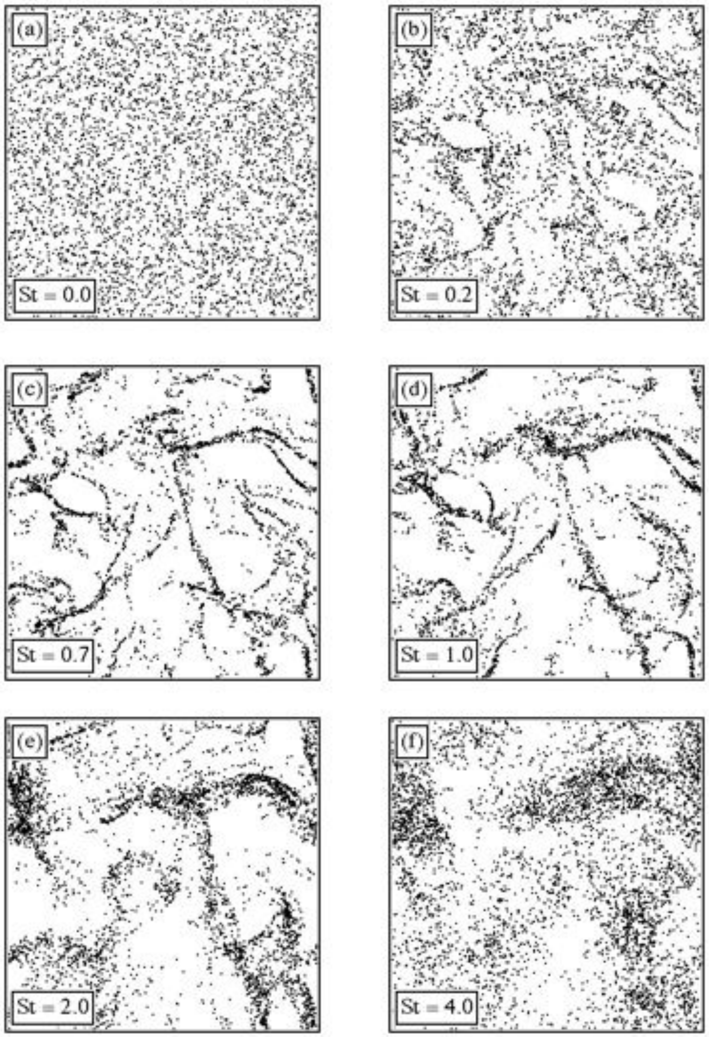

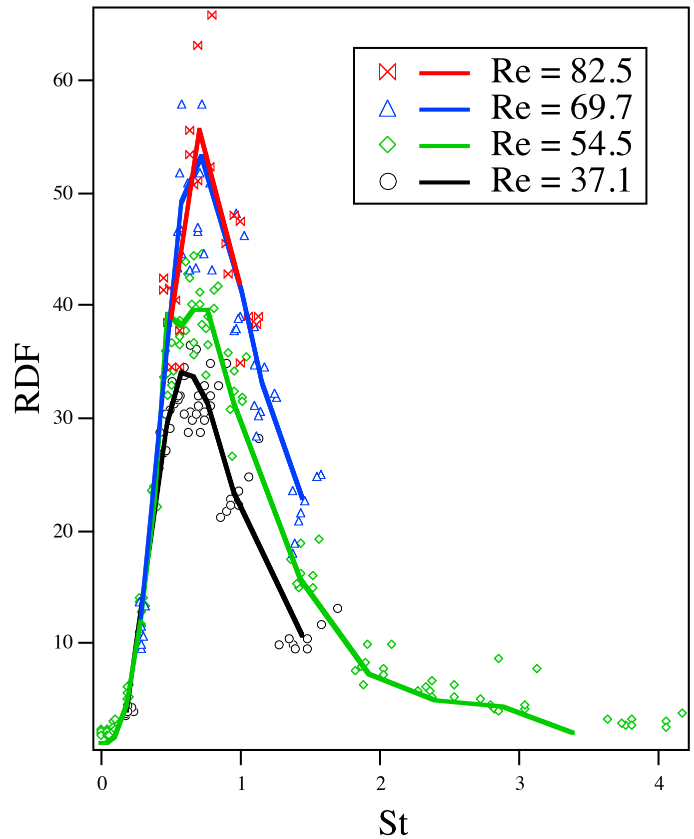

Reade & Collins (2000)

Bi-disperse RDFs

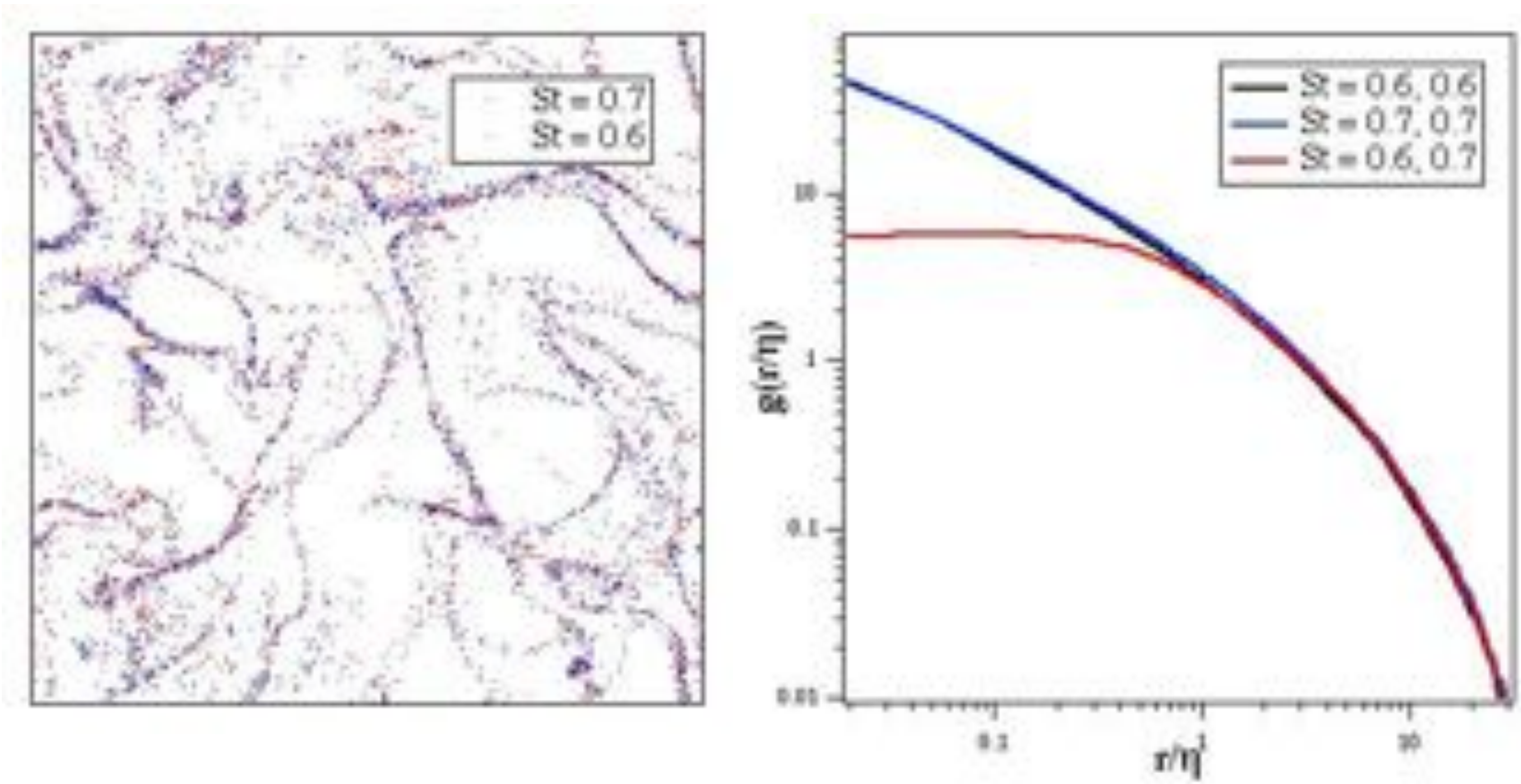

Reynolds number dependence

St = 0.4

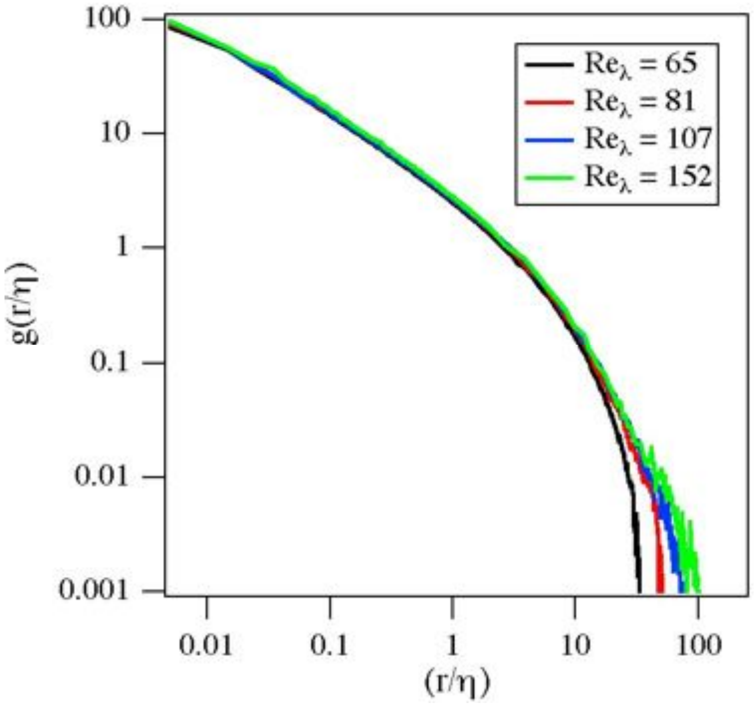

St = 0.7

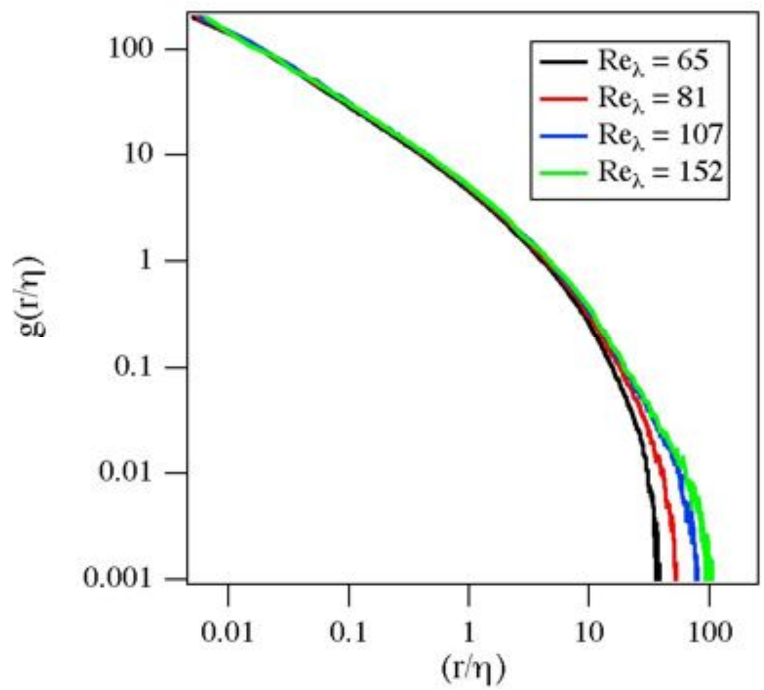

Keswani & Collins 2004

Experimental Turbulence Chamber

Hui Meng
SUNY Buffalo

Isotropic Turbulence Chamber

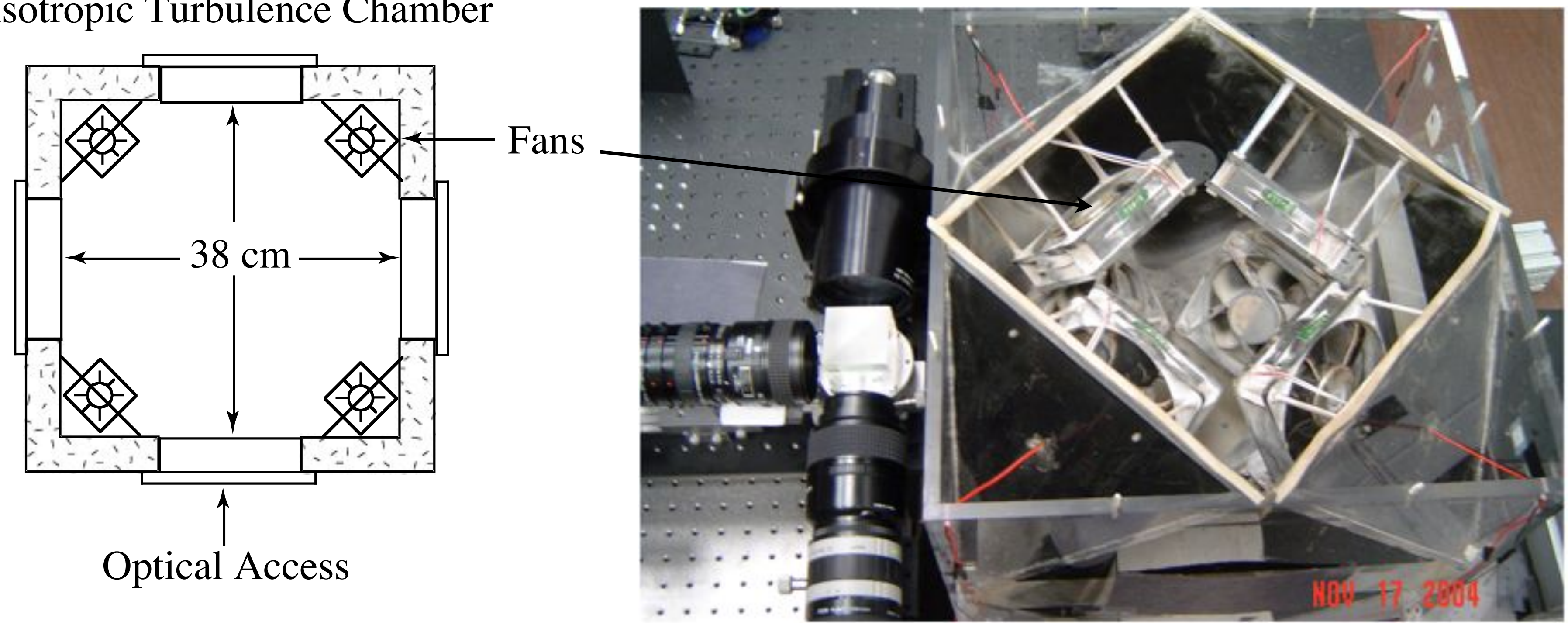

de Jong, Cao, Salazar, Collins, Woodward & Meng 2008

Exp Fluids (2009) 46:499–515
DOI 10.1007/s00348-008-0576-3

RESEARCH ARTICLE

Dissipation rate estimation from PIV in zero-mean isotropic turbulence

J. de Jong · L. Cao · S. H. Woodward ·
J. P. L. C. Salazar · L. R. Collins · H. Meng

Fit a 2nd-order structure function

$$D_{LL}(r) \approx C_2 \, (\epsilon r)^{2/3}$$

$$\text{Errors} \approx 20\%$$

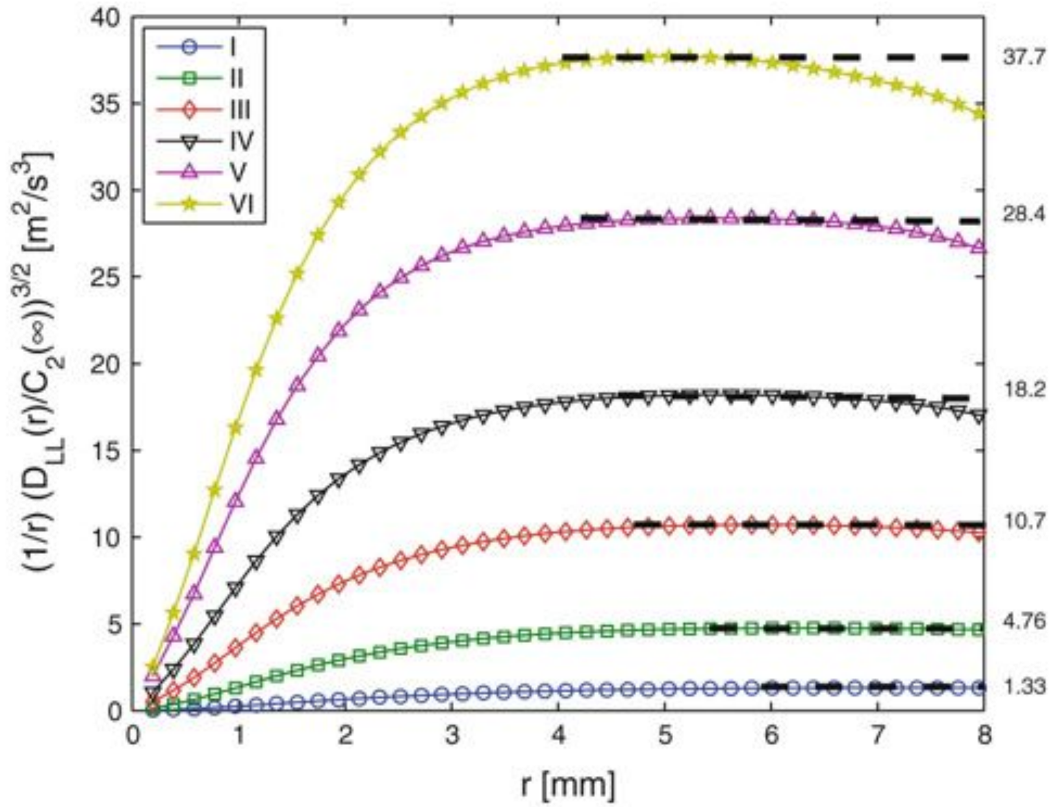

Fig. 6 Compensated second-order longitudinal velocity structure functions $D_{\mathrm{LL}}(r)$ for the six flow conditions defined in Fig. 1

J. Fluid Mech. (2002), *vol.* 459, *pp.* 93–102. © 2002 Cambridge University Press
DOI: 10.1017/S0022112002008169 Printed in the United Kingdom

Relationship between the intrinsic radial distribution function for an isotropic field of particles and lower-dimensional measurements

By GRETCHEN L. HOLTZER AND LANCE R. COLLINS†

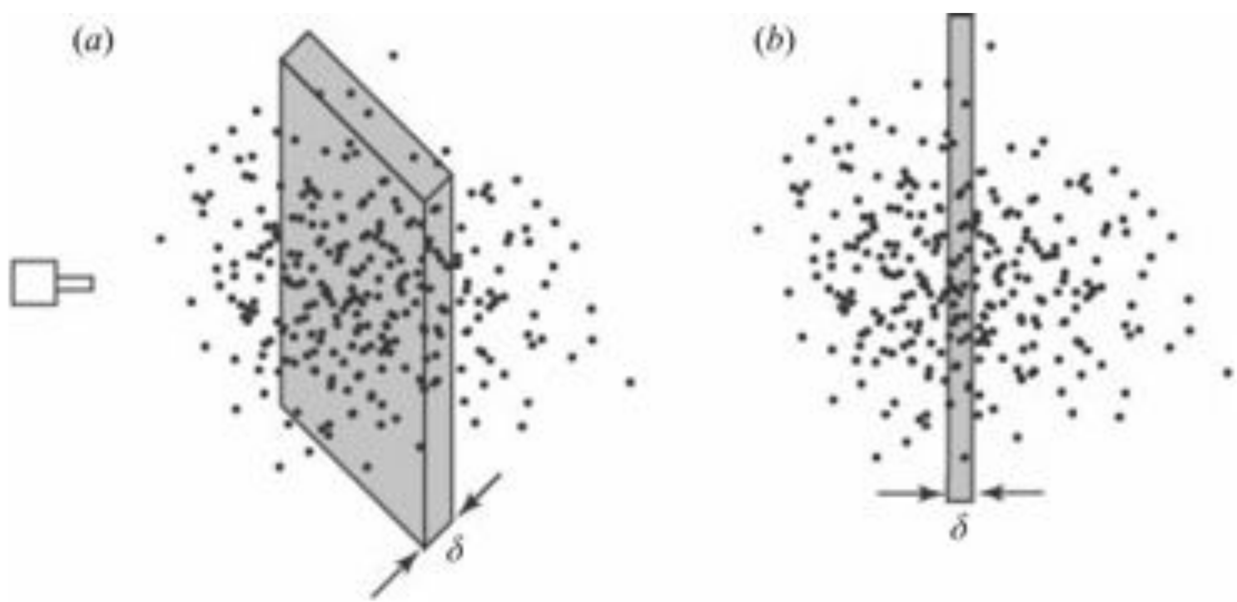

FIGURE 1. Schematic of (*a*) a two-dimensional laser sheet of thickness δ going through a three-dimensional particle field, and (*b*) a one-dimensional sampling of the same particles using a probe of cross-section δ^2.

$$g_{2D}(\epsilon_i) = 2\int_0^1 (1-v)g_{3D}\left(\sqrt{\epsilon_i^2+v^2}\right)dv \qquad \epsilon_i \equiv \frac{r_i}{\delta} \quad v \equiv \frac{x}{\delta} \quad w \equiv \frac{y}{\delta}$$

$$g_{1D}(\epsilon_i) = 4\int_0^1\int_0^1 (1-v)(1-w)g_{3D}\left(\sqrt{\epsilon_i^2+v^2+w^2}\right)dvdw$$

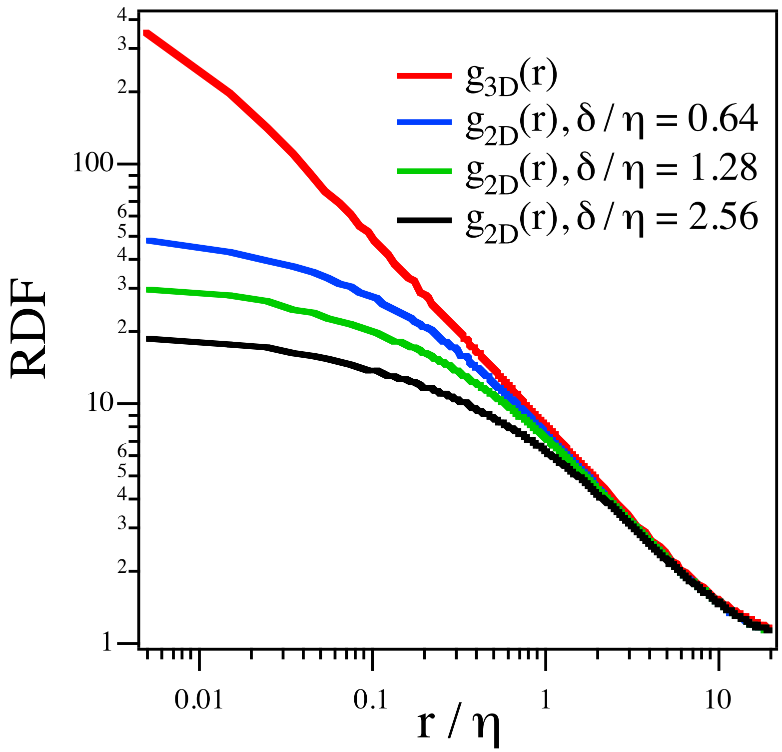

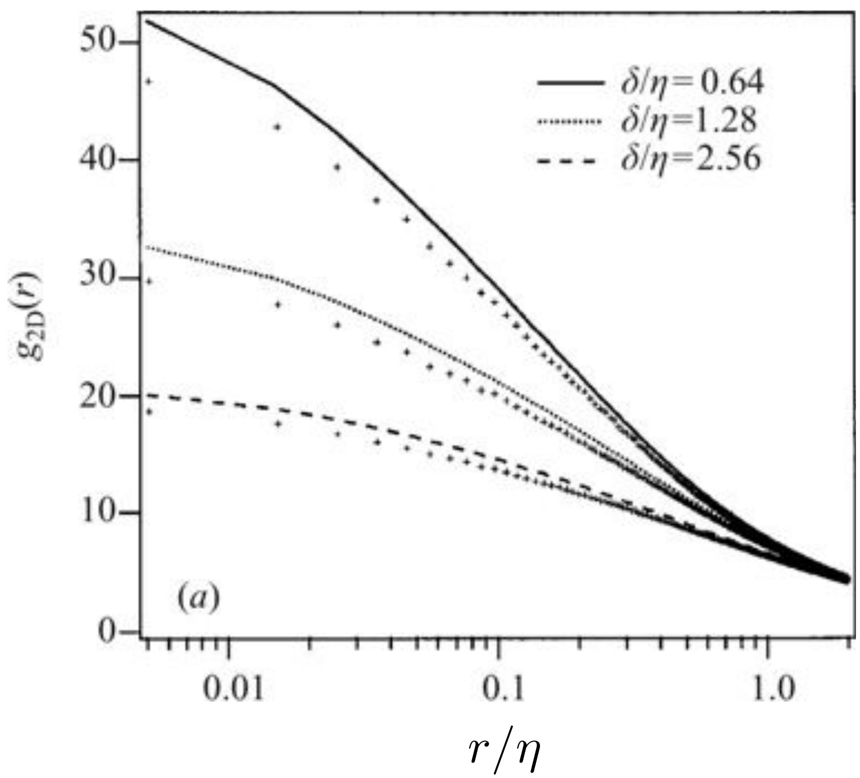

Holographic Imaging

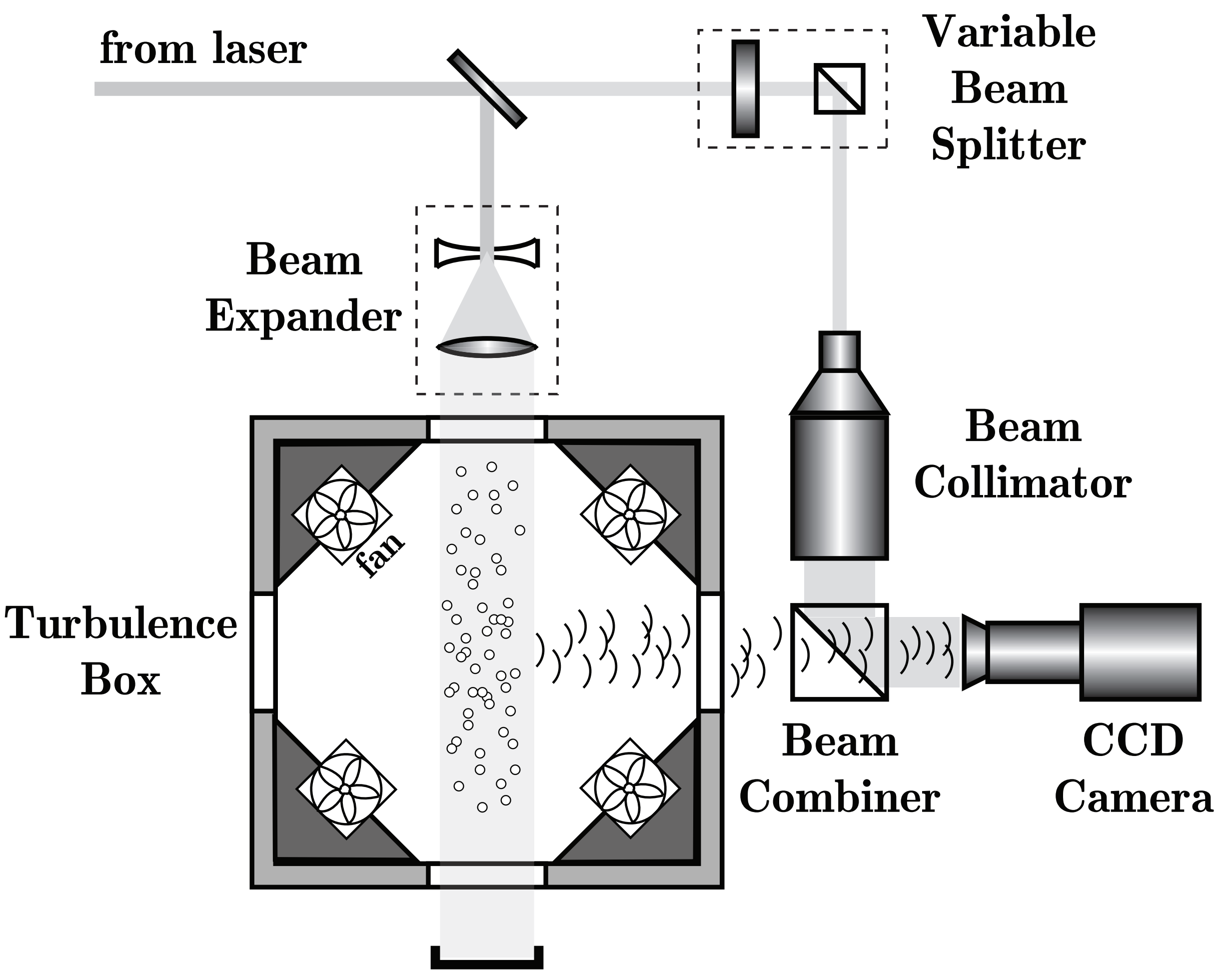

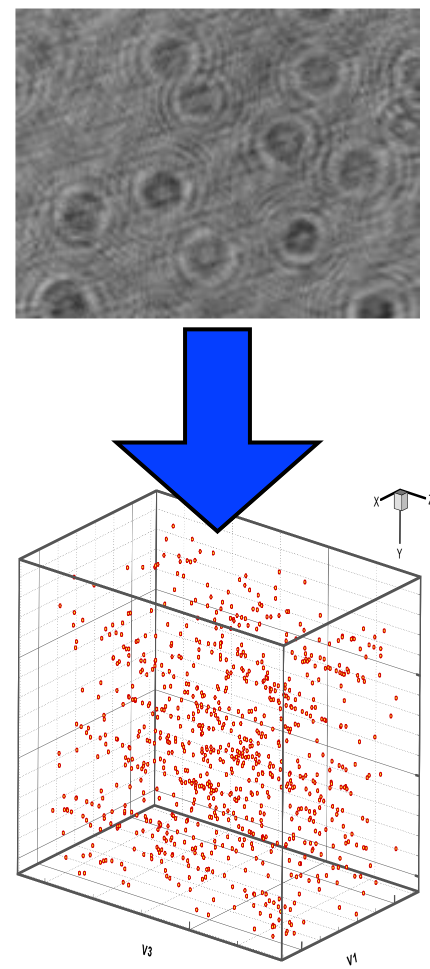

Meng, Pan & Pu 2004

Reconstructed “particle”

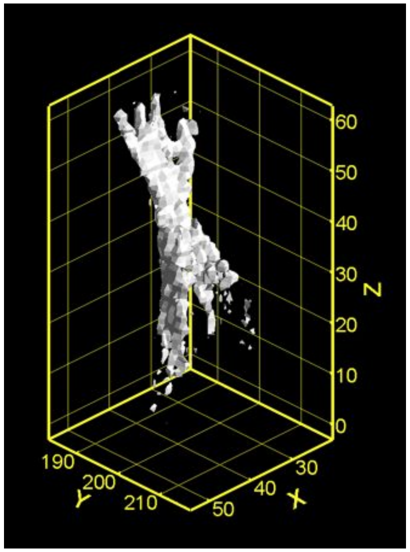

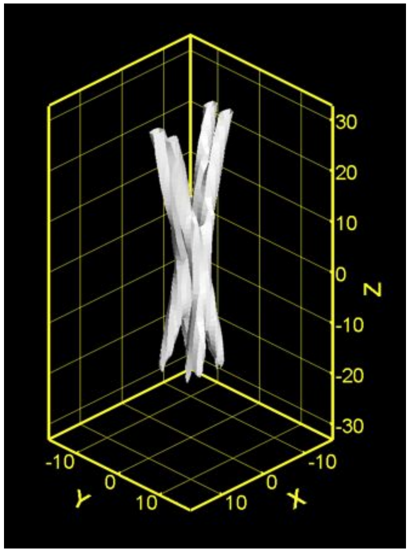

Particle reconstruction by edge detection (PRED)

Pu & Meng, Exp. Fluids 29:184-197 (2000)

Metal-Coated Hollow Glass Spheres

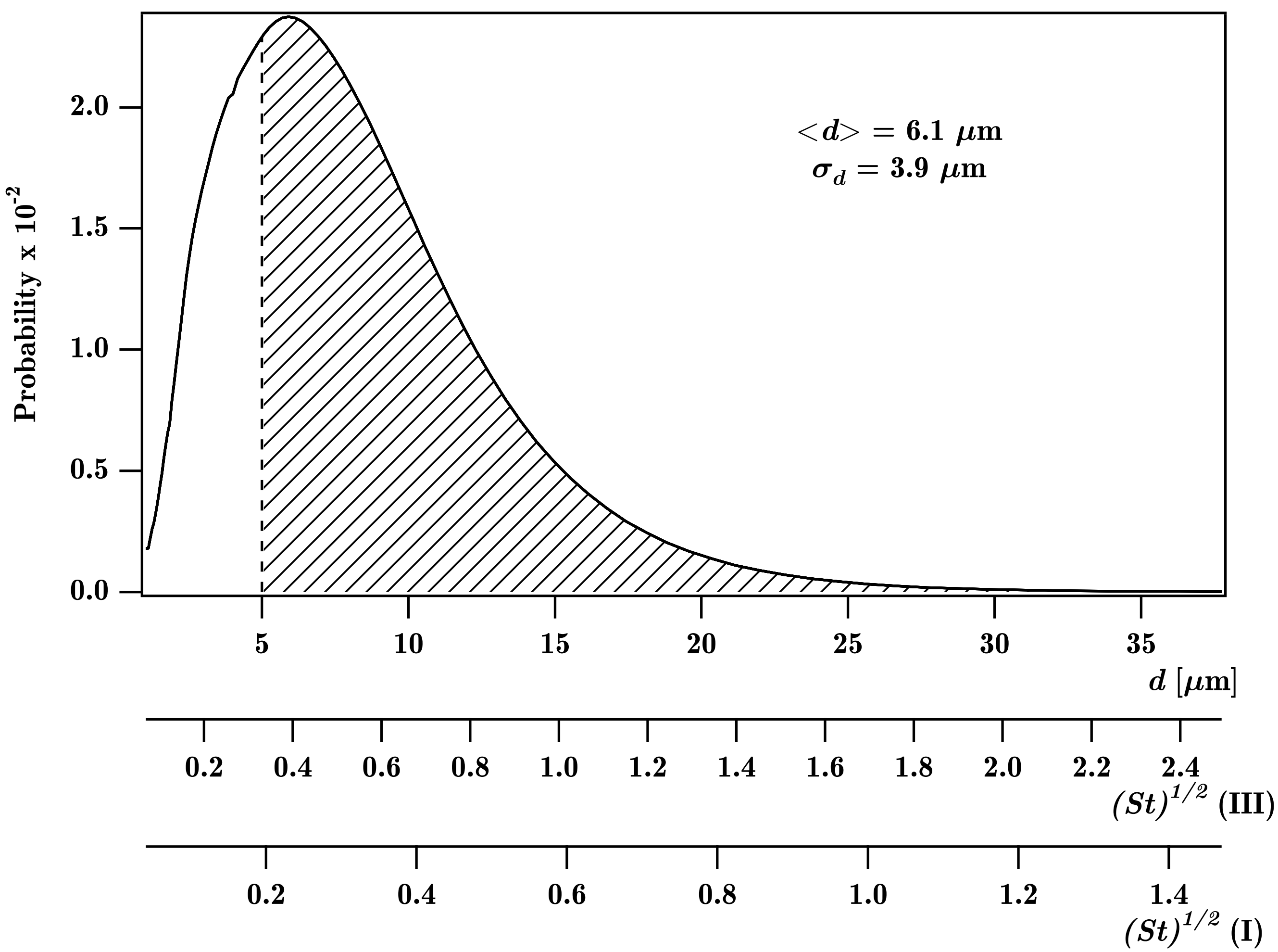

Time Evolution of RDF

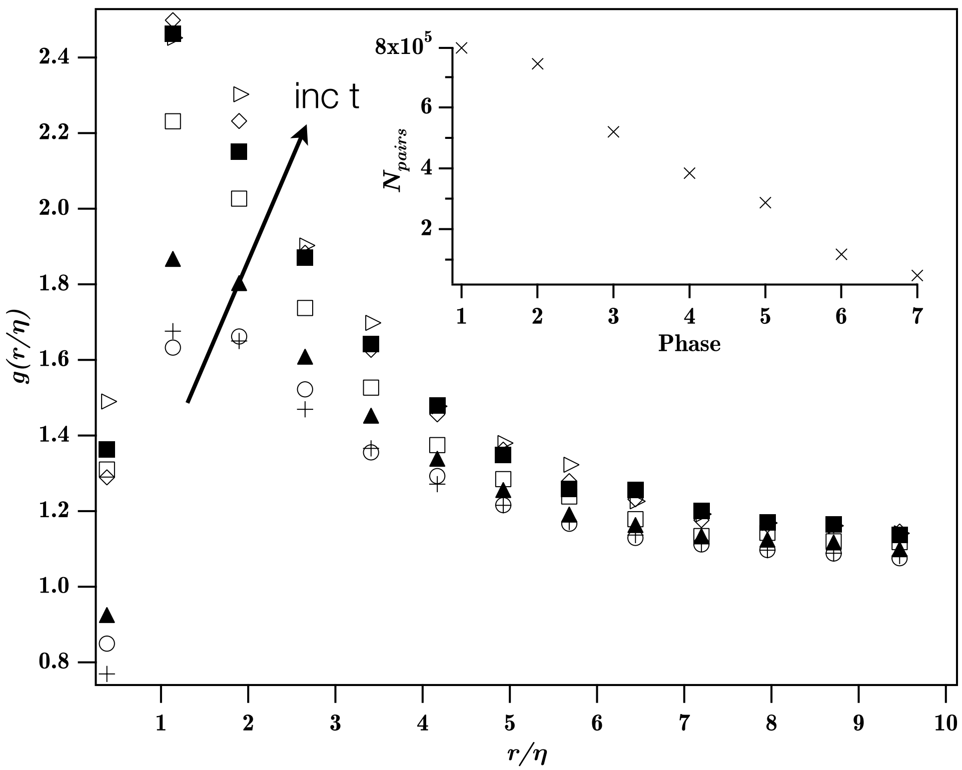

Salazar, de Jong, Cao, Woodward, Meng & Collins, J. Fluid Mech. (2008)

Comparison of RDF from Experiment and DNS

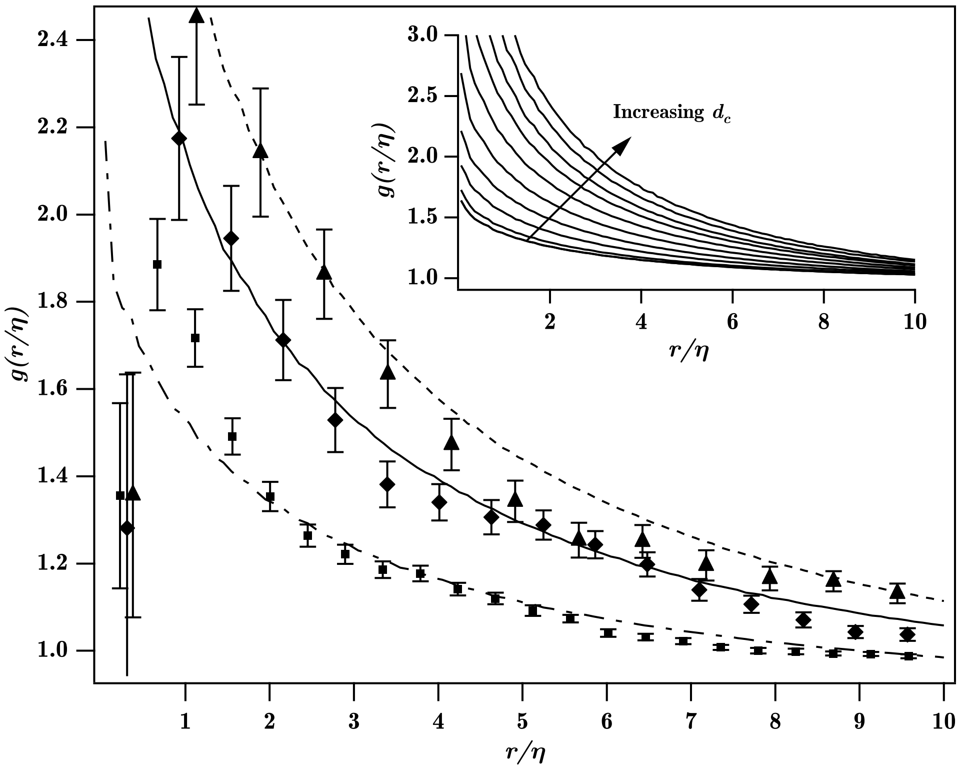

Salazar, de Jong, Cao, Woodward, Meng & Collins, J. Fluid Mech. (2008)

Particle Relative Velocities

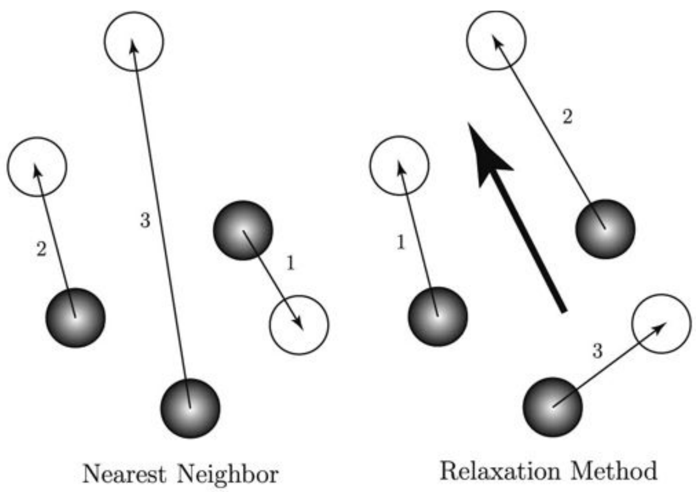

Fig. 3. Particle pairing results from the 'nearest neighbor' algorithm (left) and 'relaxation method' matching algorithm (right) for clustered particles. Black and white circles represents particles extracted from holographic images A and B, respectively. The large arrow in the relaxation method indicates the direction of the cluster motion. The numbers show the order of the pairings for each method.

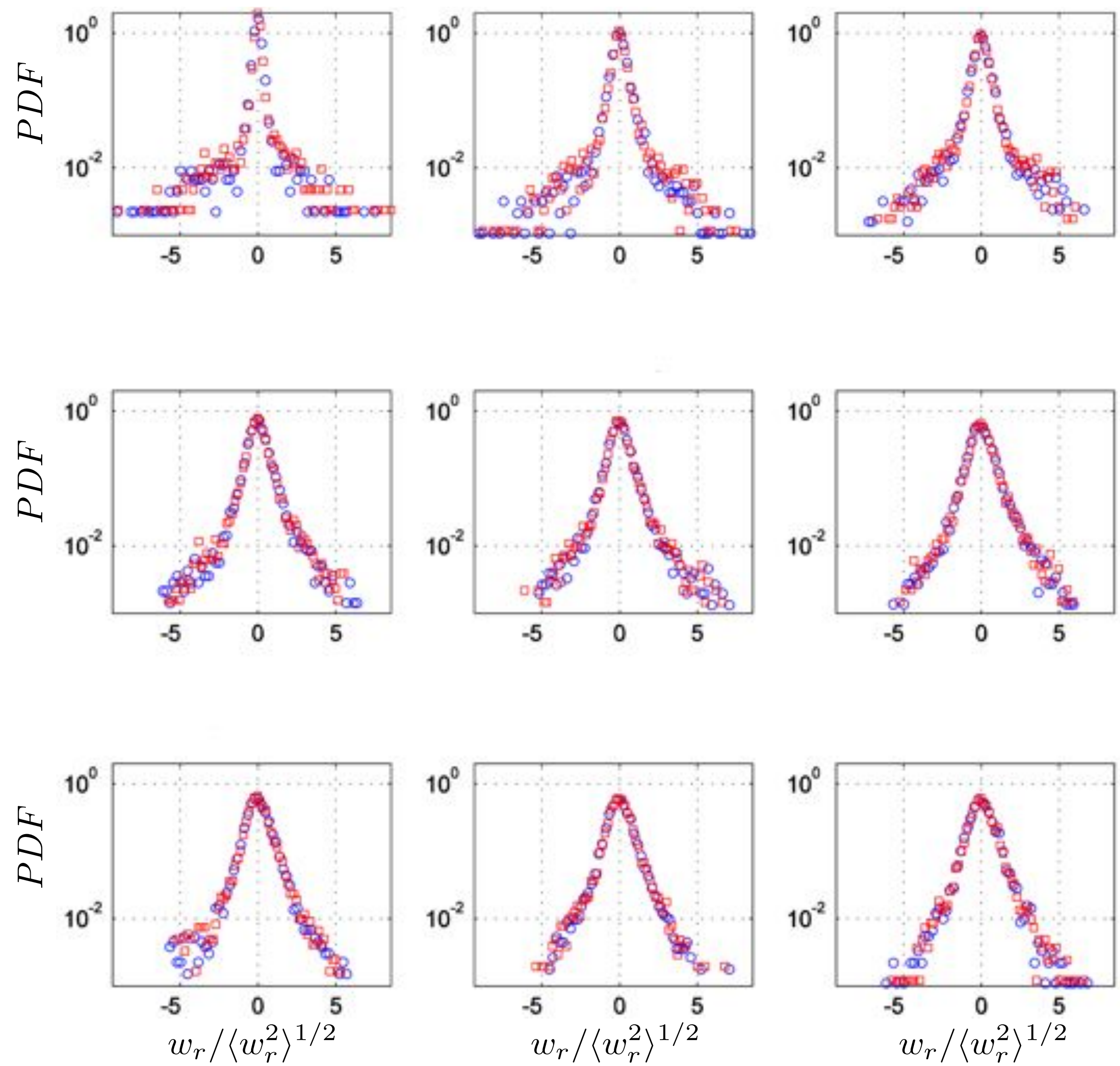

Particle Relative Velocities

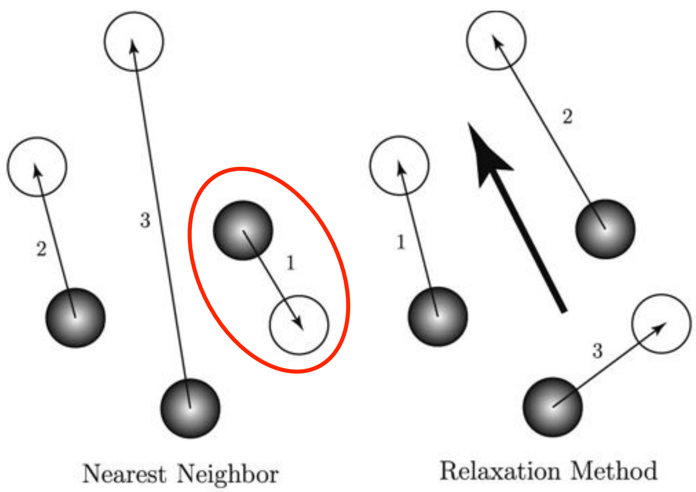

Fig. 3. Particle pairing results from the 'nearest neighbor' algorithm (left) and 'relaxation method' matching algorithm (right) for clustered particles. Black and white circles represents particles extracted from holographic images A and B, respectively. The large arrow in the relaxation method indicates the direction of the cluster motion. The numbers show the order of the pairings for each method.

"Sweet Spot"

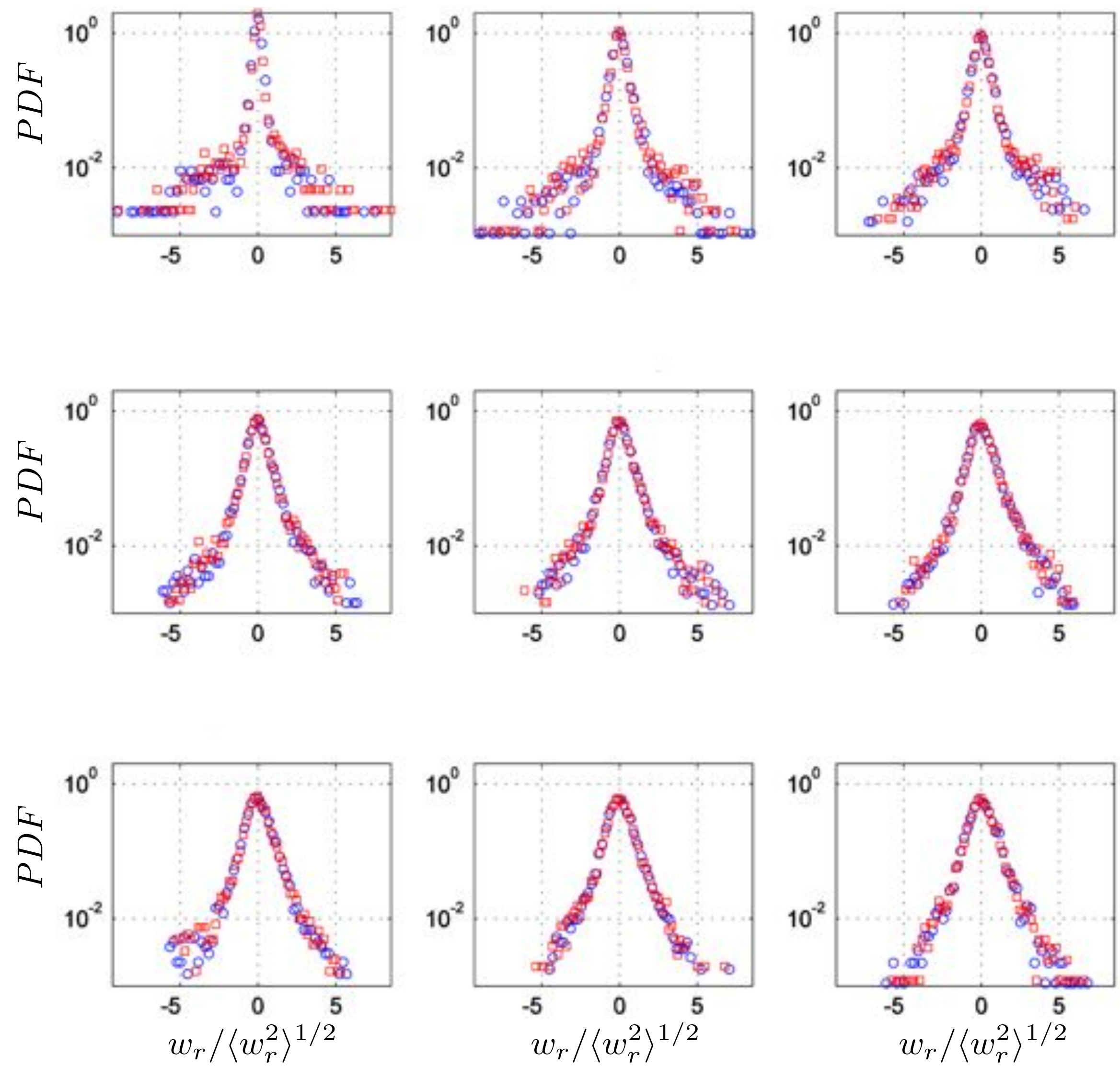

Comparison of PDFs

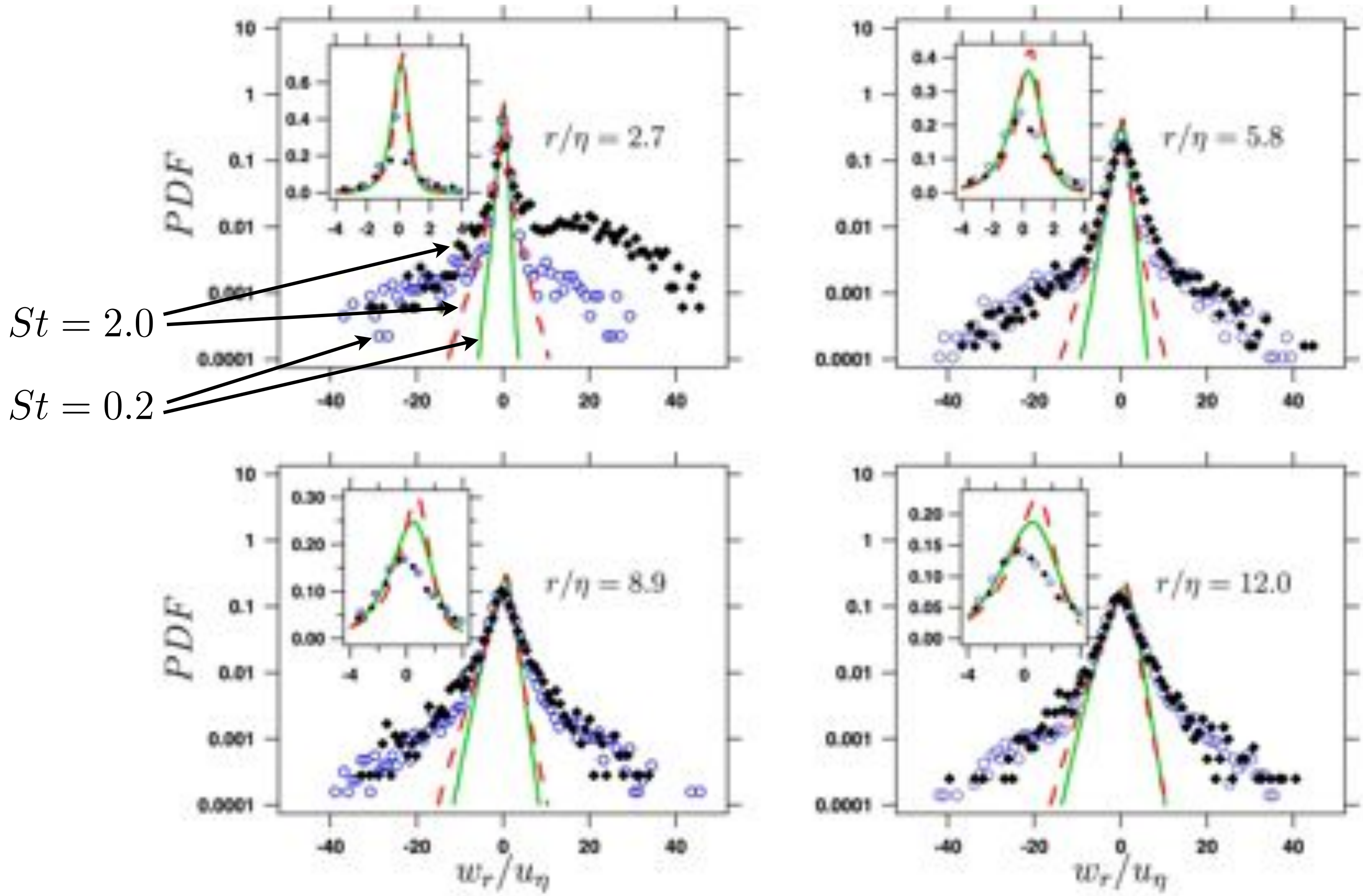

Fig. 5. Comparison of experimental (markers) and DNS (lines) radial relative velocity PDF at increasing two-particle separation distances for different St. In the experiment: Silver-coated hollow-glass spheres St = 0.2 (blue circles) and Polyimide spheres St = 2.4 (black diamonds). DNS values are for St = 0.2 (solid green line) and St = 2.0 (dashed red line).(For interpretation of the references to colour in this figure legend, the reader is referred to the web version of this article.)

Mean inward velocity

Fig 6b is obtained by filtering the errant tail in the experimental PDFs. It gives some sense of the possibility with an improved algorithm for high velocity particles.

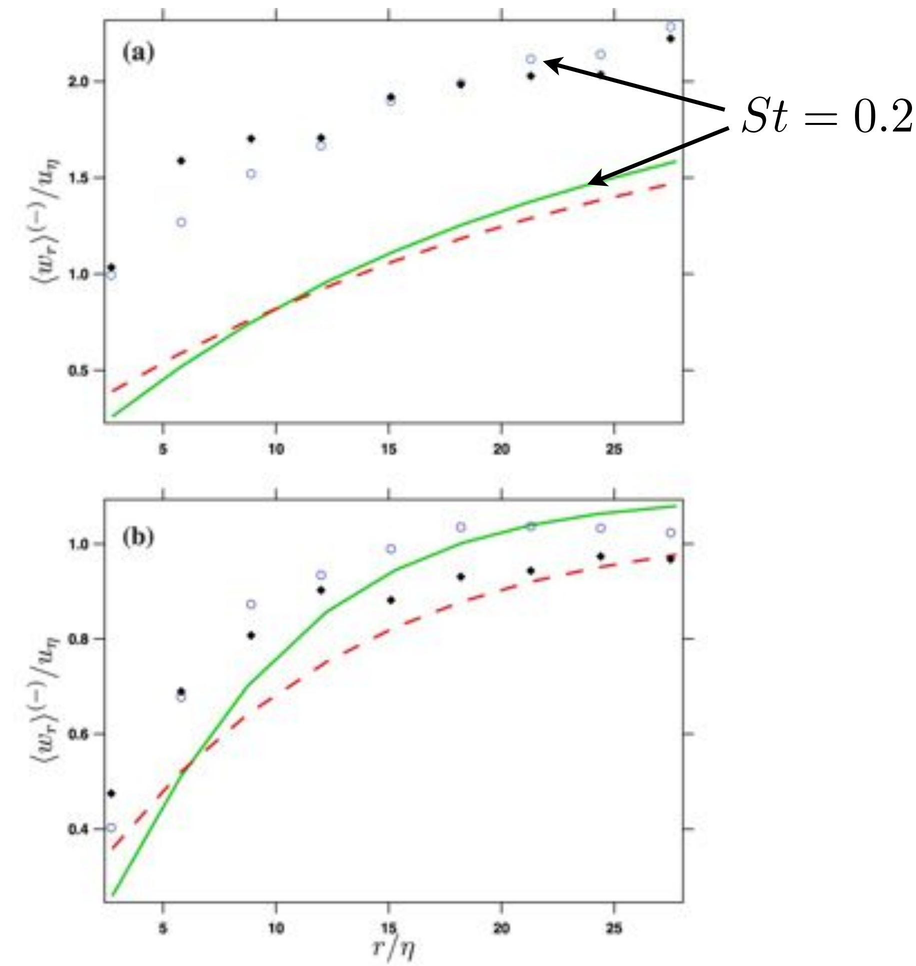

Fig. 6. Mean inward relative velocity (see Eq. (5)) comparison between DNS and experiments: (a) raw data without filtering and (b) mean inward relative velocity found by integrating the PDF over the range $-7 \leqslant w_r \leqslant 0$ for both experiment and DNS. In the experiment: Silver-coated hollow-glass spheres $St = 0.2$ (blue circles) and polyimide spheres $St = 2.4$ (black diamonds). DNS values are for $St = 0.2$ (solid green line) and $St = 2.0$ (dashed red line).(For interpretation of the references to colour in this figure legend, the reader is referred to the web version of this article.)

Summary on DNS and experiments for collisions kernel

- Experiments yield RDF in quantitative agreement with DNS when parameters are precisely matched
- Experiments yield relative velocity statistics in qualitative agreement with DNS
- We need a better matching algorithm to improve velocity measurements
- We are using DNS as virtual data to optimize `delta t` for each velocity

Eulerian view of clustering

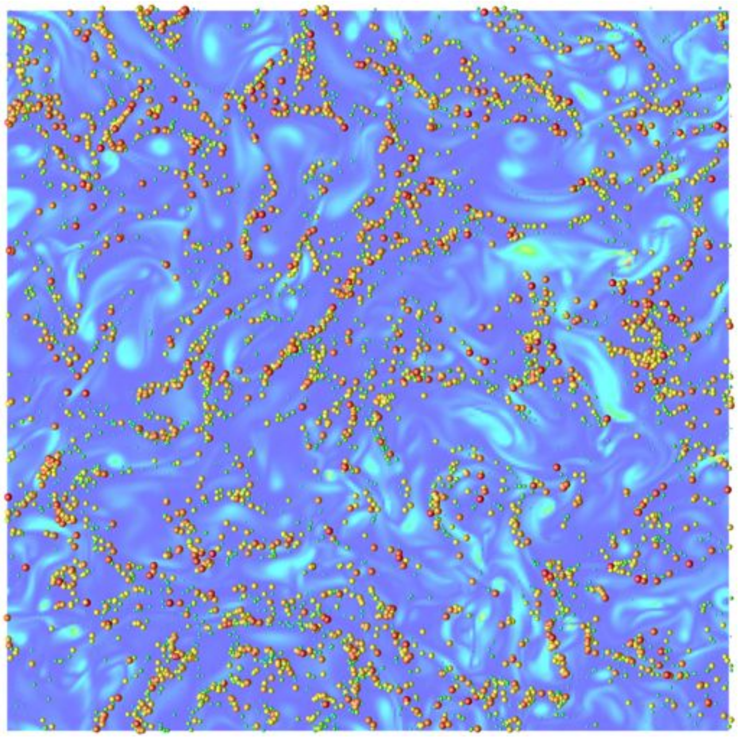

DNS

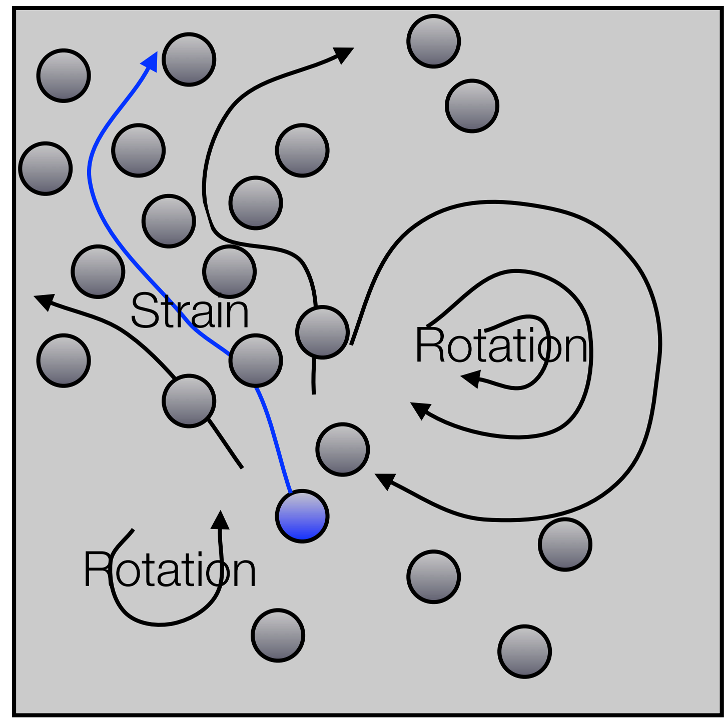

Schematic

Maxey 1987; Squires & Eaton 1991; Wang & Maxey 1993
Sundaram & Collins 1997; Reade & Collins 2000
Falkovich et al. 2002; Zaichik & Alipchenkov 2003; Chun et al. 2005

Monodisperse inward drift

$$q_r^d = -A\frac{r}{\tau_\eta}g(r)$$

$$A = \frac{St\tau_\eta^2}{3}\left[\langle S^2\rangle - \langle R^2\rangle\right]_p$$

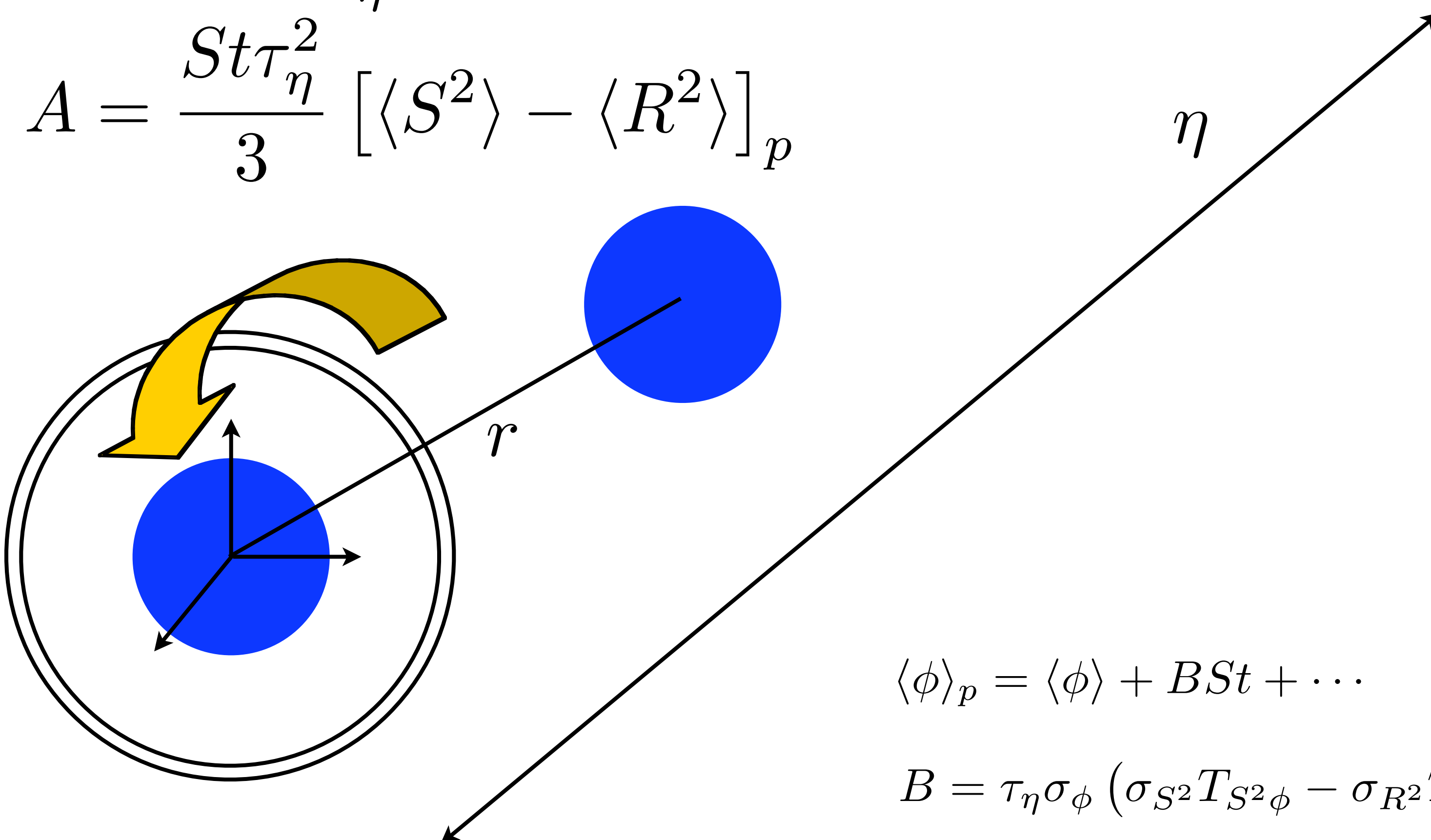

$$\langle\phi\rangle_p = \langle\phi\rangle + BSt + \cdots$$

$$B = \tau_\eta\sigma_\phi\left(\sigma_{S^2}T_{S^2\phi} - \sigma_{R^2}T_{R^2\phi}\right)$$

Maxey, JFM 174:441 (1987)
Chun, Koch, Rani, Ahluwalia & Collins, JFM 536:219 (2005)

Monodisperse outward diffusion

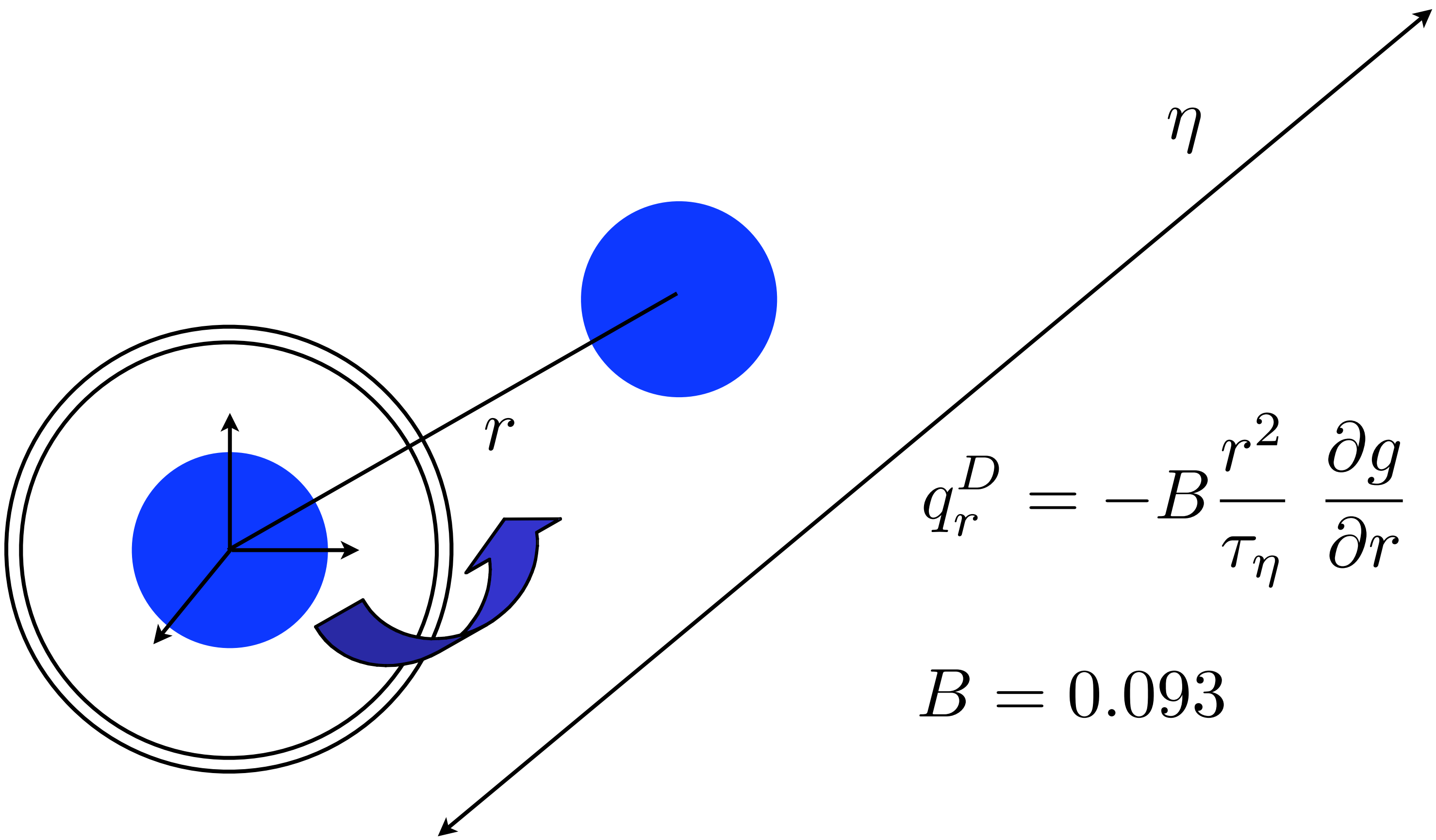

$$q_r^D = -B\frac{r^2}{\tau_\eta}\ \frac{\partial g}{\partial r}$$

$$B = 0.093$$

Chun, Koch, Rani, Ahluwalia & Collins, JFM 536:219 (2005)

Monodisperse prediction

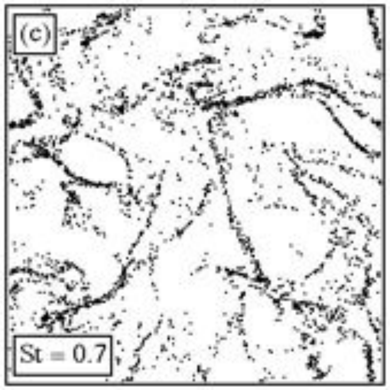

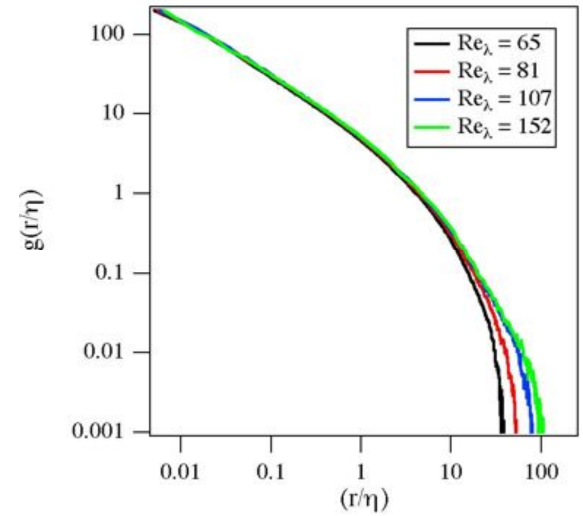

$$g(r) = \left(\frac{\eta}{r}\right)^{A/B}$$

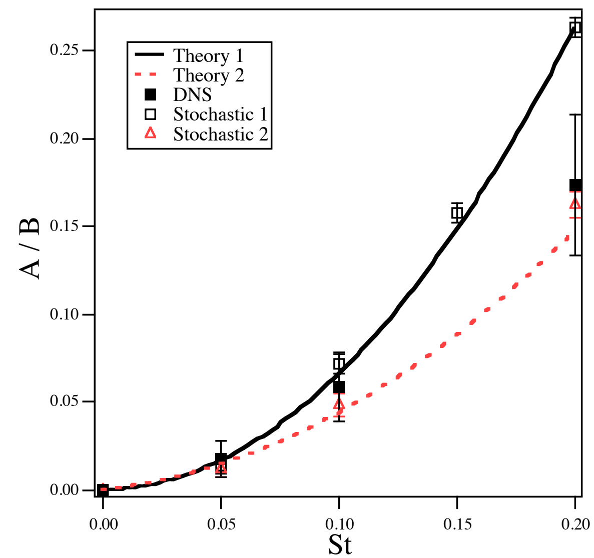

Falkovich et al., Nature 419:151 (2002)
Zaichik et al., PoF 18:035110 (2006)
Chun, Koch, Rani, Ahluwalia & Collins, JFM 536:219 (2005)

Bidisperse inward drift

$$q_r^d = -A\frac{r}{\tau_\eta}g(r)$$

$$A = \frac{St\tau_\eta^2}{3}\left[\langle S^2\rangle - \langle R^2\rangle\right]_p$$

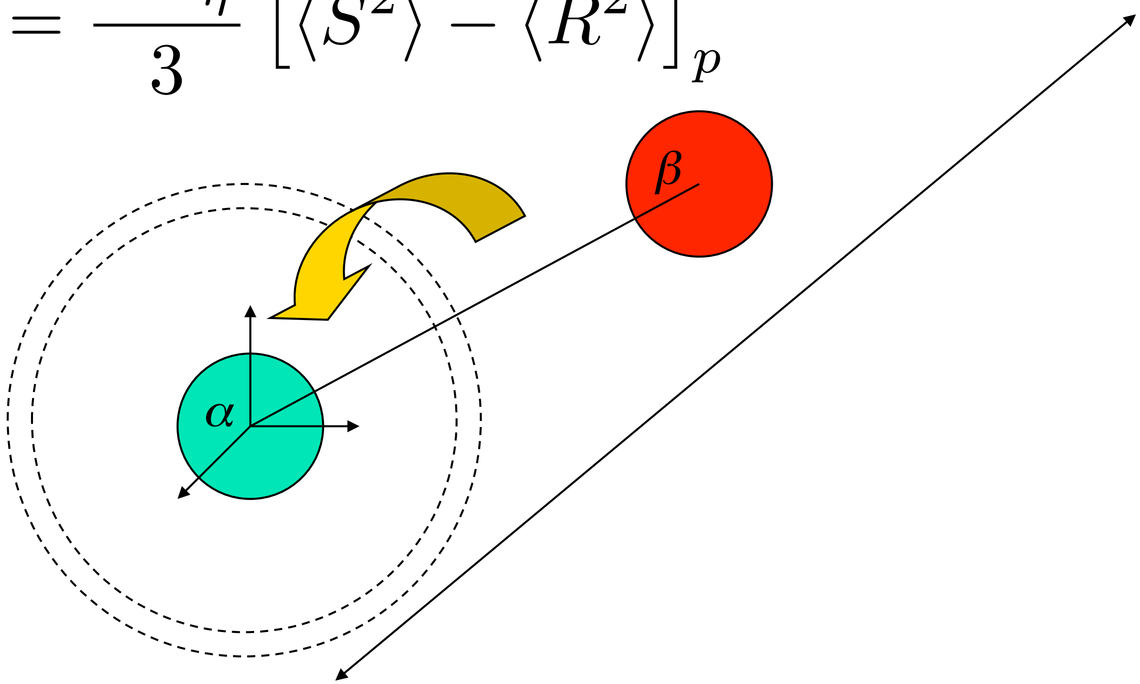

Bidisperse outward diffusion

$$q_r^D \equiv -D\frac{\partial g}{\partial r}$$

$$D = (\Delta St)^2 \, a_0 \frac{\eta^2}{\tau_\eta}$$

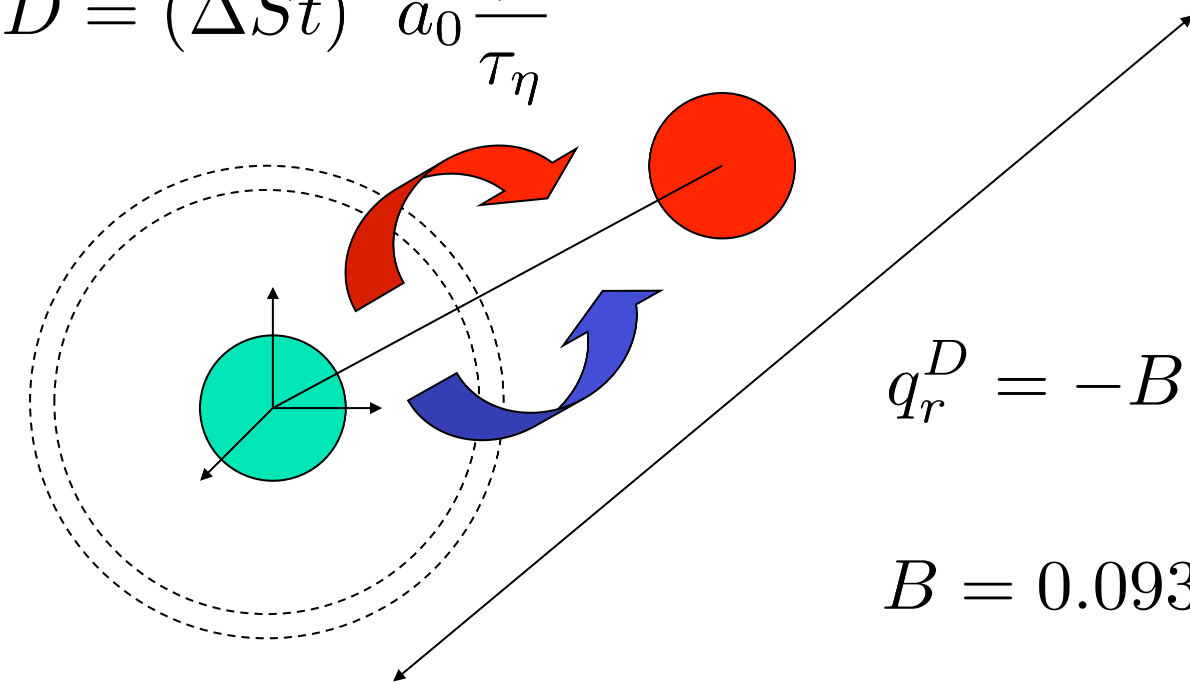

$$q_r^D = -B\frac{r^2}{\tau_\eta} \, \frac{\partial g}{\partial r}$$

$$B = 0.093$$

Bidisperse prediction

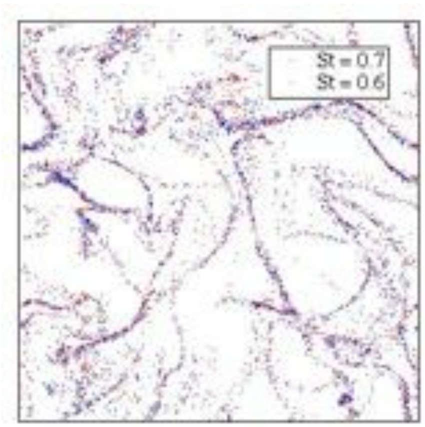

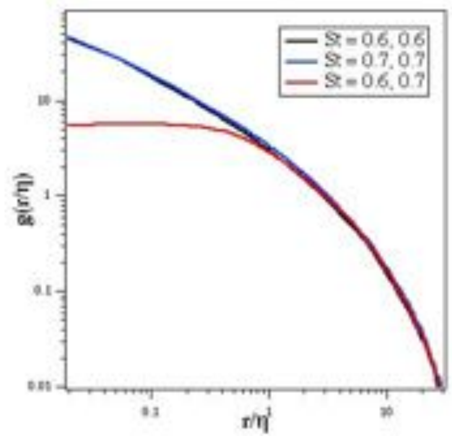

$$g(r) = \left(\frac{\eta^2}{r^2 + r_c^2} \right)^{A/2B}$$

Reynolds number dependence puzzle

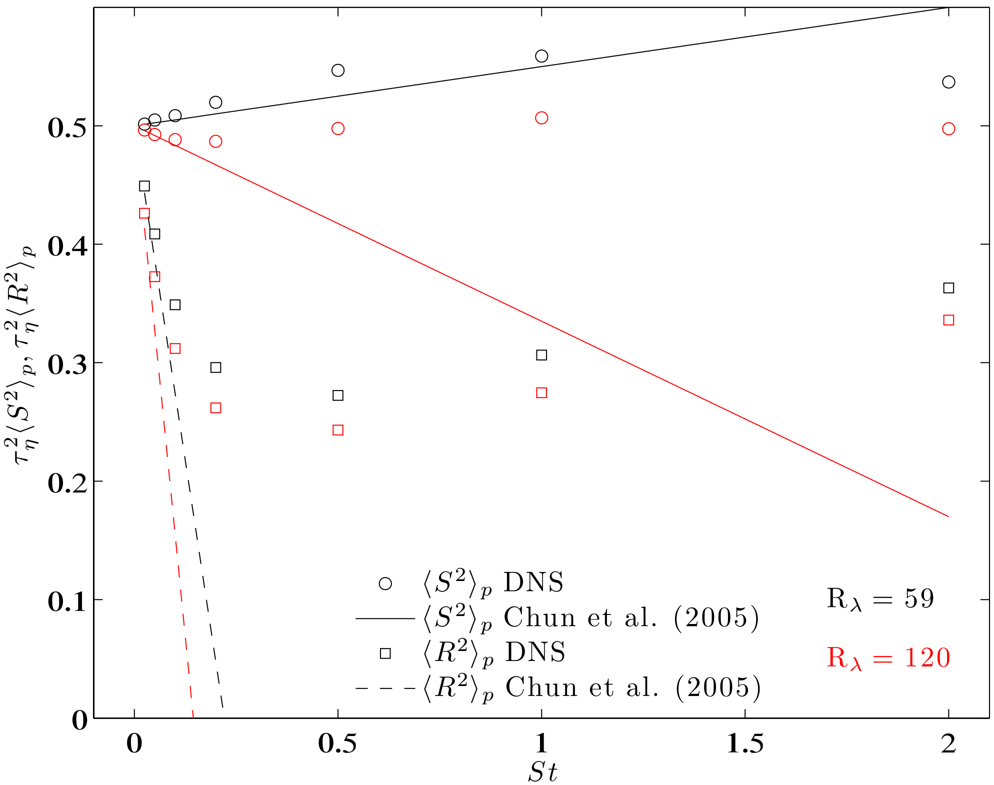

Inertial particles avoiding high strain too?

Relative Velocity PDFs have Skewness

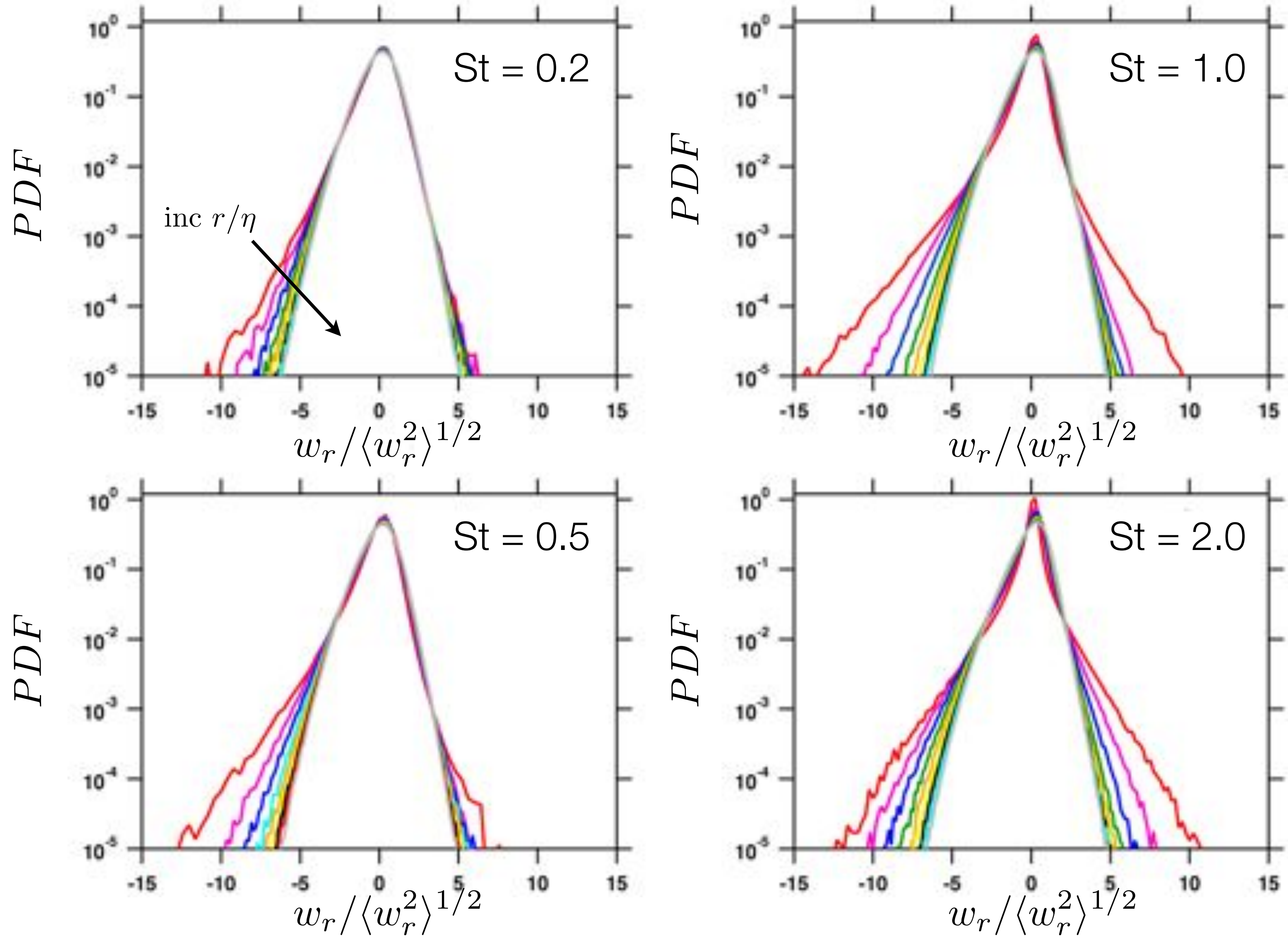

What is a “caustic”?

- …ne (1959) coined this the “crossing trajectories” effect and studied its relevance to dispersion. Both Falkovich et al. (2002) and Wilkinson et al. (2006) identified the importance of caustics (or “sling effect”) to the process of warm rain initiation.

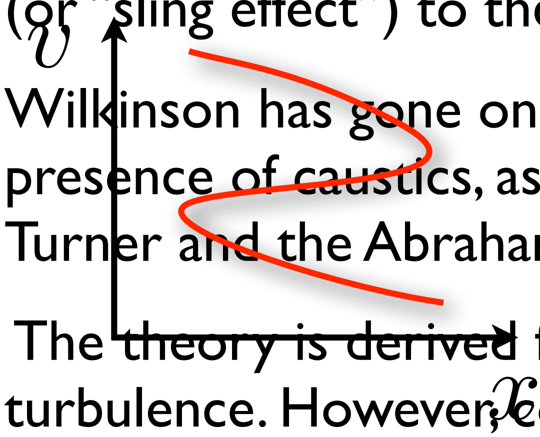

- Wilkinson has gone on to predict the collision kernel in the presence of caustics, as a weighted average of the Saffman-Turner and the Abrahamson kernels.
- The theory is derived for limits not compatible with turbulence. However, comparison with random Gaussian flows with specified space-time correlations is favorable.
- Do we see caustics?

A caustic occurs when the same point in space has more than one defined velocity

2nd order structure function

- We investigate the scaling of the inertial particle relative velocity structure function in the dissipation range and the inertial subrange

- In the dissipation range we find evidence of caustics and good agreement with the theory of Falkovich and Pumir (2007) and Wilkinson et al. (2006) for St>0.5. Scaling exponents are analyzed in the context of the model proposed by Bec et al. (2009).

- In the inertial subrange we observe reduced intermittency exponents when compared to that of the fluid. Manipulation of the particle evolution equation shows that the dominant effect is that of filtering and not biased sampling.

$$G_p^{\parallel,\perp}(r, St) \equiv \left\langle \left[\Delta\mathbf{v} \cdot \mathbf{e}^{\parallel,\perp} \right]^p \right\rangle (r)$$

$$\Delta\mathbf{v}(r, St) \equiv \mathbf{v}(\mathbf{x}+\mathbf{r}, St) - \mathbf{v}(\mathbf{x}, St)$$

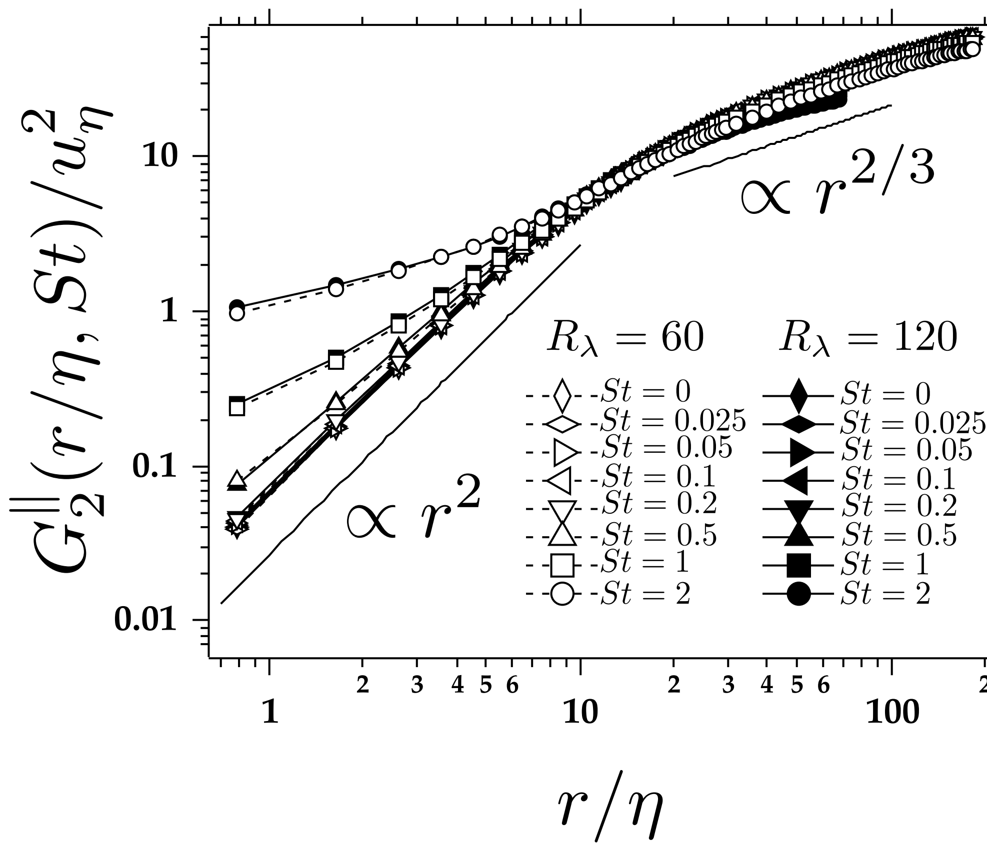

Salazar & Collins JFM, in review; Bec et al. (2010)

Bec et al. (2010)

$$G_2^{\|}(r, St) \propto r^{\xi_p(St)}$$

$$\xi_p(St) = \begin{cases} p & \text{for } p \leq \alpha \ln(7/St)\,, \\ \alpha \ln(7/St) & \text{for } St \leq 7\,, \\ 0 & \text{for } St > 7\,. \end{cases}$$

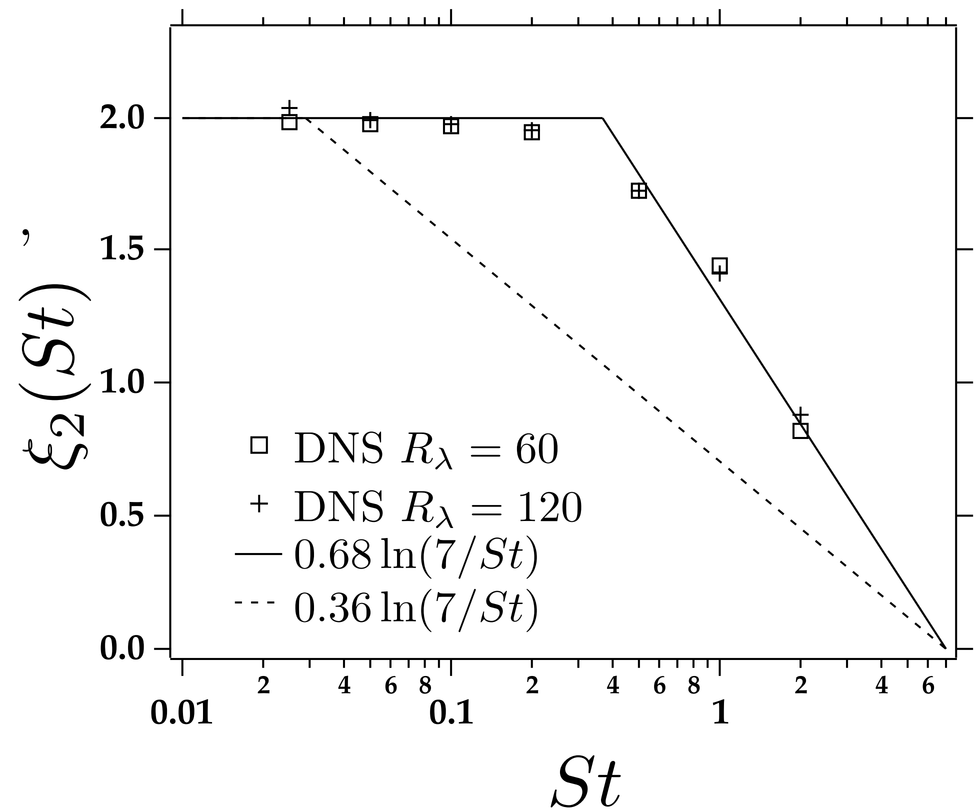

Consistent with the limits $\xi_p(St \to 0) = p$ and $\xi_p(St \to \infty) = 0$

fluid limit | ballistic limit

Decomposition in the limit r⟶0

From the evolution equation for inertial particles we can write

$$\mathbf{v} = \mathbf{u} - \tau_p \dot{\mathbf{v}}$$

$$\dot{\mathbf{v}} = \frac{d\mathbf{v}}{dt}$$

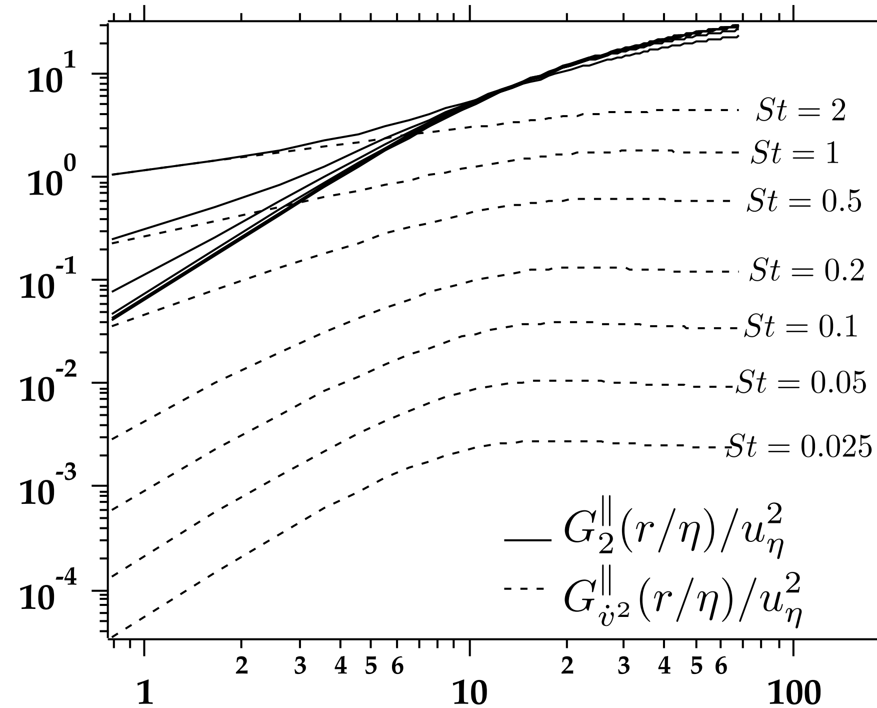

The second order structure function can be expanded as follows

$$G_2^{\parallel}(r,St) = \underbrace{\left\langle \left[\Delta\mathbf{u}\cdot\mathbf{e}^{\parallel}\right]^2 \right\rangle(r)}_{G_2^{\parallel}(r,St=0)} - 2\,\underbrace{\tau_p \left\langle \Delta\mathbf{u}\cdot\mathbf{e}^{\parallel}\Delta\dot{\mathbf{v}}\cdot\mathbf{e}^{\parallel}\right\rangle(r)}_{\equiv G_{u\dot{v}}^{\parallel}(r,St)} + \underbrace{\tau_p^2 \left\langle \left[\Delta\dot{\mathbf{v}}\cdot\mathbf{e}^{\parallel}\right]^2 \right\rangle(r)}_{\equiv G_{\dot{v}^2}^{\parallel}(r,St)}$$

Decomposition in the limit r⟶0

$$G_2^{\|}(r\to 0,St)=\underbrace{\cancel{\left\langle\left[\Delta\mathbf{u}\cdot\mathbf{e}^{\|}\right]^2\right\rangle}}_{\propto r^2}-2\,\tau_p\underbrace{\cancel{\left\langle\Delta\mathbf{u}\cdot\mathbf{e}^{\|}\Delta\dot{\mathbf{v}}\cdot\mathbf{e}^{\|}\right\rangle}}_{\propto r^2}+\tau_p^2\underbrace{\left\langle\left[\Delta\dot{\mathbf{v}}\cdot\mathbf{e}^{\|}\right]^2\right\rangle}_{\neq 0}$$

Theory of Falkovich & Pumir (2007) and Wilkinson et. al (2006) gives,

$$\langle|\Delta\mathbf{v}|^p\rangle=B^p\exp\left[-pA/St\right]$$

This in turn implies

$$G_2^{\|}(r\to 0,St)=G_{\dot{v}^2}^{\|}(r\to 0,St)=\frac{B^2}{3}\exp\left[-2A/St\right]$$

Do caustics exist at all St? Following Maxey (1987), for St<<1 we have $\dot{\mathbf{v}}=\mathbf{a}$

Hence for small St the inertial particle velocity is given by $\mathbf{v}=\mathbf{u}-\tau_p\mathbf{a}$

This suggests the Stokes number must exceed a critical value for caustics to form

Curve Fit

$$G_2^{\|}(r, St) = \alpha + \beta r^{\xi_2}$$

General Expression

$$G_2^{\parallel}(r, St) = \begin{cases} c^{\parallel}(St) r^2 & \text{for } St \le St_c \,, \\ \frac{1}{3} B^2 \exp\left[-2A/St\right] + c^{\parallel}(St) r^{\xi_2(St)} & \text{for } St_c \le St \le 7 \,, \\ \frac{1}{3} B^2 \exp\left[-2A/St\right] & \text{for } St > 7 \,. \end{cases}$$

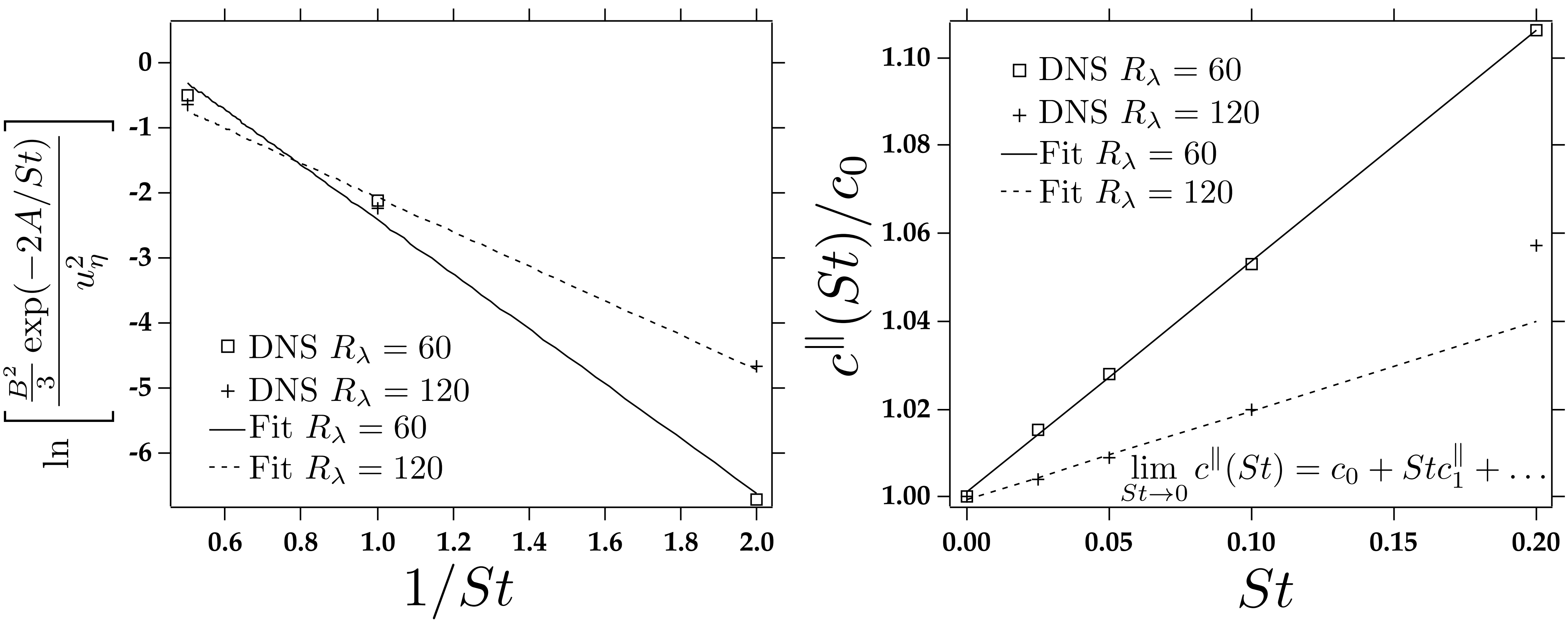

Quality of Fit

$$G_2^{\|}(r,St) = \begin{cases} c^{\|}(St)r^2 & \text{for } St \le St_c\,, \\ \frac{1}{3}B^2\exp\left[-2A/St\right] + c^{\|}(St)r^{\xi_2(St)} & \text{for } St_c \le St \le 7\,, \\ \frac{1}{3}B^2\exp\left[-2A/St\right] & \text{for } St > 7\,. \end{cases}$$

- The linear regime for $c^{\|}$ is apparent, with a Reynolds number dependent slope.
- It is difficult to establish the existence of a critical Stokes number St_c.
- Our fit to the expression for caustics given by Falkovich & Pumir (2007) and Wilkinson (2006) is reasonable. We find a similar Reynolds number dependence.
- Our proposed decomposition shows excellent convergence to $G^{\|}_{\dot{v}^2}$ in the limit of $r/\eta \ll 1$ and $St > St_c$

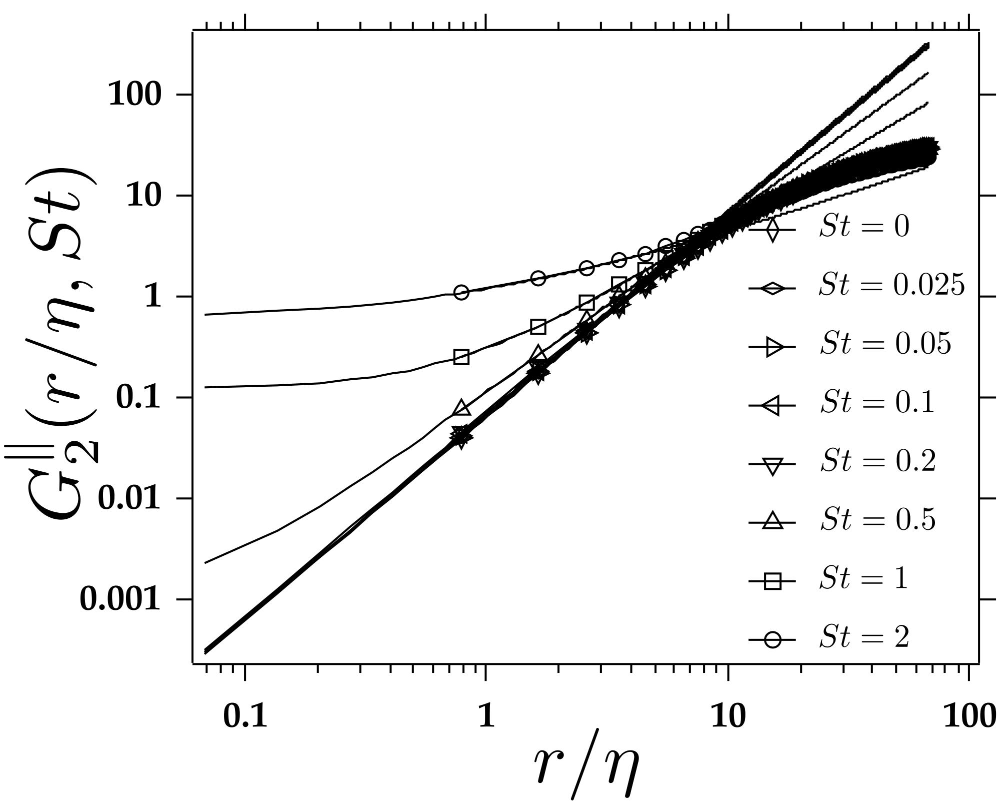

Summary on relative velocity

- Theory gives us the RDF and relative velocity PDF in the zero Stokes limit in quantitative agreement with DNS

- Theory predicts relative velocity PDF is negatively skewed (required for clustering to occur)

- Theory cannot predict the appearance of “caustics”; they are required to understand the peak in clustering at St ~ 1

- We believe there is a critical Stokes number for the appearance of caustics (between 0.2 and 0.5); consistent with Reeks (cellular flow); inconsistent with Wilkinson and Falkovich (assumed a Gaussian distribution of velocity gradients)

Large eddy simulation (LES)

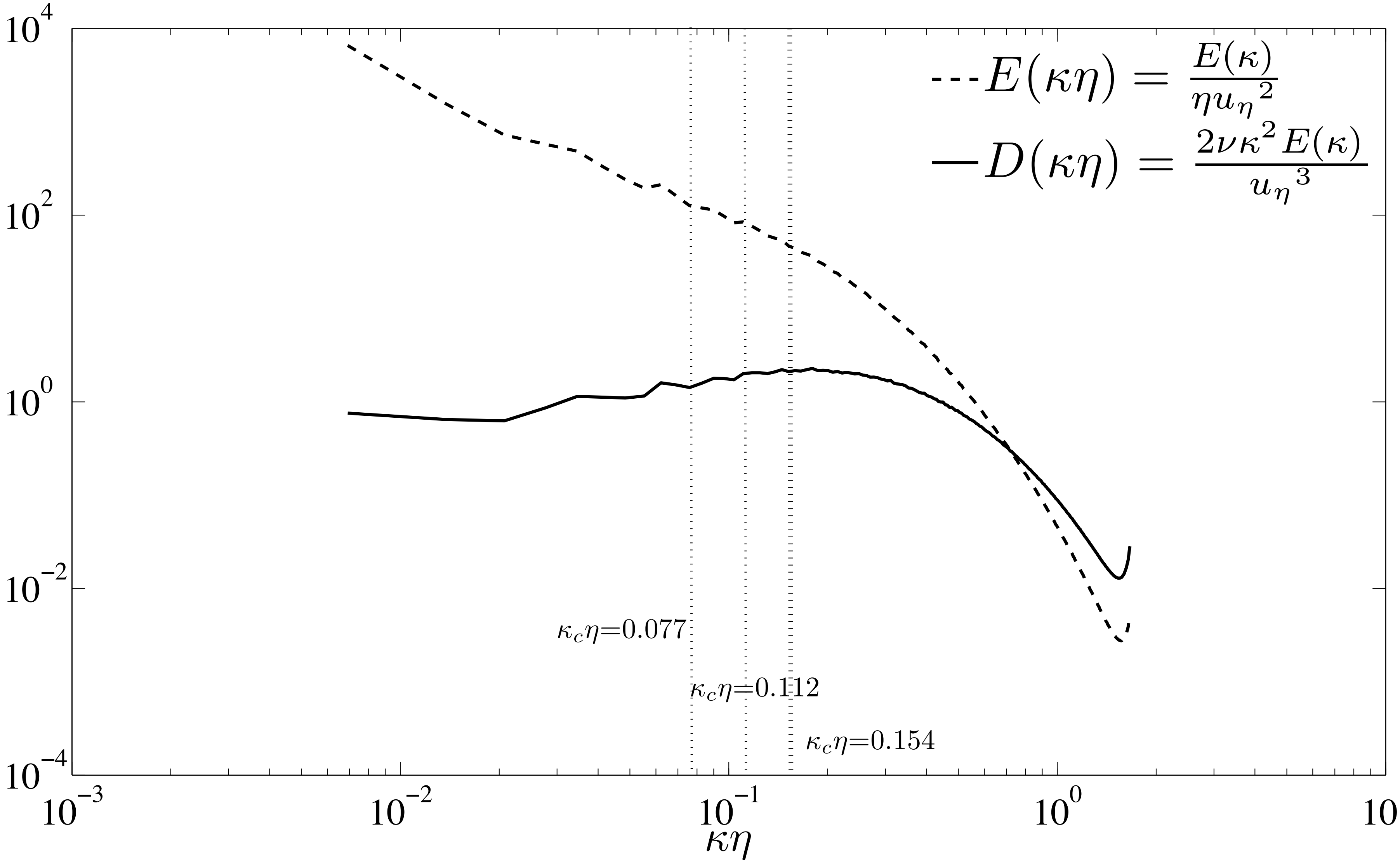

Unfiltered RDF

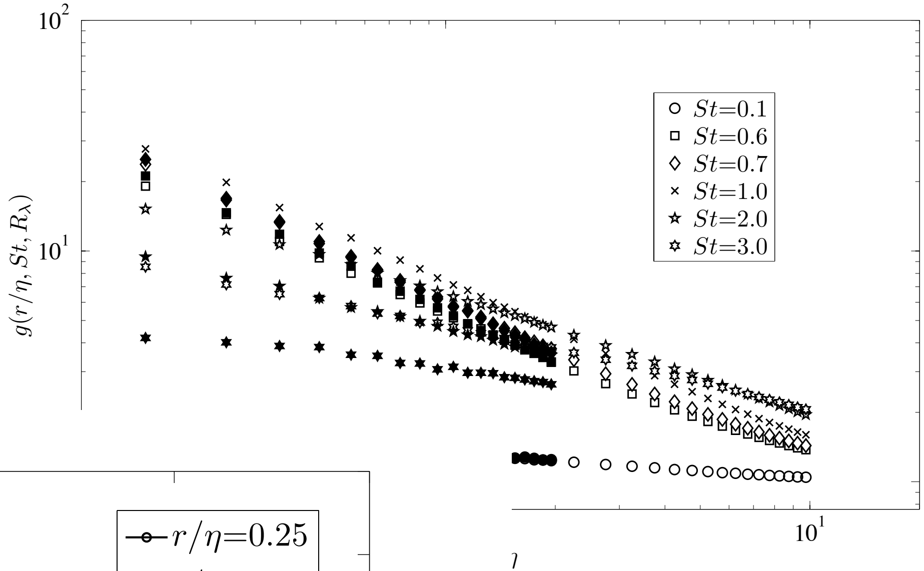

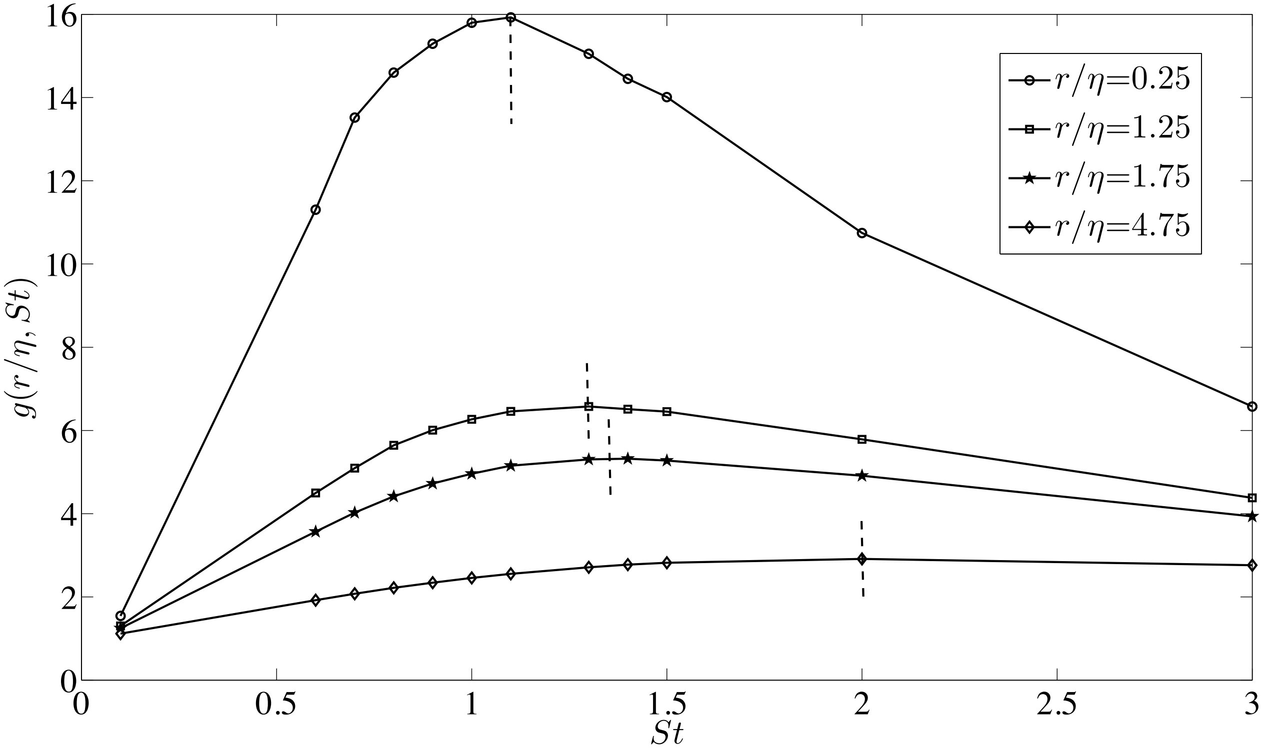

Unfiltered relative velocity PDF

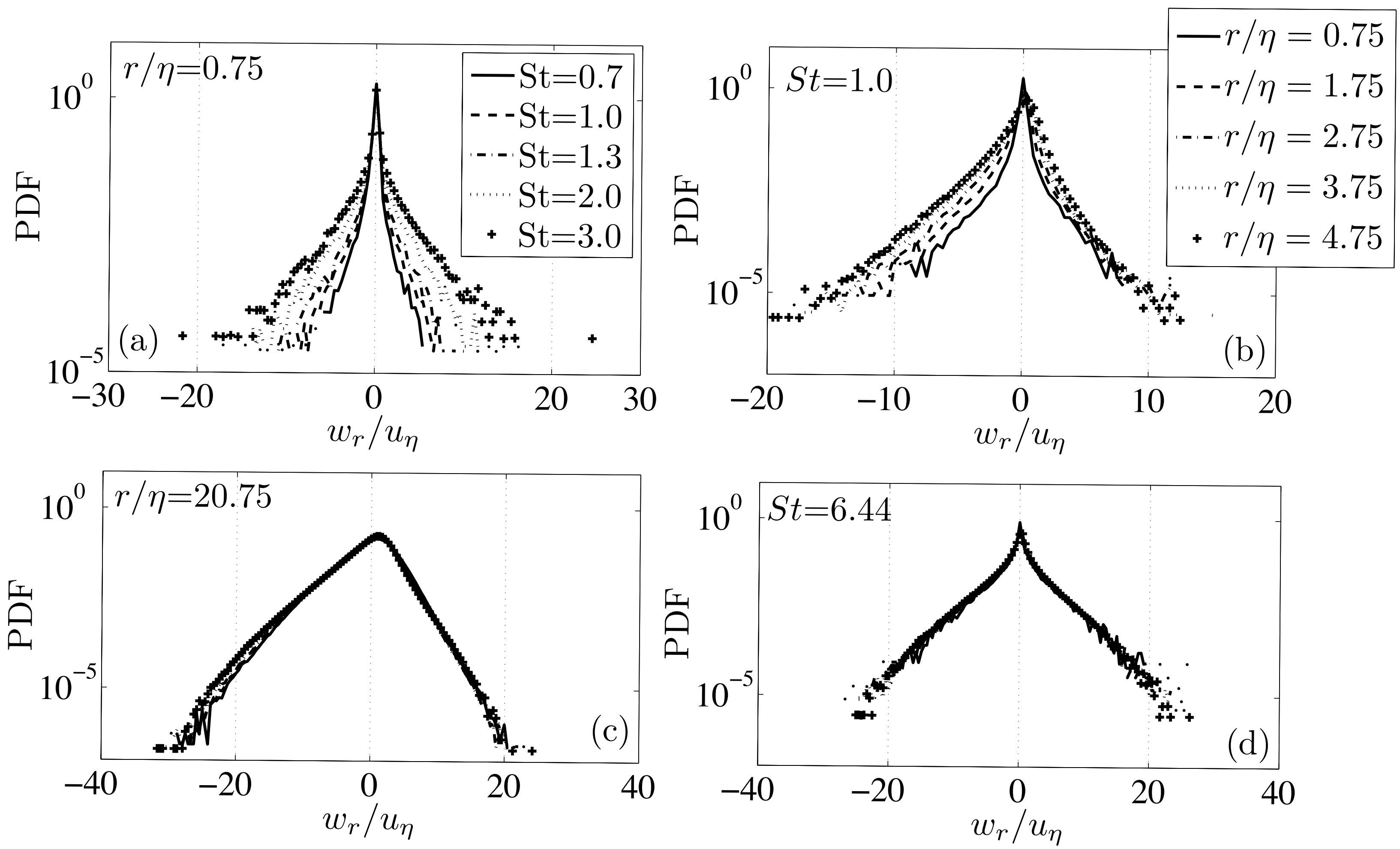

Unfiltered skewness of relative velocity

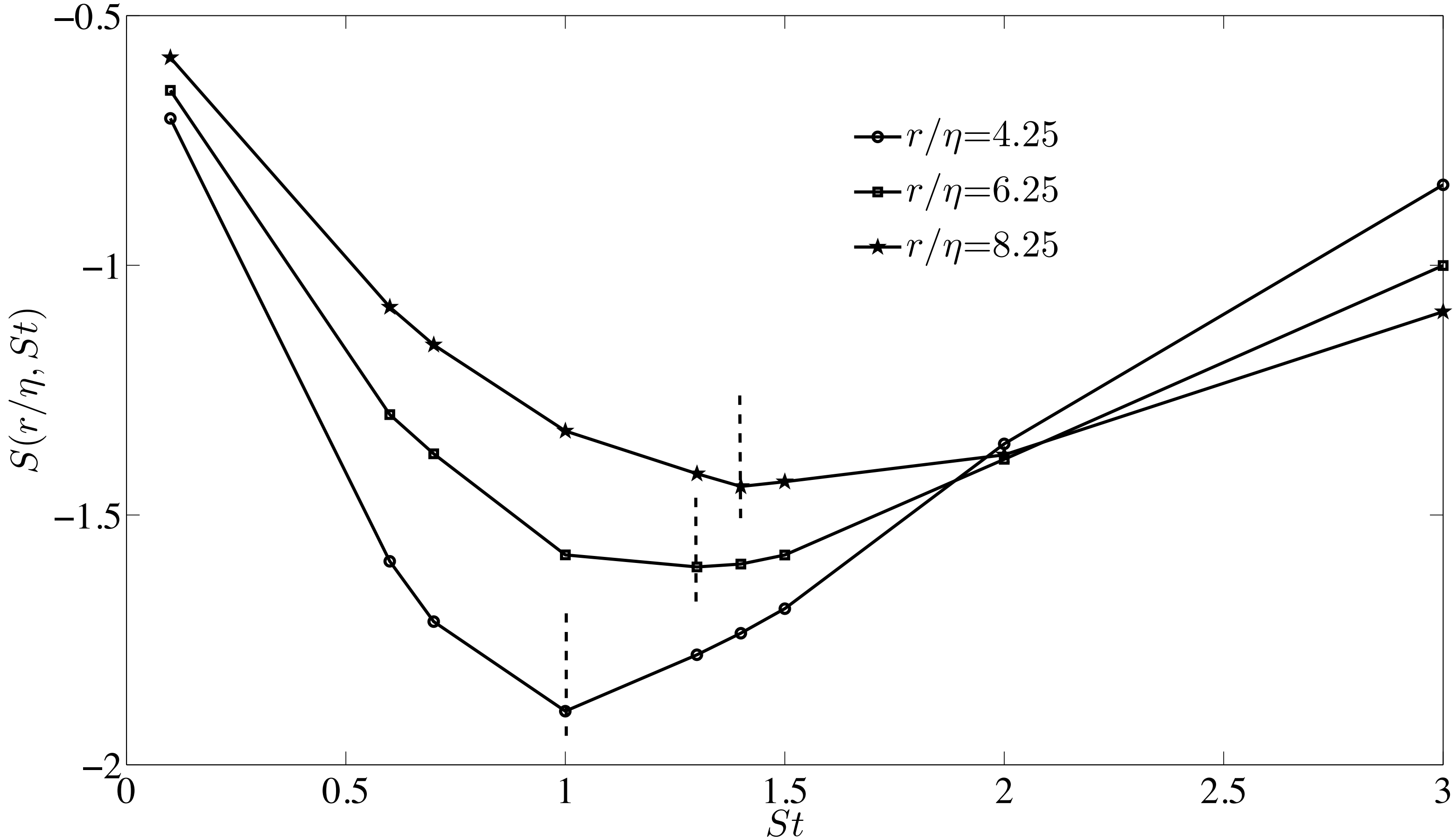

Effect of filtering on RDF

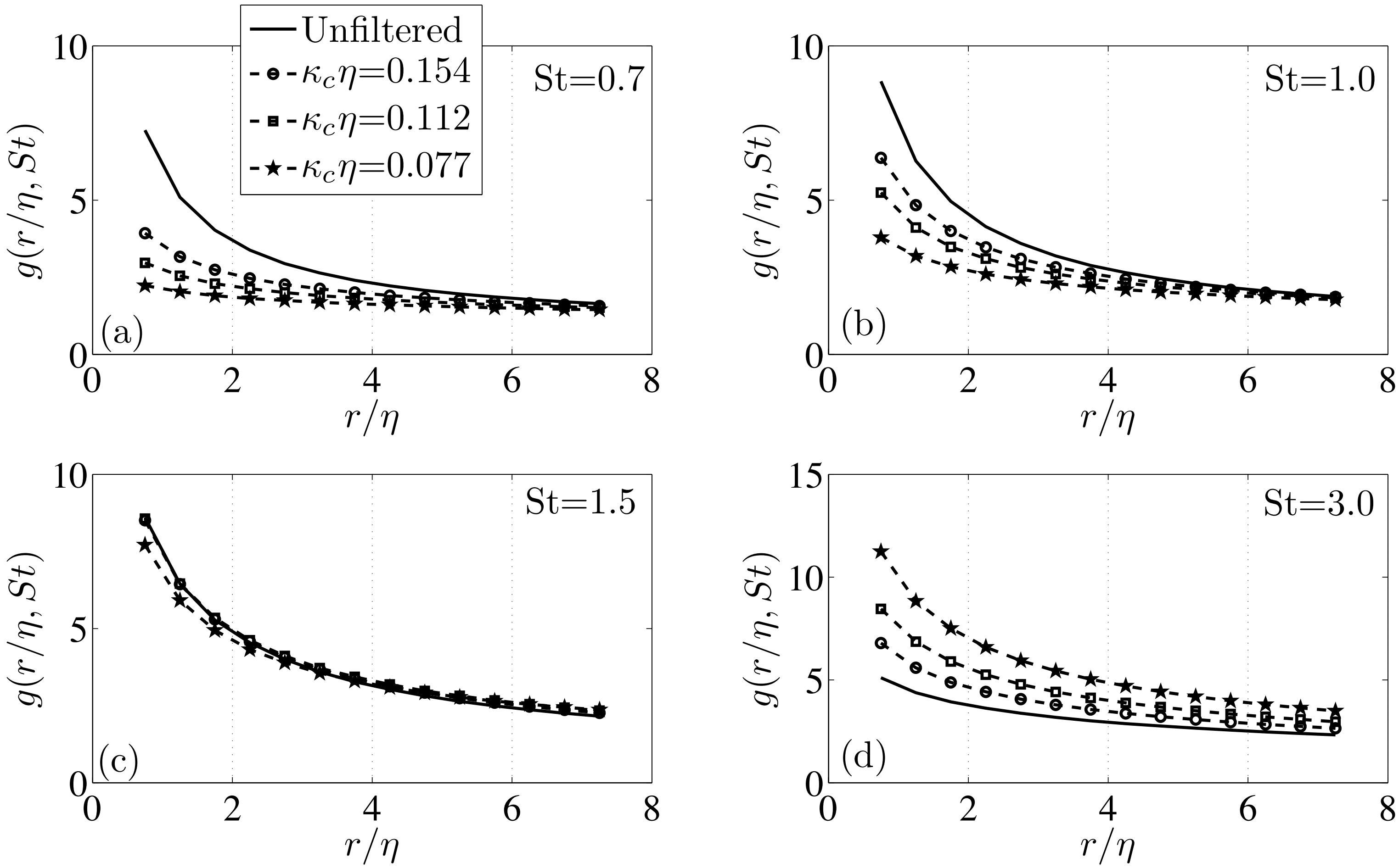

Effect of filtering on relative velocity PDF

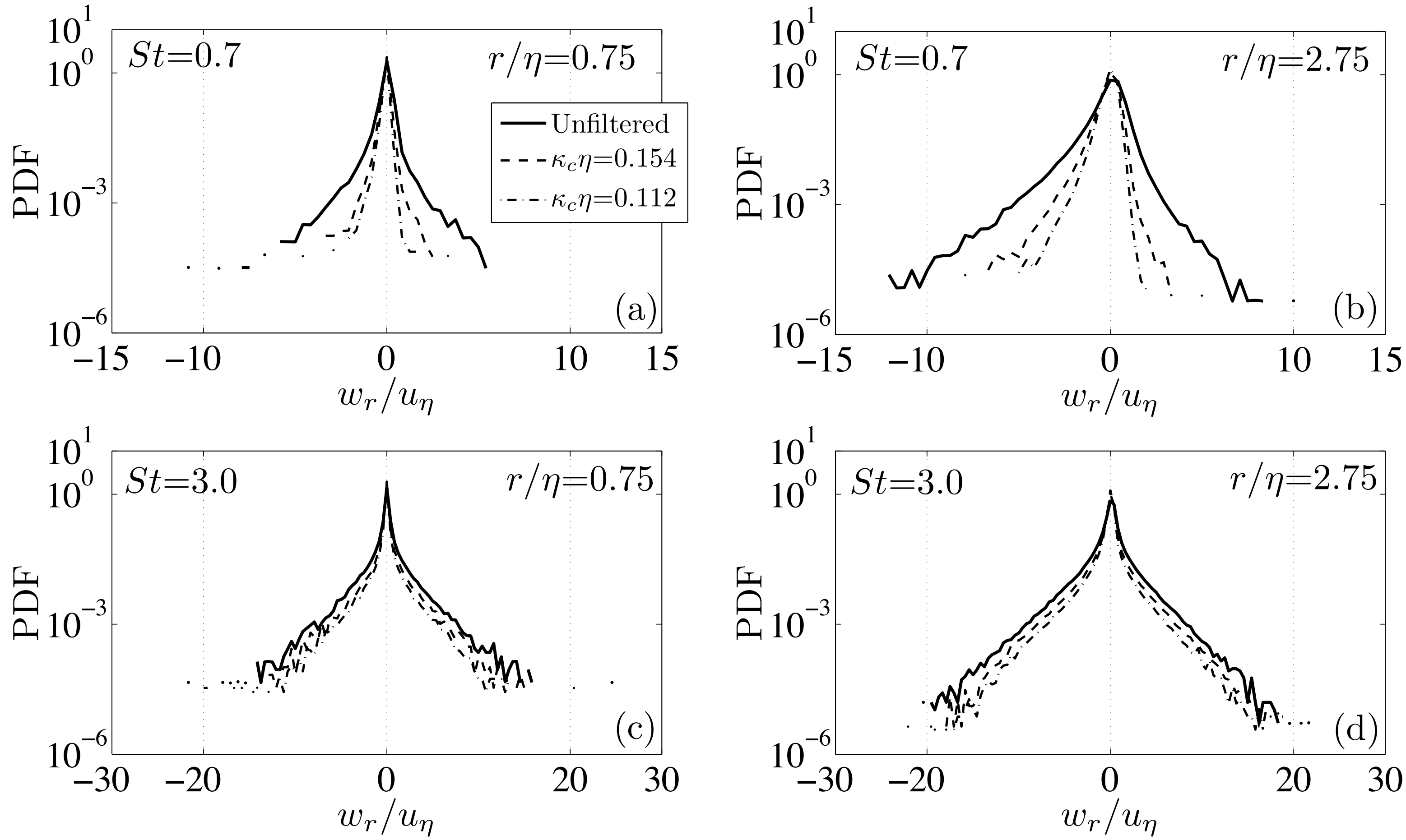

Effect of filtering on skewness of relative velocity

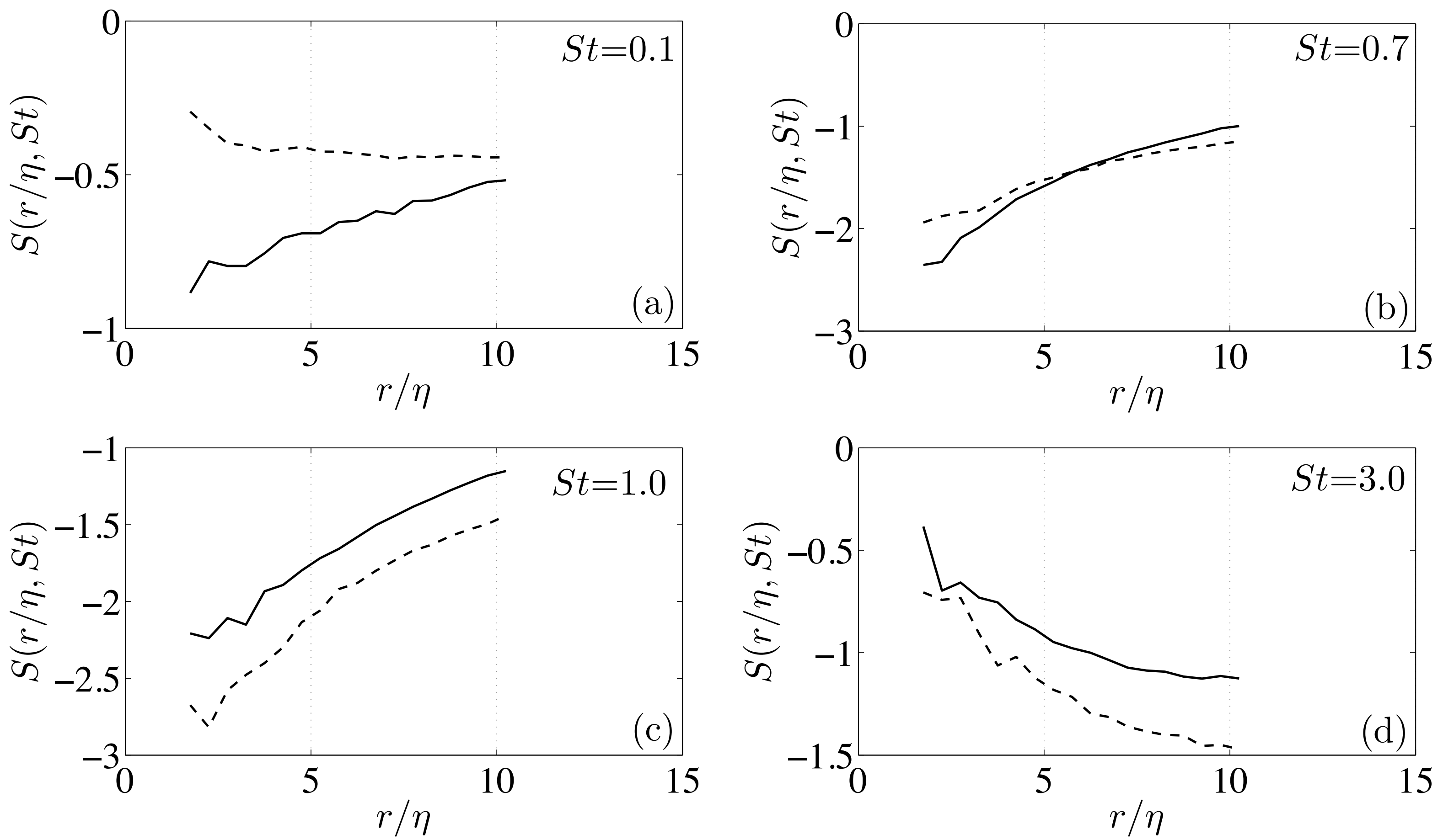

Summary of LES

- Filtering reduces clustering for low St particles, but enhances clustering for high St particles (filtered eddies “diffuse” high St particles; filtering reduces caustics as well)
- Filtering always reduces relative velocity variance
- Filtering modifies skewness in manner qualitatively similar to clustering